HAL open science

Observations: oceanic climate and sea level

N. Bindoff, J. Willebrand, V. Artale, A. Cazenave, J. Gregory, S. Gulev, K. Hanawa, C. Le Quéré, S. Levitus, Y. Nojiri, et al.

To cite this version:

N. Bindoff, J. Willebrand, V. Artale, A. Cazenave, J. Gregory, et al.. Observations: oceanic climate and sea level. Climate change 2007: The physical Science Basis, pp.385-432, 2007. hal-00287145

HAL Id: hal-00287145

https://hal.science/hal-00287145v1

Submitted on 21 Apr 2020

HAL is a multi-disciplinary open access archive for the deposit and dissemination of scientific research documents, whether they are published or not. The documents may come from teaching and research institutions in France or abroad, or from public or private research centers.

L'archive ouverte pluridisciplinaire **HAL**, est destinée au dépôt et à la diffusion de documents scientifiques de niveau recherche, publiés ou non, émanant des établissements d'enseignement et de recherche français ou étrangers, des laboratoires publics ou privés.

5

Observations: Oceanic Climate Change and Sea Level

Coordinating Lead Authors:

Nathaniel L. Bindoff (Australia), Jürgen Willebrand (Germany)

Lead Authors:

Vincenzo Artale (Italy), Anny Cazenave (France), Jonathan M. Gregory (UK), Sergey Gulev (Russian Federation), Kimio Hanawa (Japan), Corrine Le Quéré (UK, France, Canada), Sydney Levitus (USA), Yukihiro Nojiri (Japan), C.K. Shum (USA), Lynne D. Talley (USA), Alakkat S. Unnikrishnan (India)

Contributing Authors:

J. Antonov (USA, Russian Federation), N.R. Bates (Bermuda), T. Boyer (USA), D. Chambers (USA), B. Chao (USA), J. Church (Australia), R. Curry (USA), S. Emerson (USA), R. Feely (USA), H. Garcia (USA), M. González-Davíla (Spain), N. Gruber (USA, Switzerland), S. Josey (UK), T. Joyce (USA), K. Kim (Republic of Korea), B. King (UK), A. Koertzinger (Germany), K. Lambeck (Australia), K. Laval (France), N. Lefevre (France), E. Leuliette (USA), R. Marsh (UK), C. Mauritzen (Norway), M. McPhaden (USA), C. Millot (France), C. Milly (USA), R. Molinari (USA), R.S. Nerem (USA), T. Ono (Japan), M. Pahlow (Canada), T.-H. Peng (USA), A. Proshutinsky (USA), B. Qiu (USA), D. Quadfasel (Germany), S. Rahmstorf (Germany), S. Rintoul (Australia), M. Rixen (NATO, Belgium), P. Rizzoli (USA, Italy), C. Sabine (USA), D. Sahagian (USA), F. Schott (Germany), Y. Song (USA), D. Stammer (Germany), T. Suga (Japan), C. Sweeney (USA), M. Tamisiea (USA), M. Tsimplis (UK, Greece), R. Wanninkhof (USA), J. Willis (USA), A.P.S. Wong (USA, Australia), P. Woodworth (UK), I. Yashayaev (Canada), I. Yasuda (Japan)

Review Editors:

Laurent Labeyrie (France), David Wratt (New Zealand)

This chapter should be cited as:

Bindoff, N.L., J. Willebrand, V. Artale, A, Cazenave, J. Gregory, S. Gulev, K. Hanawa, C. Le Quéré, S. Levitus, Y. Nojiri, C.K. Shum, L.D. Talley and A. Unnikrishnan, 2007: Observations: Oceanic Climate Change and Sea Level. In: *Climate Change 2007: The Physical Science Basis. Contribution of Working Group I to the Fourth Assessment Report of the Intergovernmental Panel on Climate Change* [Solomon, S., D. Qin, M. Manning, Z. Chen, M. Marquis, K.B. Averyt, M. Tignor and H.L. Miller (eds.)]. Cambridge University Press, Cambridge, United Kingdom and New York, NY, USA.

Executive Summary

- The oceans are warming. Over the period 1961 to 2003, global ocean temperature has risen by 0.10°C from the surface to a depth of 700 m. Consistent with the Third Assessment Report (TAR), global ocean heat content (0–3,000 m) has increased during the same period, equivalent to absorbing energy at a rate of 0.21 ± 0.04 W m^{-2} globally averaged over the Earth's surface. Two-thirds of this energy is absorbed between the surface and a depth of 700 m. Global ocean heat content observations show considerable interannual and inter-decadal variability superimposed on the longer-term trend. Relative to 1961 to 2003, the period 1993 to 2003 has high rates of warming but since 2003 there has been some cooling.

- Large-scale, coherent trends of salinity are observed for 1955 to 1998, and are characterised by a global freshening in subpolar latitudes and a salinification of shallower parts of the tropical and subtropical oceans. Freshening is pronounced in the Pacific while increasing salinities prevail over most of Atlantic and Indian Oceans. These trends are consistent with changes in precipitation and inferred larger water transport in the atmosphere from low latitudes to high latitudes and from the Atlantic to the Pacific. Observations do not allow for a reliable estimate of the global average change in salinity in the oceans.

- Key oceanic water masses are changing; however, there is no clear evidence for ocean circulation changes. Southern Ocean mode waters and Upper Circumpolar Deep Waters have warmed from the 1960s to about 2000. A similar but weaker pattern of warming in the Gulf Stream and Kuroshio mode waters in the North Atlantic and North Pacific has been observed. Long-term cooling is observed in the North Atlantic subpolar gyre and in the central North Pacific. Since 1995, the upper North Atlantic subpolar gyre has been warming and becoming more saline. It is *very likely* that up to the end of the 20th century, the Atlantic meridional overturning circulation has been changing significantly at interannual to decadal time scales. Over the last 50 years, no coherent evidence for a trend in the strength of the meridional overturning circulation has been found.

- Ocean biogeochemistry is changing. The total inorganic carbon content of the oceans has increased by 118 ± 19 GtC between the end of the pre-industrial period (about 1750) and 1994 and continues to increase. It is *more likely than not* that the fraction of emitted carbon dioxide that was taken up by the oceans has decreased, from 42 ± 7% during 1750 to 1994 to 37 ± 7% during 1980 to 2005. This would be consistent with the expected rate at which the oceans can absorb carbon, but the uncertainty in this estimate does not allow firm conclusions. The increase in total inorganic carbon caused a decrease in the depth at which calcium carbonate dissolves, and also caused a decrease in surface ocean pH by an average of 0.1 units since 1750. Direct observations of pH at available time series stations for the last 20 years also show trends of decreasing pH at a rate of 0.02 pH units per decade. There is evidence for decreased oxygen concentrations, likely driven by reduced rates of water renewal, in the thermocline (~100–1,000 m) in most ocean basins from the early 1970s to the late 1990s.

- Global mean sea level has been rising. From 1961 to 2003, the average rate of sea level rise was 1.8 ± 0.5 mm yr^{-1}. For the 20th century, the average rate was 1.7 ± 0.5 mm yr^{-1}, consistent with the TAR estimate of 1 to 2 mm yr^{-1}. There is *high confidence* that the rate of sea level rise has increased between the mid-19th and the mid-20th centuries. Sea level change is highly non-uniform spatially, and in some regions, rates are up to several times the global mean rise, while in other regions sea level is falling. There is evidence for an increase in the occurrence of extreme high water worldwide related to storm surges, and variations in extremes during this period are related to the rise in mean sea level and variations in regional climate.

- The rise in global mean sea level is accompanied by considerable decadal variability. For the period 1993 to 2003, the rate of sea level rise is estimated from observations with satellite altimetry as 3.1 ± 0.7 mm yr^{-1}, significantly higher than the average rate. The tide gauge record indicates that similar large rates have occurred in previous 10-year periods since 1950. It is unknown whether the higher rate in 1993 to 2003 is due to decadal variability or an increase in the longer-term trend.

- There are uncertainties in the estimates of the contributions to sea level change but understanding has significantly improved for recent periods. For the period 1961 to 2003, the average contribution of thermal expansion to sea level rise was 0.4 ± 0.1 mm yr^{-1}. As reported in the TAR, it is *likely* that the sum of all known contributions for this period is smaller than the observed sea level rise, and therefore it is not possible to satisfactorily account for the processes causing sea level rise. However, for the period 1993 to 2003, for which the observing system is much better, the contributions from thermal expansion (1.6 ± 0.5 mm yr^{-1}) and loss of mass from glaciers, ice caps and the Greenland and Antarctic Ice Sheets together give 2.8 ± 0.7 mm yr^{-1}. For the latter period, the climate contributions constitute the main factors in the sea level budget, which is closed to within known errors.

- The patterns of observed changes in global ocean heat content and salinity, sea level, thermal expansion, water mass evolution and biogeochemical parameters described in this chapter are broadly consistent with the observed ocean surface changes and the known characteristics of the large-scale ocean circulation.

5.1 Introduction

The ocean has an important role in climate variability and change. The ocean's heat capacity is about 1,000 times larger than that of the atmosphere, and the oceans net heat uptake since 1960 is around 20 times greater than that of the atmosphere (Levitus et al., 2005a). This large amount of heat, which has been mainly stored in the upper layers of the ocean, plays a crucial role in climate change, in particular variations on seasonal to decadal time scales. The transport of heat and freshwater by ocean currents can have an important effect on regional climates, and the large-scale Meridional Overturning Circulation (MOC; also referred to as thermohaline circulation) influences the climate on a global scale (e.g., Vellinga and Wood, 2002). Life in the sea is dependent on the biogeochemical status of the ocean and is influenced by changes in the physical state and circulation. Changes in ocean biogeochemistry can directly feed back to the climate system, for example, through changes in the uptake or release of radiatively active gases such as carbon dioxide. Changes in sea level are also important for human society, and are linked to changes in ocean circulation. Finally, oceanic parameters can be useful for detecting climate change, in particular temperature and salinity changes in the deeper layers and in different regions where the short-term variability is smaller and the signal-to-noise ratio is higher.

The large-scale, three-dimensional ocean circulation and the formation of water masses that ventilate the main thermocline together create pathways for the transport of heat, freshwater and dissolved gases such as carbon dioxide from the surface ocean into the density-stratified deeper ocean, thereby isolating them from further interaction with the atmosphere. These pathways are also important for the transport of anomalies in these parameters caused by changes in the surface conditions. Furthermore, changes in the storage of heat and in the distribution of ocean salinity cause the ocean to expand or contract and hence change the sea level both regionally and globally.

The ocean varies over a broad range of time scales, from seasonal (e.g., in the surface mixed layer) to decadal (e.g., circulation in the main subtropical gyres) to centennial and longer (associated with the MOC). The main modes of climate variability, which are described in Chapter 3, are the El Niño-Southern Oscillation (ENSO), the Pacific Decadal Oscillation (PDO), the Northern Annular Mode (NAM), which is related to the North Atlantic Oscillation (NAO), and the Southern Annular Mode (SAM). Forcing of the oceans is often related to these modes, which cause changes in ocean circulation through changed patterns of winds and changes in surface ocean density.

The Third Assessment Report (TAR) discussed some aspects of the ocean's role. Folland et al. (2001) concluded that the global ocean has significantly warmed since the late 1950's. This assessment provides updated estimates of temperature changes for the oceans. Furthermore, it discusses new evidence for changes in the ocean freshwater budget and the ocean circulation. The TAR estimate of the total inorganic carbon increase in the ocean (Prentice et al., 2001) was based entirely on indirect evidence. This assessment provides updated indirect estimates and reports on new and direct evidence for changes in total carbon increase and for changes in ocean biogeochemistry (including pH and oxygen). Church et al. (2001) determined a range of 1 to 2 mm yr^{-1} for the observed global average sea level rise in the 20th century. This assessment provides new estimates for sea level change and the climate-related contributions to sea level change from thermal expansion and melting of ice sheets, glaciers and ice caps. The focus of this chapter is on observed changes in the global ocean basins, however some regional changes in the ocean state are also considered.

Many ocean observations are poorly sampled in space and time, and regional distributions often are quite heterogeneous. Furthermore, the observational records only cover a relatively short period of time (e.g., the 1950s to the present). Many of the observed changes have significant decadal variability associated with them, and in some cases decadal variability and/or poor sampling may prevent detection of long-term trends. When time series of oceanic parameters are considered, linear trends are often computed in order to quantify the observed long-term changes; however, this does not imply that the original signal is best represented by a linear increase in time. For plotting time series, this chapter generally uses the difference (anomaly) from the average value for the years 1961 to 1990. Wherever possible, error bars are provided to quantify the uncertainty of the observations. As in other parts of this report, 90% confidence intervals are used throughout. If not otherwise stated, values with error bars given as $x \pm e$ should hence be interpreted as a 90% chance that the true value is in the range $x - e$ to $x + e$.

5.2 Changes in Global-Scale Temperature and Salinity

5.2.1 Background

Among the major challenges in understanding the climate system are quantifying the Earth's heat balance and the freshwater balance (hydrological cycle), which both have a substantial contribution from the World Ocean. This chapter presents observational evidence that directly or indirectly helps to quantify changes in these balances.

The TAR included estimates of ocean heat content changes for the upper 3,000 m of the World Ocean. Ocean heat content change is closely proportional to the average temperature change in a volume of seawater, and is defined here as the deviation from a reference period. This section reports on updates of this estimate and presents estimates for the upper 700 m based on additional modern and historical data (Willis et al., 2004; Levitus et al., 2005b; Ishii et al., 2006). The section also presents new estimates of the temporal variability of salinity. The data used for temperature and heat content estimates are based on the World Ocean Database 2001 (e.g., Boyer et al.,

2002; Conkright et al., 2002), which has been updated with more recent data. Temperature data include measurements from reversing thermometers, expendable bathythermographs, mechanical bathythermographs, conductivity-temperature-depth instruments, Argo profiling floats, moored buoys and drifting buoys. The salinity data are described by Locarnini et al. (2002) and Stephens et al. (2002).

5.2.2 Ocean Heat Content

5.2.2.1 Long-Term Temperature Changes

Figure 5.1 shows two time series of ocean heat content for the 0 to 700 m layer of the World Ocean, updated from Ishi et al. (2006) and Levitus et al. (2005a) for 1955 to 2005, and a time series for 0 to 750 m for 1993 to 2005 updated from Willis et al. (2004). Approximately 7.9 million temperature profiles were used in constructing the two longer time series. The three heat content analyses cover different periods but where they overlap in time there is good agreement. The time series shows an overall trend of increasing heat content in the World Ocean with interannual and inter-decadal variations superimposed on this trend. The root mean square difference between the three data sets is 1.5×10^{22} J. These year-to-year differences, which are due to differences in quality control and data used, are small and now approaching the accuracies required to close the Earth's radiation budget (e.g., Carton et al., 2005). On longer time scales, the two longest time series (using independent criteria for selection, quality control, interpolation and analysis of similar data sets) show good agreement about long-term trends and also on decadal time scales.

For the period 1993 to 2003, the Levitus et al. (2005a) analysis has a linear global ocean trend of 0.42 ± 0.18 W m^{-2}, Willis et al. (2004) has a trend of 0.66 ± 0.18 W m^{-2} and Ishii et al. (2006) a trend of 0.33 ± 0.18 W m^{-2}. Overall, we assess the trend for this period as 0.5 ± 0.18 W m^{-2}. For the 0 to 700 m layer and the period 1955 to 2003 the heat content change is $10.9 \pm 3.1 \times 10^{22}$ J or 0.14 ± 0.04 W m^{-2} (data from Levitus et al., 2005a). All of these estimates are per unit area of Earth surface. Despite the fact that there are differences between these three ocean heat content estimates due to the data used, quality control applied, instrumental biases, temporal and spatial averaging and analysis methods (Appendix 5.A.1), they are consistent with each other giving a high degree of confidence for their use in climate change studies. The global increase in ocean heat content during the period 1993 to 2003 in two ocean models constrained by assimilating altimetric sea level and other observations (Carton et al., 2005; Köhl et al., 2006) is considerably larger than these observational estimates. We assess the heat content change from both of the long time series (0 to 700 m layer and the 1961 to 2003 period) to be $8.11 \pm 0.74 \times 10^{22}$ J, corresponding to an average warming of 0.1°C or 0.14 ± 0.04 W m^{-2}, and conclude that the available heat content estimates from 1961 to 2003 show a significant increasing trend in ocean heat content.

The data used in estimating the Levitus et al. (2005a) ocean temperature fields (for the above heat content estimates) do not include sea surface temperature (SST) observations,

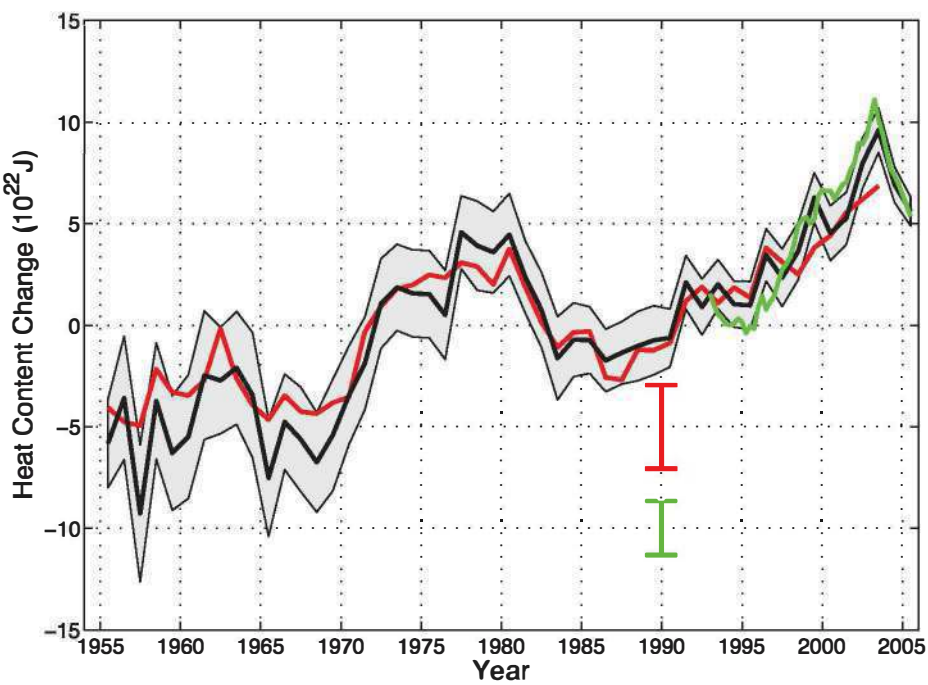

Figure 5.1. *Time series of global annual ocean heat content (10^{22} J) for the 0 to 700 m layer. The black curve is updated from Levitus et al. (2005a), with the shading representing the 90% confidence interval. The red and green curves are updates of the analyses by Ishii et al. (2006) and Willis et al. (2004, over 0 to 750 m) respectively, with the error bars denoting the 90% confidence interval. The black and red curves denote the deviation from the 1961 to 1990 average and the shorter green curve denotes the deviation from the average of the black curve for the period 1993 to 2003.*

which are discussed in Chapter 3. However, comparison of the global, annual mean time series of near-surface temperature (approximately 0 to 5 m depth) from this analysis and the corresponding SST series based on a subset of the International Comprehensive Ocean-Atmosphere Data Set (ICOADS) database (approximately 134 million SST observations; Smith and Reynolds, 2003 and additional data) shows a high correlation (r = 0.96) for the period 1955 to 2005. The consistency between these two data sets gives confidence in the ocean temperature data set used for estimating depth-integrated heat content, and supports the trends in SST reported in Chapter 3.

There is a contribution to the global heat content integral from depths greater than 700 m as documented by Levitus et al. (2000; 2005a). However, due to the lack of data with increasing depth the data must be composited using five-year running pentads in order to have enough data for a meaningful analysis in the deep ocean. Even then, there are not enough deep ocean data to extend the time series for the upper 3,000 m past the 1994–1998 pentad. There is a close correlation between the 0 to 700 and 0 to 3,000 m time series of Levitus et al. (2005a). A comparison of the linear trends from these two series indicates that about 69% of the increase in ocean heat content during 1955 to 1998 (the period when estimates from both time series are available) occurred in the upper 700 m of the World Ocean. Based on the linear trend, for the 0 to 3,000 m layer for the period 1961 to 2003 there has been an increase of ocean heat content of approximately $14.2 \pm 2.4 \times 10^{22}$ J, corresponding to a global ocean volume mean temperature increase of 0.037°C during this period. This increase in ocean heat content corresponds to an average heating rate of 0.21 ± 0.04 W m^{-2} for the Earth's surface.

The geographical distribution of the linear trend of 0 to 700 m heat content for 1955 to 2003 for the World Ocean is shown in Figure 5.2. These trends are non-uniform in space, with some regions showing cooling and others warming. Most of the Atlantic Ocean exhibits warming with a major exception being the subarctic gyre. The Atlantic Ocean accounts for approximately half of the global linear trend of ocean heat content (Levitus et al., 2005a). Much of the Indian Ocean has warmed since 1955 with a major exception being the 5°S to 20°S latitude belt. The Southern Ocean (south of 35°S) in the Atlantic, Indian and Pacific sectors has generally warmed. The Pacific Ocean is characterised by warming with major exceptions along 40°N and the western tropical Pacific.

Figure 5.3 shows the linear trends (1955 to 2003) of zonally averaged temperature anomalies (0 to 1,500 m) for the World Ocean and individual basins based on yearly anomaly fields (Levitus et al., 2005a). The strongest trends in these anomalies are concentrated in the upper ocean. Warming occurs at most latitudes in all three of the ocean basins. The regions that exhibit cooling are mainly in the shallow equatorial areas and in some high-latitude regions. In the Indian Ocean, cooling occurs at subsurface depths centred on 12°S at 150 m depth and in the Pacific centred on the equator and 150 m depth. Cooling also occured in the 32°N to 48°N region of the Pacific Ocean and the 49°N to 60°N region of the Atlantic Ocean. Regional temperature changes are discussed further in Section 5.3.

5.2.2.2 Variability of Heat Content

A major feature of Figure 5.1 is the relatively large increase in global ocean heat content during 1969 to 1980 and a sharp

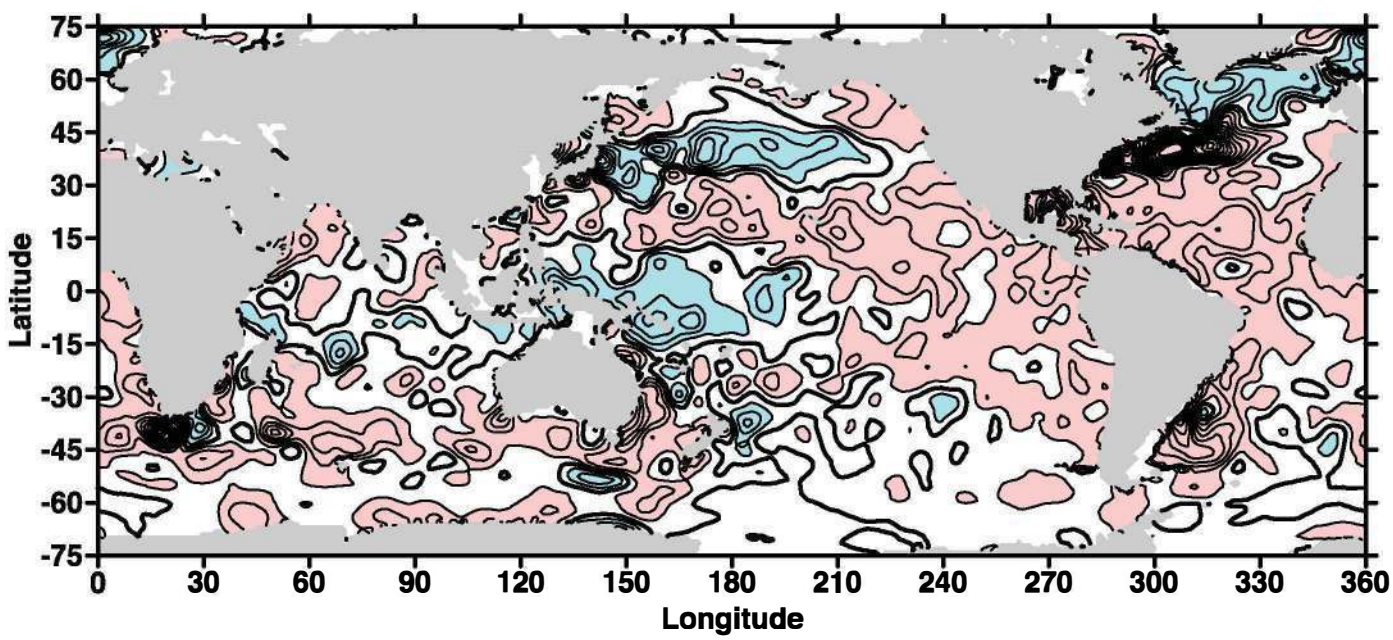

Figure 5.2. *Linear trends (1955–2003) of change in ocean heat content per unit surface area (W m^{-2}) for the 0 to 700 m layer, based on the work of Levitus et al. (2005a). The linear trend is computed at each grid point using a least squares fit to the time series at each grid point. The contour interval is 0.25 W m^{-2}. Red shading indicates values equal to or greater than 0.25 W m^{-2} and blue shading indicates values equal to or less than –0.25 W m^{-2}.*

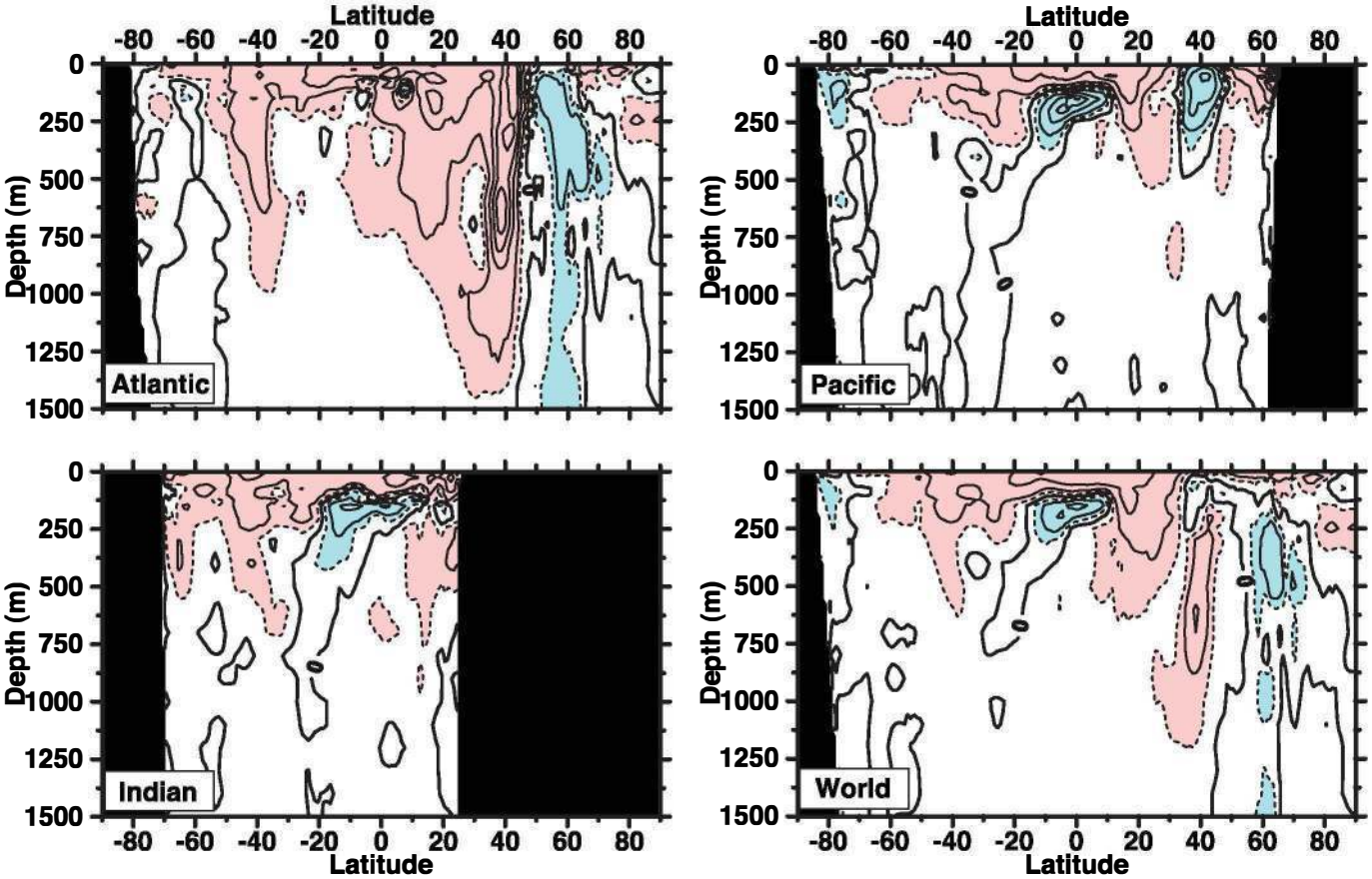

Figure 5.3. *Linear trend (1955–2003) of zonally averaged temperature in the upper 1,500 m of the water column of the Atlantic, Pacific, Indian and World Oceans. The contour interval is 0.05°C per decade, and the dark solid line is the zero contour. Red shading indicates values equal to or greater than 0.025°C per decade and blue shading indicates values equal to or less than –0.025°C per decade. Based on the work of Levitus et al. (2005a).*

decrease during 1980 to 1983. The 0 to 700 m layer cooled at a rate of 1.2 W m^{-2} during this period. Most of this cooling occurred in the Pacific Ocean and may have been associated with the reversal in polarity of the PDO (Stephens et al., 2001; Levitus et al., 2005c, see also Section 3.6.3). Examination of the geographical distribution of the differences in 0 to 700 m heat content between the 1977–1981 and 1965–1969 pentads and the 1986–1990 and 1977–1981 pentads shows that the pattern of heat content change has spatial scales of entire ocean basins and is also found in similar analyses by Ishii et al. (2006). The Pacific Ocean dominates the decadal variations of global heat content during these two periods. The origin of this variability is not well understood.

Based on model experiments, it has been suggested that errors resulting from the highly inhomogeneous distribution of ocean observations in space and time (see Appendix 5.A.1) could lead to spurious variability in the analysis (e.g., Gregory et al., 2004, AchutaRao et al., 2006). As discussed in the appendix, even in periods with overall good coverage in the observing system, large regions in Southern Hemisphere (SH) are not well sampled, and their contribution to global heat content variability is less certain. However, the large-scale nature of heat content variability, the similarity of the Levitus et al. (2005a) and the Ishii et al. (2006) analyses and new results showing a decrease in the global heat content in a period with much better data coverage (Lyman et al., 2006), gives confidence that there is substantial inter-decadal variability in global ocean heat content.

5.2.2.3 Implications for Earth's Heat Balance

To place the changes of ocean heat content in perspective, Figure 5.4 provides updated estimates of the change in heat content of various components of the Earth's climate system for the period 1961 to 2003 (Levitus et al., 2005a). This includes changes in heat content of the lithosphere (Beltrami et al., 2002), the atmosphere (e.g., Trenberth et al., 2001) and the total heat of fusion due to melting of i) glaciers, ice caps and the Antarctic and Greenland Ice Sheets (see Chapter 4) and ii) arctic sea ice (Hilmer and Lemke, 2000). The increase in ocean heat content is much larger than any other store of energy in the Earth's heat balance over the two periods 1961 to 2003 and 1993 to 2003, and accounts for more than 90% of the possible increase in heat content of the Earth system during these periods. Ocean heat content variability is thus a critical variable for detecting the effects of the observed increase in greenhouse gases in the Earth's atmosphere and for resolving the Earth's overall energy balance. It is noteworthy that whereas ice melt from glaciers, ice caps and ice sheets is very important in the sea level budget

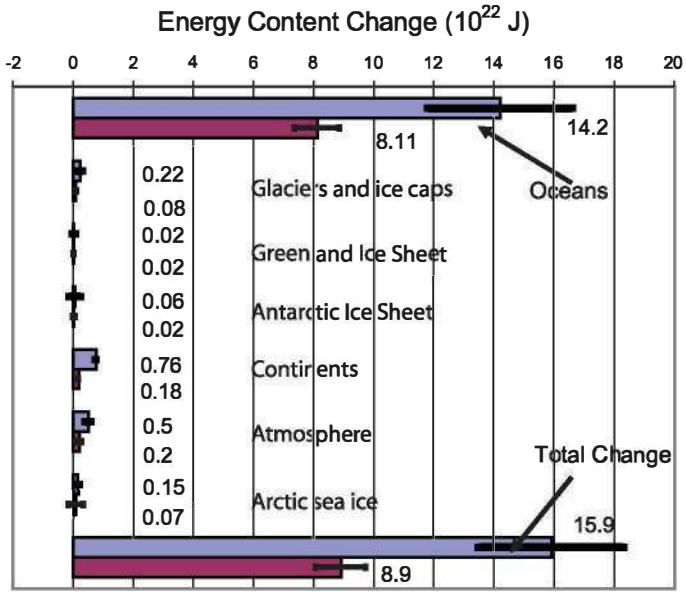

Figure 5.4. *Energy content changes in different components of the Earth system for two periods (1961–2003 and 1993–2003). Blue bars are for 1961 to 2003, burgundy bars for 1993 to 2003. The ocean heat content change is from this section and Levitus et al. (2005c); glaciers, ice caps and Greenland and Antarctic Ice Sheets from Chapter 4; continental heat content from Beltrami et al. (2002); atmospheric energy content based on Trenberth et al. (2001); and arctic sea ice release from Hilmer and Lemke (2000). Positive energy content change means an increase in stored energy (i.e., heat content in oceans, latent heat from reduced ice or sea ice volumes, heat content in the continents excluding latent heat from permafrost changes, and latent and sensible heat and potential and kinetic energy in the atmosphere). All error estimates are 90% confidence intervals. No estimate of confidence is available for the continental heat gain. Some of the results have been scaled from published results for the two respective periods. Ocean heat content change for the period 1961 to 2003 is for the 0 to 3,000 m layer. The period 1993 to 2003 is for the 0 to 700 m (or 750 m) layer and is computed as an average of the trends from Ishii et al. (2006), Levitus et al. (2005a) and Willis et al. (2004).*

(contributing about 40%), the energy associated with ice melt contributes only about 1% to the Earth's energy budget.

5.2.3 Ocean Salinity

Ocean salinity changes are an indirect but potentially sensitive indicator for detecting changes in precipitation, evaporation, river runoff and ice melt. The patterns of salinity change can be used to infer changes in the Earth's hydrological cycle over the oceans (Wong et al., 1999; Curry et al., 2003) and are an important complement to atmospheric measurements. Figure 5.5 shows the linear trends (based on pentadal anomaly fields) of zonally averaged salinity in the upper 500 m of the World Ocean and individual ocean basins (Boyer et al., 2005) from 1955 to 1998. A total of 2.3 million salinity profiles were used in this analysis, about one-third of the amount of data used in the ocean heat content estimates in Section 5.2.2.

Estimates of changes in the freshwater content of the global ocean have suggested that the global ocean is freshening (e.g., Antonov et al., 2002), however, sampling limitations due to data sparsity in some regions, particularly the SH, means that such estimates have an uncertainty that is not possible to quantify.

Between 15°S and 42°N in the Atlantic Ocean there is a salinity increase in the upper 500 m layer. This region includes the North Atlantic subtropical gyre. In the 42°N to 72°N region, including the Labrador, Irminger and Icelandic Seas, there is a freshening trend (discussed further in Section 5.3). The increase in salinity north of 72°N (Arctic Ocean) is highly uncertain because of the paucity of data in this region.

South of 50°S in the polar region of the Southern Ocean, there is a relatively weak freshening signal. Freshening occurs throughout most of the Pacific with the exception of the South Pacific subtropical gyre between 8°S and 32°S and above 300 m where there is an increase in salinity. The near-surface Indian Ocean is characterised mainly by increasing salinity. However, in the latitude band 5°S to 42°S (South Indian gyre) in the depth range of 200 to 1,000 m, there is a freshening of the water column.

The results shown here document that ocean salinity and hence freshwater are changing on gyre and basin scales, with the near-surface waters in the more evaporative regions increasing in salinity in almost all ocean basins. In the high-latitude regions in both hemispheres the surface waters are freshening consistent with these regions having greater precipitation, although higher runoff, ice melting, advection and changes in the MOC (Häkkinen, 2002) may also contribute. In addition to these meridional changes, the Atlantic is becoming saltier over much of the water column (Figure 5.5 and Boyer et al., 2005). Although the South Pacific subtropical region is becoming saltier, on average the whole water column in the Pacific Basin is becoming fresher (Boyer et al., 2005). The increasing difference in volume-averaged salinity between the Atlantic and Pacific Oceans suggests changes in freshwater transport between these two ocean basins.

We are confident that vertically coherent gyre and basin scale changes have occurred in the salinity (freshwater content) of parts of the World Ocean during the past several decades. While the available data and their analyses are insufficient to identify in detail the origin of these changes, the patterns are consistent with a change in the Earth's hydrological cycle, in particular with changes in precipitation and inferred larger water transport in the atmosphere from low latitudes to high latitudes and from the Atlantic to the Pacific (see Section 3.3.2).

5.2.4 Air-Sea Fluxes and Meridional Transports

The global average changes in ocean heat content discussed above are driven by changes in the air-sea net energy flux (see Section 5.2.2.1). At regional scales, few estimates of heat flux changes have been possible. During the last 50 years, net heat fluxes from the ocean to the atmosphere demonstrate locally decreasing values (up to 1 W m^{-2} yr^{-1}) over the southern flank of the Gulf Stream and positive trends (up to 0.5 W m^{-2} yr^{-1}) in the Atlantic central subpolar regions (Gulev et al., 2006). At the global scale, the accuracy of the flux observations is insufficient to permit a direct assessment of changes in heat flux. Air-sea fluxes are discussed in Section 3.5.6.

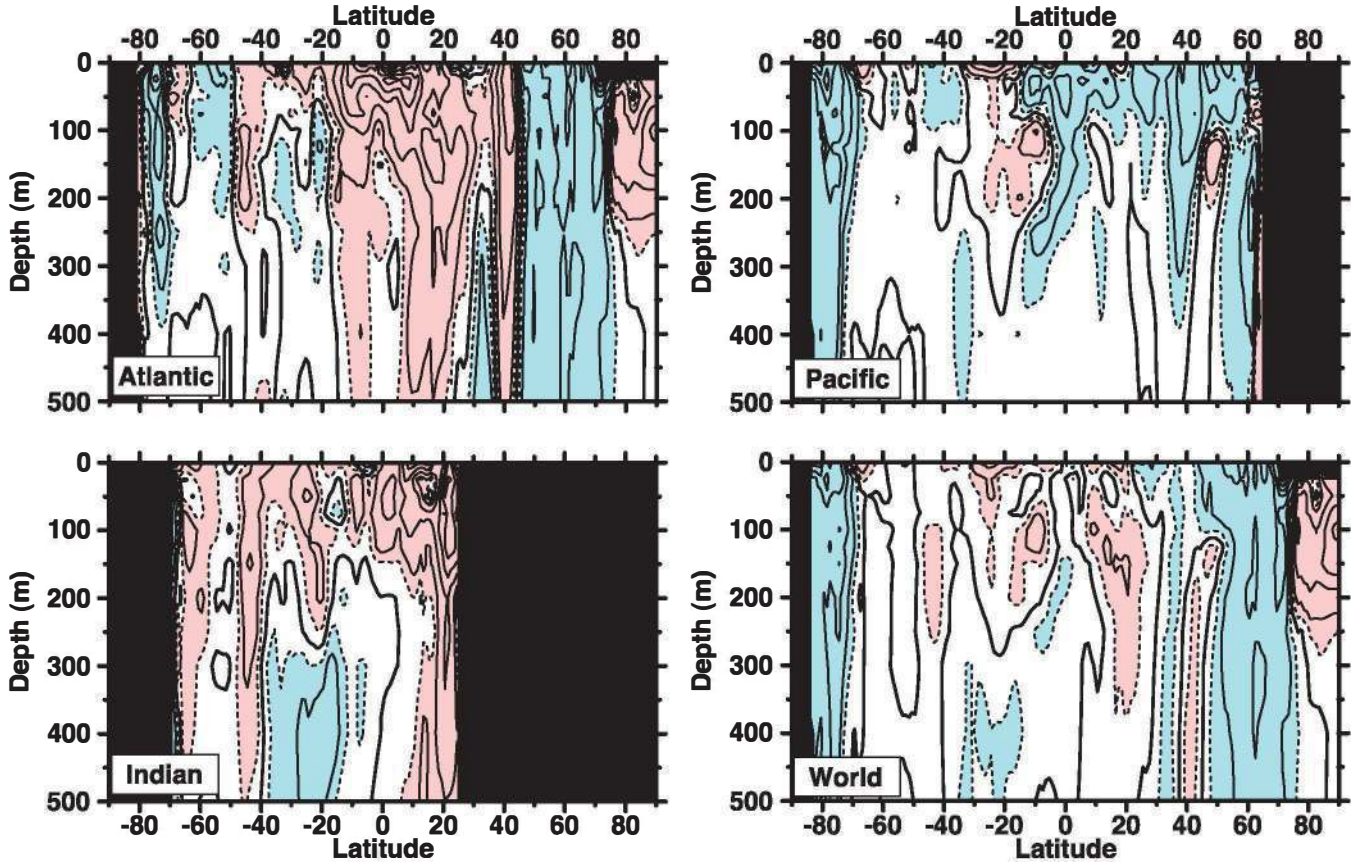

Figure 5.5: *Linear trends (1955–1998) of zonally averaged salinity (psu) in the upper 500 m of the Atlantic, Pacific, Indian and World Oceans. The contour interval is 0.01 psu per decade and dashed contours are ±0.005 psu per decade. The dark solid line is the zero contour. Red shading indicates values equal to or greater than 0.005 psu per decade and blue shading indicates values equal to or less than –0.005 psu per decade. Based on the work of Boyer et al. (2005).*

Estimates of the climatological mean oceanic meridional heat transport derived from atmospheric observations (e.g., Trenberth and Caron, 2001) and from oceanographic cross sections (e.g., Ganachaud and Wunsch, 2003) are in fair agreement, despite considerable uncertainties (see Appendix 5.A.2). The ocean heat transport estimate derived from integration of climatological air-sea heat flux fields (e.g., Grist and Josey, 2003) is in good agreement with an independent oceanographic cross section at 32°S. Estimates of changes in the Atlantic meridional heat transport are discussed in Section 5.3.2.

5.3 Regional Changes in Ocean Circulation and Water Masses

5.3.1 Introduction

Robust long-term trends in global- and basin-scale ocean heat content and basin-scale salinity were shown in Section 5.2. The observed heat and salinity trends are linked to changes in ocean circulation and other manifestations of global change such as oxygen and carbon system parameters (see Section 5.4). Global ocean changes result from regional changes in these properties, assessed in this section. Evidence for change in temperature, salinity and circulation is described globally and then for each of the major oceans. Two marginal seas with multi-decadal time series are also examined as examples of regional variations.

The upper ocean in all regions is close to the atmospheric forcing and has the largest variability; it is also the best sampled. For these reasons, Section 5.2 mainly assessed upper-ocean observations for long-term trends in heat content and salinity. However, there are important changes in heat and salinity at intermediate and abyssal depths, restricted to regions that are relatively close to the main sources of deep and intermediate waters. These sources are most vigorous in the northern North Atlantic and the Southern Ocean around Antarctica. This is illustrated well in salinity differences shown for the Atlantic (1985–1999 minus 1955–1969) and Pacific (1980s minus 1960s) in Figure 5.6. Striking changes in salinity are found from the surface to the bottom in the northern North Atlantic near water mass formation sites that fill the water colunm (Section 5.3.2); bottom changes elsewhere are small, being most prevalent at the under-sampled southern ends of both sections. At mid-depth (500 to 2,000 m), the Atlantic and southern end of the Pacific section show widespread change, but the North Pacific signal is weaker and shallower because it has only weak intermediate water formation (and no deep water formation). Changes in intermediate and deep waters can ultimately affect

the ocean's vertical stratification and overturning circulation; the topic of the overturning circulation in the North Atlantic is considered in Section 5.3.2.

The observed changes in salinity are of global scale, with similar patterns in different ocean basins (Figure 5.6). The subtropical waters have increased in salinity and the subpolar surface and intermediate waters have freshened in both the Atlantic and Pacific Oceans during the period from the 1960s to the 1990s and in both hemispheres in each ocean. The waters that underlie the near-surface subtropical waters have freshened due to equatorward circulation of the freshened subpolar surface waters; in particular, the fresh intermediate water layer (at ~1,000 m) in the SH has freshened in both the Atlantic and Pacific Oceans. In the Northern Hemisphere (NH), the Pacific intermediate waters have freshened, and the underlying deep waters did not change, consistent with no local bottom water source in the North Pacific. In the central North Atlantic, the intermediate layer (approximately 900–1,200 m) became saltier due to increased salinity in the outflow from the Mediterranean that feeds this layer.

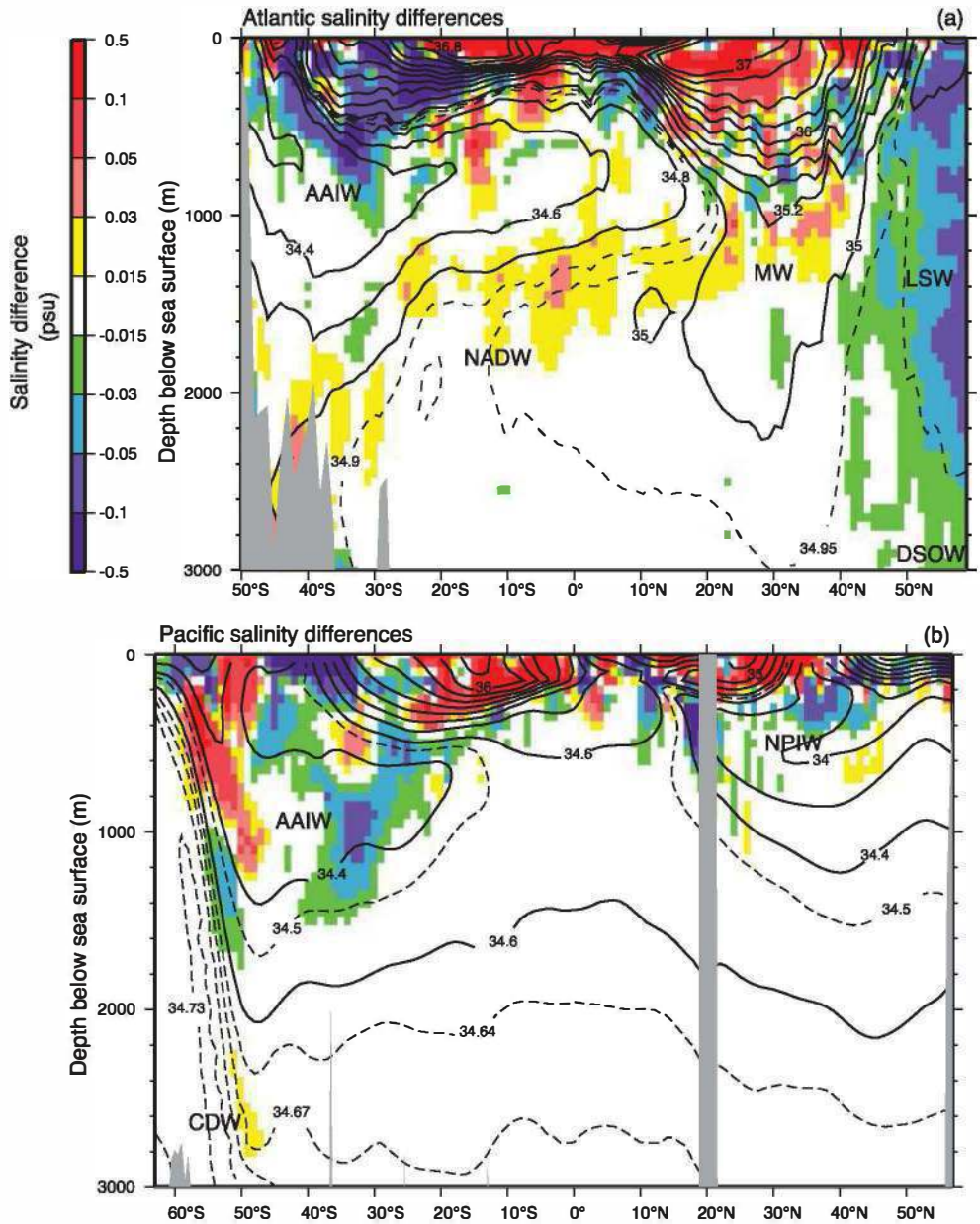

Figure 5.6. *Meridional sections of differences in salinity (psu) of the a) Atlantic Ocean for the period 1985 to 1999 minus 1955 to 1969 and b) Pacific Ocean for the World Ocean Circulation Experiment (WOCE) 150°W section (1991–1992) and historical data from 1968 plus or minus 7.5 years. Contours are the mean salinity fields along each section and show the key features. The salinity differences are differences along isopycnals that have been mapped to pressure surfaces. The Atlantic section is along the western side of the Atlantic Ocean and the Pacific section is along 150°W. The two figures are redrafted from Curry et al. (2003) and Wong et al (2001). Water masses shown include Antarctic Intermediate Water (AAIW), Circumpolar Deep Water (CDW), North Atlantic Deep Water (NADW), Mediterranean Water (MW), Labrador Sea Water (LSW), Denmark Strait Overflow Water (DSOW) and North Pacific Intermediate Water NPIW). The areas shaded in grey represent the seafloor and oceanic crust.*

5.3.2 Atlantic and Arctic Oceans

The North Atlantic Ocean has a special role in long-term climate assessment because it is central to one of the two global-scale MOCs (see Box 5.1), the other location being the Southern Ocean. The long-term trends in depth-integrated Atlantic heat content for the period 1955 to 2003 (Figure 5.2) are broadly consistent with the warming tendencies identified from the global analyses of SST (see Section 3.2.2.3). The subtropical gyre warmed and the subpolar gyre cooled over that period, consistent with a predominantly positive phase of the NAO during the last several decades. The warming extended down to below 1,000 m, deeper than anywhere else in the World Ocean (Figure 5.3 Atlantic), and was particularly pronounced under the Gulf Stream and North Atlantic Current near 40°N. Long-term trends in salinity towards freshening in the subpolar regions and increased salinity in the subtropics through the mid-1990s (Figure 5.5 Atlantic and Figure 5.6a) are consistent with the global tendencies for freshening of relatively fresher regions and increased salinity in saltier regions (Section 5.2.3).

5.3.2.1 *North Atlantic Subpolar Gyre, Labrador Sea and Nordic Seas*

In the North Atlantic subpolar gyre, Labrador Sea and Nordic Seas, large salinity changes have been observed that have been associated with changed inputs of fresh water (ice melt, ocean circulation and river runoff) and with the NAO. Advection of these surface and deep salinity anomalies has been traced around the whole subpolar gyre including the Labrador and Nordic Seas. These anomalies are often called 'Great Salinity Anomalies' (GSAs; e.g., Dickson et al., 1988; Belkin, 2004). During a positive phase of the NAO, the subpolar gyre strengthens and expands towards the east, resulting in lower surface salinity in the central subpolar region (Levitus, 1989; Reverdin et al., 1997; Bersch, 2002). Three GSAs have been thoroughly documented: one from 1968 to 1978, one in the 1980s and one in the 1990s. Observational and modelling studies show that the relative influence of local events and advection differ between different GSA events and regions (Houghton and Visbeck, 2002; Josey and Marsh, 2005).

These surface salinity anomalies have affected the Labrador Sea and the production of Labrador Sea Water (LSW), a major component of the North Atlantic Deep Water (NADW) and contributor to the lower limb of the MOC. The LSW appears to alternate between dense, cold types and less dense, warm types (Yashayaev et al., 2003; Kieke et al., 2006) possibly with more production of dense LSW during years of positive-phase NAO (Dickson et al., 1996). Since 1965 to 1970, the LSW has had a significant freshening trend with a superimposed variability consisting of three saltier periods, coinciding with warmer water, and two freshening and cooling periods in the 1970s and 1990s (Figure 5.7). During the period 1988 to 1994, an exceptionally large volume of cold, fresh and dense LSW was produced (Sy et al., 1997; Lazier et al., 2002), unprecedented in the sparse time series that extends back to the 1930s (Talley and McCartney, 1982). The Labrador Sea has now returned to a warmer, more saline state; most of the excess volume of the dense LSW has disappeared, the mid-layers became warmer and saltier, and the production of LSW shifted to the warmer type (e.g., Lazier et al., 2002; Yashayaev et al., 2003; Stramma et al., 2004). This warming and increased salinity and reduction in LSW was associated with the weakening of the North Atlantic subpolar gyre, seen also in satellite altimetry data (Häkkinen and Rhines, 2004).

The eastern half of the subpolar North Atlantic also freshened through the 1980s and into the 1990s, but the upper ocean has been increasing in salinity or remaining steady since then, depending on location. About two-thirds of the freshening in this region has been attributed to an increase in precipitation associated with a climate pattern known as the East Atlantic Pattern (Josey and Marsh, 2005), with the NAO playing a secondary role. From 1965 to 1995, the subpolar freshening amounted to an equivalent freshwater layer of approximately 3 m spread evenly over its total area (Belkin, 2004; Curry and Mauritzen, 2005).

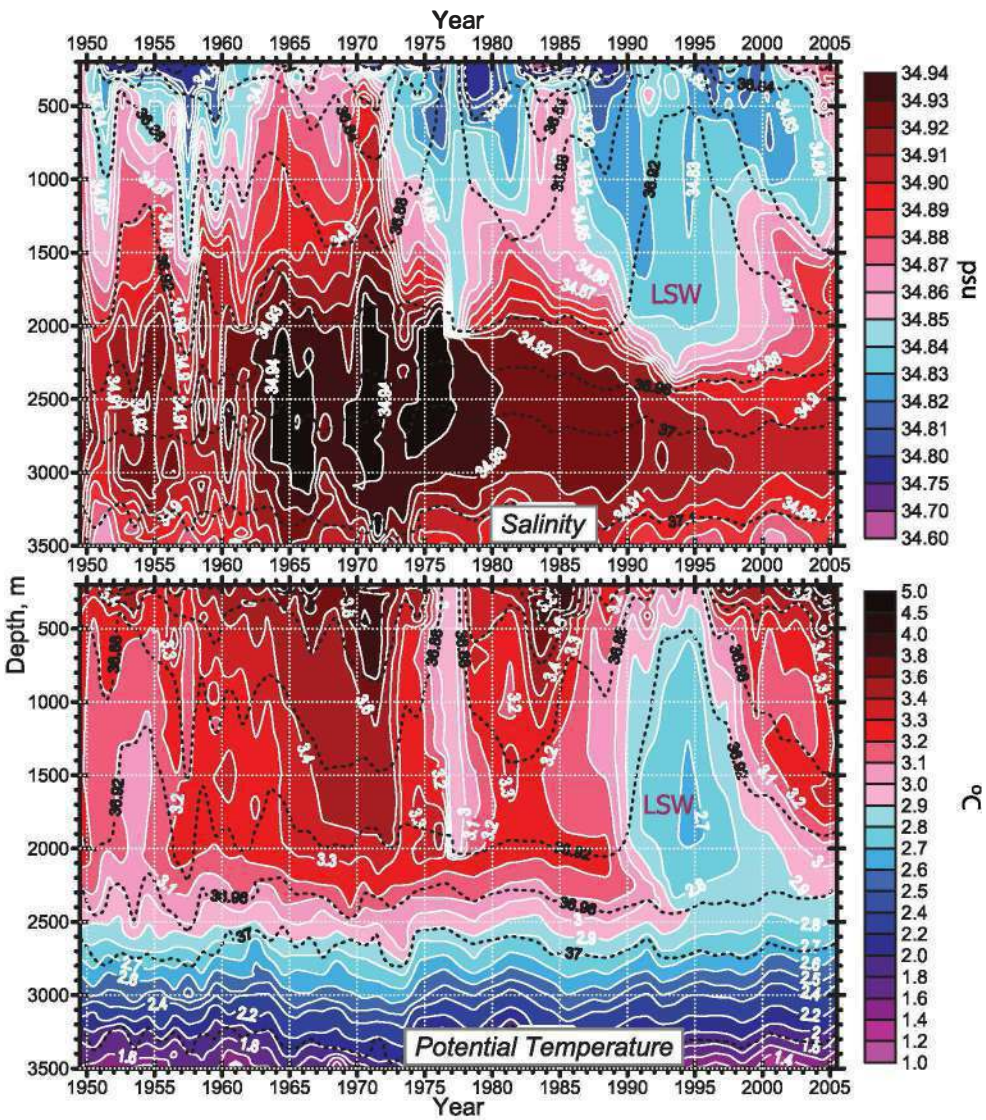

Figure 5.7. *The longest available time series of salinity (psu; upper panel) and potential temperature (°C, lower panel) in the central Labrador Sea from 1949 to 2005 (updated from Yashayaev et al., 2003). The dashed lines are contours of potential density (kg m^{-3}, difference from 1,000 kg m^{-3}) and are the same on both panels.*

Box 5.1: Has the Meridional Overturning Circulation in the Atlantic Changed?

The global Meridional Overturning Circulation consists primarily of dense waters that sink to the abyssal ocean at high latitudes in the North Atlantic Ocean and near Antarctica. These dense waters then spread across the equator with comparable flows of approximately 17 and 14 Sv (10^6 m^3 s^{-1}), respectively (Orsi et al., 2002; Talley et al., 2003a). The North Atlantic overturning circulation (henceforth 'MOC') is characterised by an inflow of warm, saline upper-ocean waters from the south that gradually increase in density from cooling as they move northward through the subtropical and subpolar gyres. They also freshen, which reduces the density increase. The inflows reach the Nordic Seas (Greenland, Iceland and Norwegian Seas) and the Labrador Sea, where they are subject to deep convection, sill overflows and vigorous mixing. Through these processes NADW is formed, constituting the southward-flowing lower limb of the MOC.

Climate models show that the Earth's climate system responds to changes in the MOC (e.g., Vellinga and Wood, 2002), and also suggest that the MOC might gradually decrease in transport in the 21st century as a consequence of anthropogenic warming and additional freshening in the North Atlantic (Bi et al., 2001; Gregory et al., 2005; see also Chapter 10). However, observations of changes in the MOC strength and variability are fragmentary; the best evidence for observational change comes from the North Atlantic.

There is evidence for a link between the MOC and abrupt changes in surface climate during the past 120 kyr, although the exact mechanism is not clear (Clark et al., 2002). At the end of the last glacial period, as the climate warmed and ice sheets melted, there were a number of abrupt oscillations, for example, the Younger Dryas and the 8.2 ka cold event (see Section 6.4), which may have been caused by changes in ocean circulation. The variability of the MOC during the Holocene after the 8.2 ka cooling event is clearly much smaller than during glacial times (Keigwin et al., 1994; see Section 6.4).

Observed changes in MOC transport, water properties and water mass formation are inconclusive about changes in the MOC strength (see Section 5.3.2.2). This is partially due to decadal variability and partially due to inadequate long-term observations. From repeated hydrographic sections in the subtropics, Bryden et al. (2005) concluded that the MOC transport at 25°N had decreased by 30% between 1957 and 2004, but the presence of significant unsampled variability in time and the lack of supporting direct current measurements reduces confidence in this estimate. Direct measurements of the two major sill overflows have shown considerable variability in the dominant Denmark Strait Overflow without enough years of coverage to discern long-term trends (Macrander et al., 2005). The observed freshening of the overflows and the associated reduction in density from 1965 to 2000 (see Section 5.3.2) has so far not led to a significant weakening of the MOC (Dickson et al., 2003; Curry and Mauritzen, 2005). Moreover, large decadal variability observed since 1960 in salinity and temperature of the surface waters, including the recent increase in salinity of the surface waters feeding the MOC, obscures the long-term trend (Hátún et al., 2005; ICES 2005) and hence conclusions about potential MOC changes.

Changes in the MOC can also be caused by changes in Labrador Sea convection, with strong convection corresponding to higher MOC. Convection was strong from the 1970s to 1995, but thereafter the Labrador Sea warmed and re-stratified (Lazier et al., 2002; Yashayaev et al., 2003) and convection has been weaker. Based on observed SST patterns, it was concluded that the MOC transport has increased by about 10% from 1970 to the 1990s (Knight et al., 2005; Latif et al., 2006). From direct current meter observations at the exit of the subpolar North Atlantic, Schott et al. (2004) concluded that the Deep Water outflow, while varying at shorter time scales, had no significant trend during the 1993 to 2001 period.

In summary, it is very likely that up to the end of the 20th century the MOC was changing significantly at interannual to decadal time scales. Given the above evidence from components of the MOC as well as uncertainties in the observational records, over the modern instrumental record no coherent evidence for a trend in the mean strength of the MOC has been found.

Subsurface salinity in the Nordic Seas has also decreased markedly since the 1970s (Dickson et al., 2003), directly affecting the salinity of the Nordic Sea overflow waters that contribute to NADW. This decrease in subsurface salinity was associated with lower salinity of the Atlantic waters entering the Nordic seas and related to the high NAO index and intensification of the subpolar gyre. Since 1994, the salinity of the inflow from the North Atlantic has been increasing, reaching the highest values since 1948, largely due to a weakening of the subpolar gyre circulation that allowed more warm water into the Nordic Seas, associated with a decreasing NAO index (Hátún et al., 2005).

The densest waters contributing to NADW and to the deep limb of the MOC arise as overflows from the upper 1,500 m of the Nordic Seas through the Denmark Strait and Faroe Channel. The marked freshening of the overflow water masses exiting the Arctic was associated with growing sea ice export from the Arctic and precipitation in the Nordic Seas (Dickson et al., 2002, 2003). The transports of the overflow waters, of which the largest component is through Denmark Strait, have varied by about 30% (Macrander et al., 2005), but there has been no clear trend in this location. Overall, the overflows that contribute to NADW from the Nordic Seas have remained constant to within the known variability.

The overall pattern of change in the North Atlantic subpolar gyre is one of a trend towards fresher values over most of the water colunm from the mid-1960s until the mid-1990s. Since then, there has been a return to warmer and more saline waters

(Figure 5.7), which coincides with the change in NAO and East Atlantic Pattern. However, this return to saltier waters has not been sustained for a long enough period to change the sign of the long-term trends (Figure 5.5 Atlantic).

5.3.2.2 Arctic Ocean

Climate change in the Arctic Ocean and Nordic Seas is closely linked to the North Atlantic subpolar gyre (Østerhus et al., 2005). Within the Arctic Ocean and Nordic Seas, surface temperature has increased since the mid-1980s and continues to increase (Comiso, 2003). In the Atlantic waters entering the Nordic Seas, a temperature increase in the late 1980s and early 1990s (Quadfasel et al., 1991; Carmack et al., 1995) has been associated with the transition in the 1980s towards more positive NAO states. Warm Atlantic waters have also been observed to enter the Arctic as pulses via Fram Strait and then along the slope to the Laptev Sea (Polyakov et al., 2005); the increased heat content and increased transport in the pulses both contribute to net warming of the arctic waters (Schauer et al., 2004). Multi-decadal variability in the temperature of the Atlantic Water core affecting the top 400 m in the Arctic Ocean has been documented (Polyakov et al., 2004). Within the Arctic, salinity increased in the upper layers of the Amundsen and Makarov Basins, while salinity of the upper layers in the Canada Basin decreased (Morison et al., 1998). Compared to the 1980s, the area of upper waters of Pacific origin has decreased (McLaughlin et al., 1996; Steele and Boyd, 1998).

During the 1990s, changed winds caused eastward redirection of river runoff from the Laptev Sea (Lena River, etc.), reducing the low-salinity surface layer in the central Arctic Ocean (Steele and Boyd, 1998), thus allowing greater convection and heat transport into the surface arctic layer from the more saline subsurface Atlantic layer. Thereafter, however, the stratification in the central Arctic (Amundsen Basin) increased and a low-salinity mixed layer was again observed at the North Pole in 2001, possibly due to a circulation change that restored the river water input (Björk et al., 2002). Circulation variability that shifts the balance of fresh and saline surface waters in the Arctic, with associated changes in sea ice, might be associated with the NAM (Proshutinsky and Johnson, 1997; Rigor et al., 2002), however, the long-term decline in arctic sea ice cover appears to be independent of the NAM (Comiso, 2002). While there is significant decadal variability in the Arctic Ocean, no systematic long-term trend in subsurface arctic waters has been identified.

5.3.2.3 Subtropical and Equatorial Atlantic

In the North Atlantic subtropical gyre, circulation, SST, the thickness of near-surface Subtropical Mode Water (STMW, Hanawa and Talley, 2001) and thermocline ventilation are all highly correlated with the NAO, with some time lags. A more positive NAO state, with westerlies shifted northwards, results in a decreased Florida Current transport (Baringer and Larsen, 2001), a likely delayed northward shift of the Gulf Stream position (Joyce et al., 2000; Seager et al., 2001; Molinari, 2004), and decreased subtropical eddy variability (Penduff et al., 2004). In the STMW, low thickness and production and higher temperature result from a high NAO index (e.g., Talley, 1996; e.g., Hazeleger and Drijfhout, 1998; Marsh, 2000). The volume of STMW is likely to lag changes in the NAO by two to three years, and low (high) volumes are associated with high (low) surface layer temperatures because of changes in both convective forcing and location of STMW formation. While quasi-cyclic variability in STMW renewal is apparent over the 1960 to 1980 period, the total volume of STMW has remained low through 2000 since a peak in 1983 to 1984, associated with a relatively persistent positive NAO phase during the late 1980s and early 1990s (Lazier et al., 2002; Kwon and Riser, 2004).

In the subtropics at depths of 1,000 to 2,000 m, the temperature has increased since the late 1950s at Bermuda, at 24°N, and at 52°W and 66°W in the Gulf Stream (Bryden et al., 1996; Joyce and Robbins, 1996; Joyce et al., 1999). These warming trends reflect reduced production of LSW (Lazier, 1995) and increased salinity and temperature of the waters from the Mediterranean (Roether et al., 1996; Potter and Lozier, 2004). After the mid-1990s at greater depths (1,500–2,500 m), temperature and salinity decreased, reversing the previous warming trend, most likely due to delayed appearance of the new colder and fresher Labrador Sea Water produced in the mid-1990s.

Intermediate water (800–1,200 m) in the mid-latitude eastern North Atlantic is strongly influenced by the saline Mediterranean Water (MW; Section 5.3.2.3). This saline layer joins the southward-flowing NADW and becomes part of it in the tropical Atlantic. This layer has warmed and become more saline since at least 1957 (Bryden et al., 1996), continuing during the last decade (1994–2003) at a rate of more than 0.2°C per decade with a rate of 0.4°C per decade at some levels (Vargas-Yáñez et al., 2004). In the Bay of Biscay (44°N; González-Pola et al., 2005) and at Gibraltar (Millot et al., 2006), similar warming was observed through the thermocline and into the core of the MW. From 1955 to 1993, the trend was about 0.1°C per decade in a zone west of Gibraltar (Potter and Lozier, 2004), and of almost the same magnitude even west of the mid-Atlantic Ridge (Curry et al., 2003).

Surface waters in the Southern Ocean, including the high-latitude South Atlantic, set the initial conditions for bottom water in the (SH). This extremely dense Antarctic Bottom Water (AABW), which is formed around the coast of Antarctica (see Section 5.3.5.2), spreads equatorward and enters the Brazil Basin through the narrow Vema Channel of the Rio Grande Rise at 31°S. Ongoing observations of the lowest bottom temperatures there have revealed a slow but consistent increase of the order 0.002°C yr^{-1} in the abyssal layer over the last 30 years (Hogg and Zenk, 1997).

In the tropical Atlantic, the surface water changes are partly associated with the variability of the marine Inter-tropical Convergence Zone, which has strong seasonal variability (Mitchell and Wallace, 1992; Biasutti et al., 2003; Stramma et al., 2003). Tropical Atlantic variability on interannual to decadal time scales can be influenced by a South Atlantic dipole in SST

(Venegas et al., 1998), associated with latent heat fluxes related to changes in the subtropical high (Sterl and Hazeleger, 2003). The South Equatorial Current provides a region for subduction of the water masses (Hazeleger et al., 2003) and may also maintain a propagation pathway for water mass anomalies towards the north (Lazar et al., 2002).

The North Atlantic Oscillation is an important driver of the oceanic water mass variations in the upper North Atlantic subtropical gyre. Its effects are also observed at depths greater than 1,500 m within the subtropical gyre consistent with the large-scale circulation and changes in source waters in the North Atlantic Ocean. While there are coherent changes in the long-term trends in temperature and salinity (Section 5.2), decadal variations are an important climate signal for this region.

5.3.2.4 Mediterranean Sea

Marked changes in thermohaline properties have been observed throughout the Mediterranean (Manca et al., 2002). In the western basin, the Western Mediterranean Deep Water (WMDW), formed in the Gulf of Lions, warmed during the last 50 years, interrupted by a short period of cooling in the early 1980s, the latter reflected in cooling of the Levantine Intermediate Water between the late 1970s and mid-1980s (Brankart and Pinardi, 2001). The WMDW warming is in agreement with recent atmospheric temperature changes over the Mediterranean (Luterbacher et al., 2004). The salt content of the WMDW has also been steadily increasing during the last 50 years, mainly attributed to decreasing precipitation over the region since the 1940s (Krahmann and Schott, 1998; Mariotti et al., 2002) and to anthropogenic reduction in the freshwater inflow (Rohling and Bryden, 1992). These changes in water properties and circulation are linked to the long-term variability of surface fluxes (Krahmann and Schott, 1998) with contributions from the NAO (Vignudelli et al., 1999) that produce consistent changes in surface heat fluxes and a net warming of the Mediterranean Sea (Rixen et al., 2005).

These changes in the temperature and salinity within the Mediterranean have affected the outflow of water into the North Atlantic at Gibraltar (see also Section 5.3.2.3). Part of this shift in Mediterranean outflow properties has been traced to the Eastern Mediterranean. During 1987 to 1991, the Eastern Mediterranean Deep Water became warmer and saltier due to the switch of its source water from the Adriatic to the Aegean (Klein et al., 2000; Gertman et al., 2006), most likely related to changes in the heat and freshwater flux anomalies in the Aegean Sea (Tsimplis and Rixen, 2002; Josey, 2003; Rupolo et al., 2003). This 1987 to 1991 switch of source waters has continued and increased its impact, with density of the westward outflow in Sicily Strait now denser (Gasparini et al., 2005). While there are strong natural variations in the Mediterranean, overall there is a discernible trend of increased salinity and warmer temperature in key water masses over the last 50 years and this signal is observable in the North Atlantic.

5.3.3 Pacific Ocean

The upper Pacific Ocean has been warming and freshening overall, as revealed in global heat and freshwater analyses (Section 5.2, Figure 5.5). The subtropical North and South Pacific have been warming. In the SH, the major warming footprint is associated with the thick mode waters north of the Antarctic Circumpolar Current. The North Pacific has cooled along 40°N. Long-term trends are rather difficult to discern in the upper Pacific Ocean because of the strong interannual and decadal variability (ENSO and the PDO) and the relatively short length of the observational records. Changes associated with ENSO are described in Section 3.6.2 and are not included here. Overall, the Pacific is freshening but there are embedded salinity increases in the subtropical upper ocean, where strong evaporation dominates.

5.3.3.1 Pacific Upper Ocean Changes

In the North Pacific, the zonally averaged temperature warming trend from 1955 to 2003 (Figure 5.3) is dominated by the PDO increase in the mid-1970s. The strong cooling between 50 and 200 m is due to relaxation and subsequent shallowing of the tropical thermocline, resulting from a decrease in the shallow tropical MOC and a relaxation of the equatorial thermocline (McPhaden and Zhang, 2002), although after 1998 this shallow overturning circulation returned to levels almost as high as in the 1970s (McPhaden and Zhang, 2004).

Warming in the North Pacific subtropics, cooling around 40°N and slight warming farther north is the pattern associated with a positive PDO (strengthened Aleutian Low; Miller and Douglas, 2004; see Figure 3.28). Within the North Pacific Ocean, a positive PDO state such as occurred after 1976 is characterised by a strengthened Kuroshio Extension. After 1976, the Kuroshio Extension and North Pacific Current transport increased by 8% and expanded southward (Parrish et al., 2000). The Kuroshio's advection of temperature anomalies has been shown to be of similar importance to variations in ENSO and the strength of the Aleutian Low in maintaining the positive PDO (Schneider and Cornuelle, 2005). The Oyashio penetrated farther southward along the coast of Japan during the 1980s than during the preceding two decades, consistent with a stronger Aleutian Low (Sekine, 1988; Hanawa, 1995; Sekine, 1999). A shoaling of the halocline in the centre of the western subarctic gyre and a concurrent southward shift of the Oyashio extension front during 1976 to 1998 vs. 1945 to 1975 has been detected (Joyce and Dunworth-Baker, 2003). Similarly, mixed layer depth decreased throughout the eastern subarctic gyre, with a distinct trend over 50 years (Freeland et al., 1997; Li et al., 2005).

Temperature changes in upper-ocean water masses in response to the more positive phase of the PDO after 1976 are well documented. The thick water mass just south of the Kuroshio Extension in the subtropical gyre (Subtropical Mode Water) warmed by 0.8°C from the mid-1970s to the late 1980s, associated with stronger Kuroshio advection, and the thick water mass along the subtropical-subpolar boundary near 40°N

(North Pacific Central Mode Water) cooled by 1°C following the shift in the PDO after 1976 (Yasuda et al., 2000; Hanawa and Kamada, 2001).

Trends towards increased heat content include a major signal in the subtropical South Pacific, within the thick mixed layers just north of the Antarctic Circumpolar Current (Willis et al., 2004; Section 5.3.5). The strength of the South Pacific subtropical gyre circulation increased more than 20% after 1993, peaking in 2003, and subsequently declined. This spin up is linked to an increase of Ekman pumping over the gyre due to an increase in the SAM index (Roemmich et al., 2007).

The marginal seas of the Pacific Ocean are also subject to climate variability and change. Like the Mediterranean in the North Atlantic, the Japan (or East) Sea is nearly completely isolated from the adjacent ocean basin, and forms all of its own waters beneath the shallow pycnocline. Because of this sea's limited size, it responds quickly through its entire depth to surface forcing changes. The warming evident through the global ocean is clearly apparent in this isolated basin, which warmed by 0.1°C at 1,000 m and 0.05°C below 2,500 m since the 1960s. Salinity at these depths also changed, by 0.06 psu per century for depths of 300 to 1,000 m and by –0.02 psu per century below 1,500 m (Kwon et al., 2004). These changes have been attributed to reduced surface heat loss and increased surface salinity, which have changed the mode of ventilation (Kim et al., 2004). Deep water production in the Japan (East) Sea slowed for many decades, with a marked decrease in dissolved oxygen from the 1930s to 2000 at a rate of about 0.8 μmol kg^{-1} yr^{-1} (Gamo et al., 1986; Minami et al., 1998). However, possibly because of weakened vertical stratification at mid-depths associated with the decades-long warming, deep-water production reappeared after the 2000–2001 severe winter (e.g., Kim et al., 2002; Senjyu et al., 2002; Talley et al., 2003b). Nevertheless, the overall trend has continued with lower deep-water production in subsequent years.

5.3.3.2 Intermediate and Deep Circulation and Water Property Changes

Since the 1970s, the major mid-depth water mass in the North Pacific, North Pacific Intermediate Water (NPIW), has been freshening and has become less ventilated, as measured by oxygen content (see Section 5.4.3). The NPIW is formed in the subpolar North Pacific, with most influence from the Okhotsk Sea, and reflects changes in northern North Pacific surface conditions. The salinity of NPIW decreased by 0.1 and 0.02 psu in the subpolar and subtropical gyres, respectively (Wong et al., 2001; Joyce and Dunworth-Baker, 2003). An oxygen decrease and nutrient increase in the NPIW south of Hokkaido from 1970 to 1999 was reported (Ono et al., 2001), along with a subpolar basin-wide oxygen decrease from the mid-1980s to the late 1990s (Watanabe et al., 2001). Warming and freshening occurred in the Okhotsk Sea in the latter half of the 20th century (Hill et al., 2003). The Okhotsk Sea intermediate water thickness was reduced and its density decreased in the 1990s (Yasuda et al., 2001).

In the southwest Pacific, in the deepest waters originating from the North Atlantic and Antarctica, cooling and freshening of 0.07°C and 0.01 psu from 1968 to 1991 was observed (Johnson and Orsi, 1997) and attributed to a change in the relative importance of Antarctic and North Atlantic source waters and weakening bottom transport. Bottom waters in the North Pacific are farther from the surface sources than any other of the world's deep waters. They are also the most uniform, in terms of spatial temperature and salinity variations. A large-scale, significant warming of the bottom 1,000 m across the entire North Pacific of the order of 0.002°C occurred between 1985 and 1999, measurable because of the high accuracy of modern instruments (Fukasawa et al., 2004). The cause of this warming is uncertain, but could have resulted from warming of the deep waters in the South Pacific and Southern Ocean, where mid-depth changes since the 1950s are as high as 0.17°C (Gille, 2002; see Figure 5.8), and/or from the declining bottom water transport into the deep North Pacific (Johnson et al., 1994).

5.3.4 Indian Ocean

The upper Indian Ocean has been warming everywhere except in a band centred at about 12°S (South Equatorial Current), as seen in Section 5.2 (Figure 5.3). In the tropical and eastern subtropical Indian Ocean (north of 10°S), warming in the upper 100 m (Qian et al., 2003) is consistent with the significant warming of the sea surface from 1900 to 1999 (see Section 3.2.2 and Figure 3.9). The surface warming trend during the period 1900 to 1970 was relatively weak, but increased significantly in the 1970 to 1999 period, with some regions exceeding 0.2°C per decade.

The global-scale circulation includes transport of warm, relatively fresh waters from the Pacific passing through the Indonesian Seas to the Indian Ocean and then onward into the South Atlantic. Much of this throughflow occurs in the tropics south of the equator, and is strongly affected by ENSO and the Indian Ocean Dipole (see Section 3.6.7.2). The latter causes pronounced thermocline variability (Qian et al., 2003) and includes propagation of upper-layer thickness anomalies by Rossby waves (Xie et al., 2002; Feng and Meyers, 2003; Yamagata et al., 2004) in the 3°S to 15°S latitude band that includes the westward-flowing throughflow water.

Long-term trends in transport and properties of the throughflow have not been reported. The mean transport into the Indonesian Seas measured at Makassar Strait from 1996 to 1998 was 9 to 10 Sv (Vranes et al., 2002), matching transports exiting the Indonesian Seas (e.g., Sprintall et al., 2004). Large variability in this transport is associated with varying tropical Pacific and Indian winds (Wijffels and Meyers, 2004), including a strong ENSO response (e.g., Meyers, 1996), and may be associated with changes in SST in the tropical Indian Ocean.

Models suggest that upper-ocean warming in the south Indian Ocean can be attributed to a reduction in the southeast trade winds and associated decrease in the southward transport of heat from the tropics to the subtropics (Lee, 2004). The export of heat from the northern Indian Ocean to the south

across the equator is accomplished by a wind-driven, shallow cross-equatorial cell; data assimilation analysis has shown a significant decadal reduction in the mass exchange during 1950 to 1990 but little change in heat transport (Schoenefeldt and Schott, 2006).

Changes in Indian subtropical gyre circulation since the 1960s include a 20% slowdown from 1962 to 1987 (Bindoff and McDougall, 2000) and a 20% speedup from 1987 to 2002 (Bryden et al., 2003; McDonagh et al., 2005), with the speedup mainly between 1995 and 2002 (Palmer et al., 2004). The upper thermocline warmed during the slowdown, and then cooled during speedup. Simulations of this region and the analysis of climate change scenarios show that the slowdown and speedup were part of an oscillatory pattern in the upper part of this gyre over periods of decades (Murray et al., 2007; Stark et al., 2006). On the other hand, the lower thermocline (<10°C) freshened and warmed from 1936 to 2002 (Bryden et al., 2003), consistent with heat content increases discussed in Section 5.2 and earlier results.

5.3.5 Southern Ocean

The Southern Ocean, which is the region south of 30°S, connects the Atlantic, Indian and Pacific Oceans together, allowing inter-ocean exchange. This region is active in the formation and subduction of waters that contributed strongly to the storage of anthropogenic carbon and heat (see Section 5.2). It is also the location of the densest part of the global overturning circulation, through formation of bottom waters around Antarctica, fed by deep waters from all of the oceans to the north. Note that some observed changes found in the Atlantic, Indian and Pacific Oceans are related to changes in the Southern Ocean waters but have largely been described in those sections.

5.3.5.1 Upper-Ocean Property Changes

The upper ocean in the SH has warmed since the 1960s, dominated by changes in the thick near-surface layers called Subantarctic Mode Water (SAMW), located just north of the Antarctic Circumpolar Current (ACC) that encircles Antarctica. The observed warming of SAMW is consistent with the subduction of warmer surface waters from south of the ACC (Wong et al., 2001; Aoki et al., 2003). In the Upper Circumpolar Deep Water (UCDW) in the Indian and Pacific sectors of the Southern Ocean, temperature and salinity have been increasing (on density surfaces) and oxygen has been decreasing between the Subantarctic Front near 45°S and the Antarctic Divergence near 60°S (Aoki et al., 2005a). These changes just below the mixed layer (~100 to 300 m) are consistent with the mixing of warmer and fresher surface waters with UCDW, suggesting an increase in stratification in the surface layer of this polar region.

Mid-depth waters of the Southern Ocean have also warmed in recent decades. As shown in Figure 5.8, temperatures increased near 900 m depth between the 1950s and the 1980s throughout most of the Southern Ocean (Aoki et al., 2003; Gille, 2004).

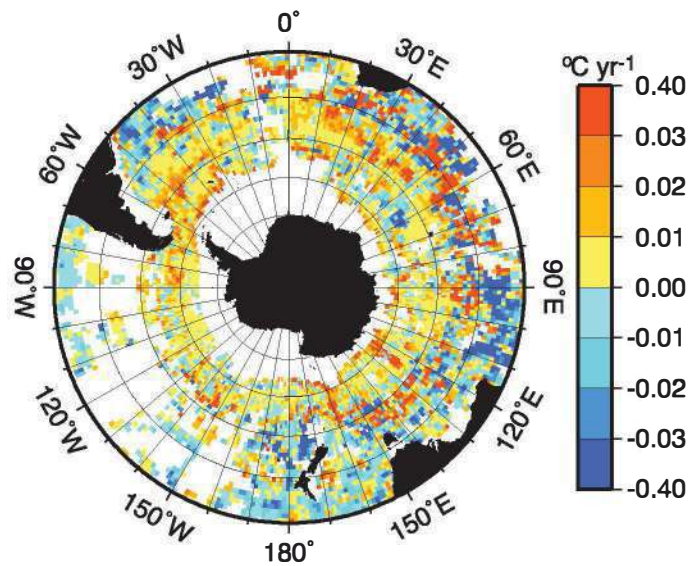

Figure 5.8. *Temperature trends (°C yr^{-1}) at 900 m depth using data collected from the 1930s to 2000, including shipboard profile and Autonomous LAgrangian Current Explorer float data. The largest warming occurs in subantarctic regions, and a slight cooling occurs to the north. From Gille (2002).*

The largest changes are found near the Antarctic Circumpolar Current, where the warming at 900 m depth is similar in magnitude to the increase in regional surface air temperatures. Analysis of altimeter and Argo float profile data suggests that, over the last 10 years, the zonally averaged warming in the upper 400 m of the ocean near 40°S (Willis et al. 2004) is much larger than that seen in long-term trends (see Section 5.2, Figure 5.3 World). The warming results from these analyses have been attributed to a southward shift and increased intensity of the SH westerlies, which would shift the ACC slightly southward and intensify the subtropical gyres (e.g., Cai, 2006).

The major mid-depth water mass in the SH, Antarctic Intermediate Water (AAIW), has also been freshening since the 1960s (Wong et al., 1999; Bindoff and McDougall, 2000; see Figure 5.6). The Atlantic freshening of AAIW is also supported by direct observations of a freshening of southern surface waters (Curry et al., 2003).

5.3.5.2. Antarctic Regions and Antarctic Circumpolar Current

The ACC, the longest current system in the world, has a transport through Drake Passage of about 130 Sv, with significant interannual variability. Measurements over 25 years across Drake Passage show no evidence for a systematic trend in total volume transport between the 1970s and the present (Cunningham et al., 2003), although continuous subsurface pressure measurements suggest that trends in seasonality of transport are highly correlated with similar trends in the SAM index (Meredith and King, 2005).

There is growing evidence for the changes in the AABW and intermediate depth waters around Antarctica. In the Weddell Sea, the deep and bottom water properties varied in the 1990s

(Robertson et al., 2002; Fahrbach et al., 2004). Changes in bottom water properties have also been observed downstream of these source regions (Hogg, 2001; Andrie et al., 2003) and in the South Atlantic (Section 5.3.2.3). The upper ocean adjacent to the West Antarctic Peninsula warmed by more than 1°C and became more saline by 0.25 psu from 1951 to 1994 (Meredith and King, 2005). The warming is likely to have resulted from large regional atmospheric warming (Vaughan et al., 2003) and reduced winter sea ice observed in this region.

In the Ross Sea and near the Ross Ice Shelf, significant decreases in salinity of 0.003 psu yr^{-1} (and density decreases) over the last four decades (Jacobs et al., 2002) have been observed. Downstream of the Ross Ice Shelf in the Australian-Antarctic Basin, AABW has also cooled and freshened (Aoki et al., 2005b). These observed decreases are significantly greater than earlier reports of AABW variability (Whitworth, 2002) and suggest that changes in the antarctic shelf waters can be quite quickly communicated to deep waters. Jacobs et al. (2002) concluded that the freshening appears to have resulted from a combination of factors including increased precipitation, reduced sea ice production and increased melting of the West Antarctic Ice Sheet.

5.3.6 Relation of Regional to Global Changes

5.3.6.1 Changes in Global Water Mass Properties

The regional analyses described in the previous sections have global organisation, as described partially in Section 5.3.1 (Figure 5.6), and as reflected in the global trend analyses in Section 5.2. The data sets used for the largest-scale descriptions over the last 30 to 50 years are reliable; different types of data and widely varying methods yield similar results, increasing confidence in the reality of the changes found in both the global and regional analyses.

The regional and global analyses of ocean warming generally show a pattern of increased ocean temperature in the regions of very thick surface mixed layer (mode water) formation. This is clearest in the North Atlantic and North Pacific and in all sectors of the Southern Ocean (Figure 5.3). There are also regions of decreased ocean temperature in both the global and regional analyses in parts of the subpolar and equatorial regions.

Both the global and regional analyses show long-term freshening in the subpolar waters in the North Atlantic and North Pacific and a salinity increase in the upper ocean (<100 m deep) at low to mid-latitudes. This is consistent with an increase in the atmospheric hydrological cycle over the oceans and could result in changes in ocean advection (Section 5.3.2). In the North Atlantic, the subpolar freshening occurred throughout the entire water column, from the 1960s to the mid-1990s (Figure 5.5 and Figure 5.6a). Increased salinity and temperature in the upper water column in the subpolar North Atlantic after 1994 are not apparent from the linear trend applied to the full time series in Figure 5.5, but are clear in all regional time series (Section 5.3.2). Freshening in the North Pacific subpolar gyre north of 45°N is apparent in both regional analyses (Section 5.3.3.2) and global analyses (Figure 5.5). Freshening of intermediate depth waters (>300 m) from Southern Ocean sources (Section 5.3.5) is apparent in both the global and regional analyses (e.g., Figure 5.5 World).

Many of the observed changes in the temperature and salinity fields have been linked to atmospheric forcing through correlations with atmospheric indices associated with the NAO, PDO and SAM. Indeed, most of the few time series of ocean measurements or repeat measurements of long sections (see Sections 5.3.2 and 5.3.4) show evidence of decadal variability. Because of the long time scales of these natural climate patterns, it is difficult to discern if observed decadal oceanic variability is natural or a climate change signal; indeed, changes in these natural patterns themselves might be related to climate change. In the North Atlantic, freshening at high latitudes and increased evaporation at subtropical latitudes prior to the mid-1990s might have been associated with an increasing NAO index, and the reversal towards higher salinity at high latitudes thereafter with a decreasing NAO index after 1990 (see Figure 3.31). Likewise in the Pacific, freshening at high latitudes and increased evaporation in the subtropics, cooling in the central North Pacific, warming in the eastern and tropical Pacific and reduced ventilation in the Kuroshio region, Japan and Okhotsk Seas could be associated with the extended positive phase of the PDO. The few detection and attribution studies of ocean changes are discussed in Section 9.5.1.

At a global scale, the observed long-term patterns of zonal temperature and salinity changes tend to be approximately symmetric around the equator (Figure 5.6) and occur simultaneously in different ocean basins (Figures 5.3 and 5.5). The scale of these patterns, which extends beyond the regions of influence normally associated with the NAO, PDO and SAM, suggests that these coherent changes between both hemispheres are associated with a global phenomenon.

5.3.6.2 Consistency with the Large-Scale Ocean Circulation

The observed changes are broadly consistent with scientific understanding of the circulation of the global oceans. The North Atlantic and antarctic regions, where the oceans ventilate the deep waters over short time scales (<50 years), show strong evidence of change over the instrumental record. For example, the North Atlantic shows evidence of a deep warming and freshening. There is evidence of change in the Southern Ocean bottom waters consistent with the sinking of fresher antarctic shelf waters. Deep waters that are far from the North Atlantic and Antarctic, remote from interaction with the atmosphere, and with replenishment rates that are long compared with the instrumental record, typically show no significant changes. Mode waters, key global water masses found in every ocean basin equatorward of major oceanic frontal systems or separated boundary currents, have a relatively rapid formation and ventilation rate (<20 years) and provide a pathway for heat (and salinity) to be transported into the main subtropical gyres of the global oceans as observed.

5.4 Ocean Biogeochemical Changes

5.4.1 Introduction

The observed increase in atmospheric carbon dioxide (CO_2; see Chapter 2) and the observed changes in the physical properties of the ocean reported in this chapter can affect marine biogeochemical cycles (here mainly carbon, oxygen, and nutrients). The increase in atmospheric CO_2 causes additional CO_2 to dissolve in the ocean. Changes in temperature and salinity affect the solubility and chemical equilibration of gases. Changes in circulation affect the supply of carbon and nutrients from below, the ventilation of oxygen-depleted waters and the downward penetration of anthropogenic carbon. The combined physical and biogeochemical changes also affect biological activity, with further consequences for the biogeochemical cycles.

The increase in surface ocean CO_2 has consequences for the chemical equilibrium of the ocean. As CO_2 increases, surface waters become more acidic and the concentration of carbonate ions decreases. This change in chemical equilibrium causes a reduction of the capacity of the ocean to take up additional CO_2. However, the response of marine organisms to ocean acidification is poorly known and could cause further changes in the marine carbon cycle with consequences that are difficult to estimate (see Section 7.3.4 and Chapter 4 of the Working Group II contribution to the IPCC Fourth Assessment Report).

Dissolved oxygen (O_2) in the ocean is affected by the same physical processes that affect CO_2, but in contrast to CO_2, O_2 is not affected by changes in its atmospheric concentration (which are only of the order of 10^{-4} of its mean concentration). Changes in oceanic O_2 concentration thus provide information on the changes in the physical or biological processes that occur within the ocean, such as ventilation (here used to describe the rate of renewal of thermocline waters), mode water formation, upwelling or biological export and respiration. Furthermore, changes in the oceanic O_2 content are needed to estimate the CO_2 budget from atmospheric O_2/molecular nitrogen (N_2) ratio measurements. However, the method currently estimates the change in air-sea fluxes of O_2 indirectly based on heat flux changes (see Section 7.3.2).

This section reports observed changes in biogeochemical cycles and assesses their consistency with observed changes in physical properties. Changes in oceanic nitrous oxide (N_2O) and methane (CH_4) have not been assessed because of the lack of large-scale observations. Observations of the mean fluxes of N_2O and CH_4 (including CH_4 hydrates) are discussed in Chapter 7.

5.4.2 Carbon

5.4.2.1 Total Change in Dissolved Inorganic Carbon and Air-Sea Carbon Dioxide Flux

Direct observations of oceanic dissolved inorganic carbon (DIC; i.e., the sum of CO_2 plus carbonate and bicarbonate) reflect changes in both the natural carbon cycle and the uptake of anthropogenic CO_2 from the atmosphere. Links between the main modes of climate variability and the marine carbon cycle have been observed on interannual time scales in several regions of the world (see Section 7.3.2.4 for quantitative estimates). In the equatorial Pacific, the reduced upwelling associated with El Niño events decreases the regional outgas of natural CO_2 to the atmosphere (Feely et al., 1999). In the subtropical North Atlantic, reduced mode water formation and reduced deep winter mixing during the positive NAO phase increase the storage of carbon in the intermediate ocean (Bates et al., 2002). These observations show that variability in the content of natural DIC in the ocean has occurred in association with climate variability.

Longer observations exist for the partial pressure of CO_2 (pCO_2) at the surface only. Over more than two decades, the oceanic pCO_2 increase has generally followed the atmospheric CO_2 within the given uncertainty, although regional differences have been observed (Feely et al., 1999; Takahashi et al., 2006). The three stations with the longest time series, all in the northern subtropics, show pCO_2 increases at a rate varying between 1.6 and 1.9 µatm yr^{-1} (Figure 5.9), indistinguishable from the atmospheric increase of 1.5 to 1.9 µatm yr^{-1}. Variability on the order of 20 µatm over periods of five years was observed in the three time series, as well as in other data sets, and has been associated with regional changes in the natural carbon cycle driven by changes in ocean circulation and by climate variability (Gruber et al., 2002; Dore et al., 2003) or with variations in biological activity (Lefèvre et al., 2004).

Direct surface pCO_2 observations have been used to compute a global air-sea CO_2 flux of 1.6 ± 1 GtC yr^{-1} for the year 1995 (Takahashi et al., 2002; Section 7.3.2.3.2, Figure 7.8). It is not yet possible to detect large-scale changes in the global air-sea CO_2 flux from direct observations because of the large influence of climate variability. However, estimates from inverse methods of the air-sea CO_2 flux from the spatio-temporal distribution of atmospheric CO_2 suggest that the global air-sea CO_2 flux increased by 0.1 to 0.6 GtC yr^{-1} between the 1980s and 1990s, consistent with results from ocean models (Le Quéré et al., 2003).

5.4.2.2 Anthropogenic Carbon Change

The recent uptake of anthropogenic carbon in the ocean is well constrained by observations to a decadal mean of 2.2 ± 0.4 GtC yr^{-1} for the 1990s (see Section 7.3.2, Table 7.1). The uptake of anthropogenic carbon over longer time scales can be estimated from oceanic measurements. Changes in DIC between two time periods reflect the anthropogenic carbon uptake plus the changes in DIC concentration due to changes in water masses and biological activity. To estimate the contribution of anthropogenic carbon alone, several corrections must be applied. From observed DIC changes between surveys in the 1970s and the 1990s, an increase in anthropogenic carbon has been inferred down to depths of 1,100 m in the North Pacific (Peng et al., 2003; Sabine et al., 2004a), 200 to 1,200 m in the Indian Ocean (Peng et al., 1998; Sabine et al., 1999) and 1,900 m in the Southern Ocean (McNeil et al., 2003).

An indirect method was used to estimate anthropogenic carbon from observations made at a single time period based on well-known processes that control the distribution of natural DIC in the ocean. The method corrects the observed DIC concentration for organic matter decomposition and dissolution of carbonate minerals, and removes an estimate of the DIC concentration of the water when it was last in contact with the atmosphere (Gruber et al., 1996). With this method, a global DIC increase of 118 ± 19 GtC between pre-industrial times (roughly 1750) and 1994 has been estimated, using 9,618 profiles from the 1990s (Sabine et al., 2004b; see Figure 5.10). The uncertainty of ±19 GtC in this estimate is based on uncertainties in the anthropogenic DIC estimates and mapping errors, which have characteristics of random error, and on an estimate of potential biases, which are not necessarily centred on the mean value. Potential biases of up to 7% in the technique have been identified, mostly caused by assumptions about the time evolution of CO_2, the age or the identification of water masses (Matsumoto and Gruber, 2005), and the recent changes in surface warming and stratification (Keeling, 2005). Potential biases from assumptions of constant carbon and nutrient uptake ratios for biological activity have not been assessed. While the magnitude and direction of all potential biases are not yet clear, the given uncertainty of ±16% appears realistic compared to the biases already identified.

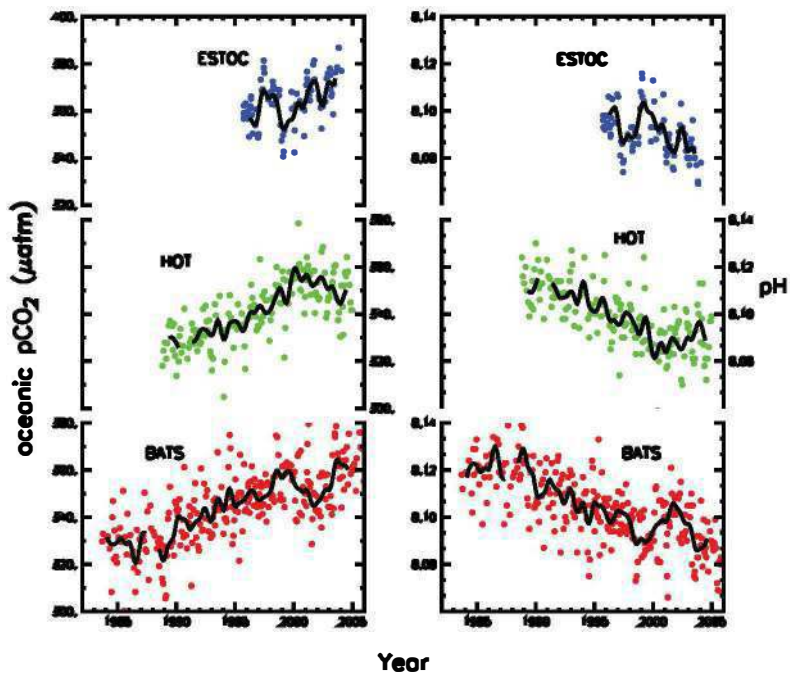

Figure 5.9. *Changes in surface oceanic pCO_2 (left; in µatm) and pH (right) from three time series stations: Blue: European Station for Time-series in the Ocean (ESTOC, 29°N, 15°W; Gonzalez-Dávila et al., 2003); green: Hawaii Ocean Time-Series (HOT, 23°N, 158°W; Dore et al., 2003); red: Bermuda Atlantic Time-series Study (BATS, 31/32°N, 64°W; Bates et al., 2002; Gruber et al., 2002). Values of pCO_2 and pH were calculated from DIC and alkalinity at HOT and BATS; pH was directly measured at ESTOC and pCO_2 was calculated from pH and alkalinity. The mean seasonal cycle was removed from all data. The thick black line is smoothed and does not contain variability less than 0.5 years period.*

Because of the limited rate of vertical transport in the ocean, more than half of the anthropogenic carbon can still be found in the upper 400 m, and it is undetectable in most of the deep ocean (Figure 5.11). The vertical penetration of anthropogenic carbon is consistent with the DIC changes observed between two cruises (Peng et al., 1998, 2003). Anthropogenic carbon has penetrated deeper in the North Atlantic and subantarctic Southern Ocean compared to other basins, due to a combination of: i) high surface alkalinity (in the Atlantic) which favours the uptake of CO_2, and ii) more active vertical exchanges caused by intense winter mixing and by the formation of deep waters (Sabine et al., 2004b). The deeper penetration of anthropogenic carbon in these regions is consistent with similar features observed in the oceanic distribution of chlorofluorocarbons (CFCs) of atmospheric origin (Willey et al., 2004), confirming that it takes decades to many centuries to transport carbon from the surface into the thermocline and the deep ocean. Deeper penetration in the North Atlantic and subantarctic Southern Ocean is also observed in the changes in heat content shown in Figure 5.3. The large storage of anthropogenic carbon observed in the subtropical gyres is caused by the lateral transport of carbon from the region of mode water formation towards the lower latitudes (Figure 5.10).

The fraction of the net CO_2 emissions taken up by the ocean (the uptake fraction) was possibly lower during 1980 to 2005 (37% ± 7%) compared to 1750 to 1994 (42% ± 7%); however the uncertainty in the estimates is larger than the difference between the estimates (Table 5.1). The net CO_2 emissions

Table 5.1. *Fraction of CO_2 emissions taken up by the ocean for different time periods.*

Time Period	Oceanic Increase	Net CO_2 Emissions[a] (GtC)	Uptake Fraction (%)	Reference
1750–1994	**(GtC)** 118 ± 19	283 ± 19	42 ± 7	Sabine et al., 2004b
1980–2005[b]	53 ± 9	143 ± 10	37 ± 7	Chapter 7[c]

Notes:
[a] Sum of emissions from fossil fuel burning, cement production, land use change and the terrestrial biosphere response.
[b] The longest possible time period was used for the recent decades to minimise the effect of the variability in atmospheric CO_2.
[c] Sum of the estimates for the 1980s, 1990s and 2000 to 2005 from Table 7.1.

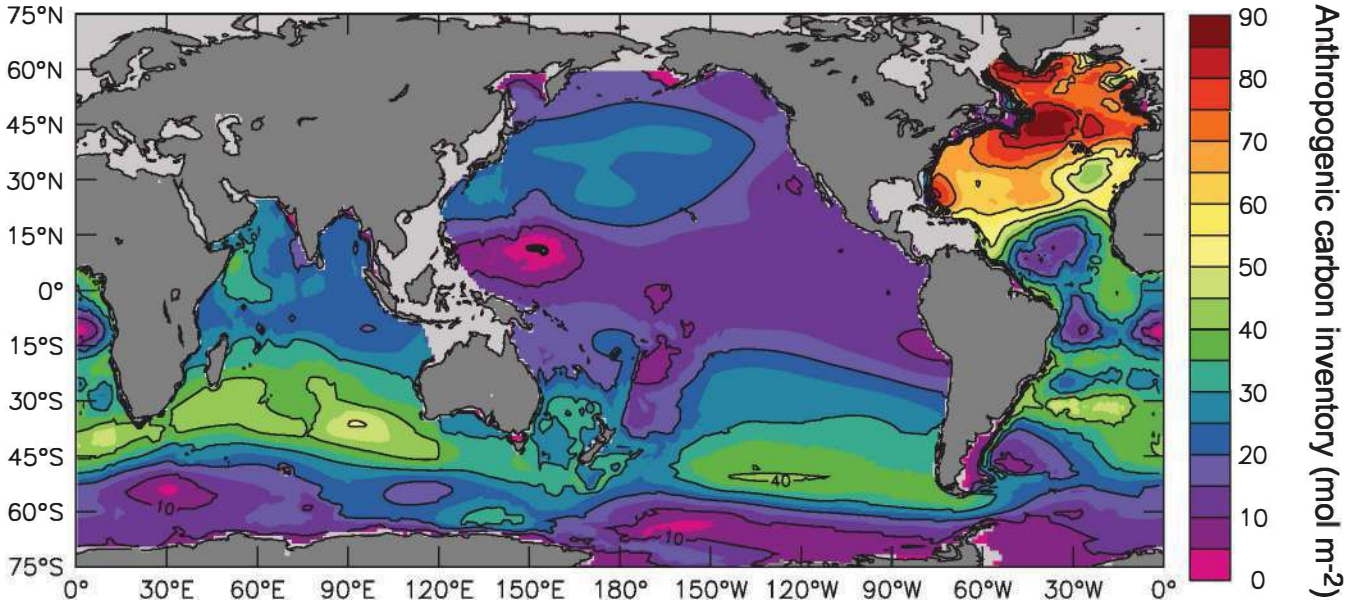

Figure 5.10. *Column inventory of anthropogenic carbon (mol m^{-2}) as of 1994 from Sabine et al. (2004b). Anthropogenic carbon is estimated indirectly by correcting the measured DIC for the contributions of organic matter decomposition and dissolution of carbonate minerals, and taking into account the DIC concentration the water had in the pre-industrial ocean when it was last in contact with the atmosphere. The global inventory of anthropogenic carbon taken up by the ocean between 1750 and 1994 is estimated to be 118 ± 19 GtC.*

include all emissions that have an influence on the atmospheric CO_2 concentration (i.e., emissions from fossil fuel burning, cement production, land use change and the terrestrial biosphere response). It is equivalent to the sum of the atmospheric and oceanic CO_2 increase. Because the atmospheric CO_2 is well constrained by observations, the uncertainty in the net CO_2 emissions is nearly equal to the uncertainty in the oceanic CO_2 increase. The decrease in oceanic uptake fraction would be consistent with the understanding that the ocean CO_2 sink is limited by the transport rate of anthropogenic carbon from the surface to the deep ocean, and also with the nonlinearity in carbon chemistry that reduces the CO_2 uptake capacity of water as its CO_2 concentration increases (Sarmiento et al., 1995).

5.4.2.3 Ocean Acidification by Carbon Dioxide

The uptake of anthropogenic carbon by the ocean changes the chemical equilibrium of the ocean. Dissolved CO_2 forms a weak acid.[1] As CO_2 increases, pH decreases, that is, the ocean becomes more acidic. Ocean pH can be computed from measurements of DIC and alkalinity. A decrease in surface pH of 0.1 over the global ocean was calculated from the estimated uptake of anthropogenic carbon between 1750 and 1994 (Sabine et al., 2004b; Raven et al., 2005), with the lowest decrease (0.06) in the tropics and subtropics, and the highest decrease (0.12) at high latitudes, consistent with the lower buffer capacity of the high latitudes compared to the low latitudes. The mean pH of surface waters ranges between 7.9 and 8.3 in the open

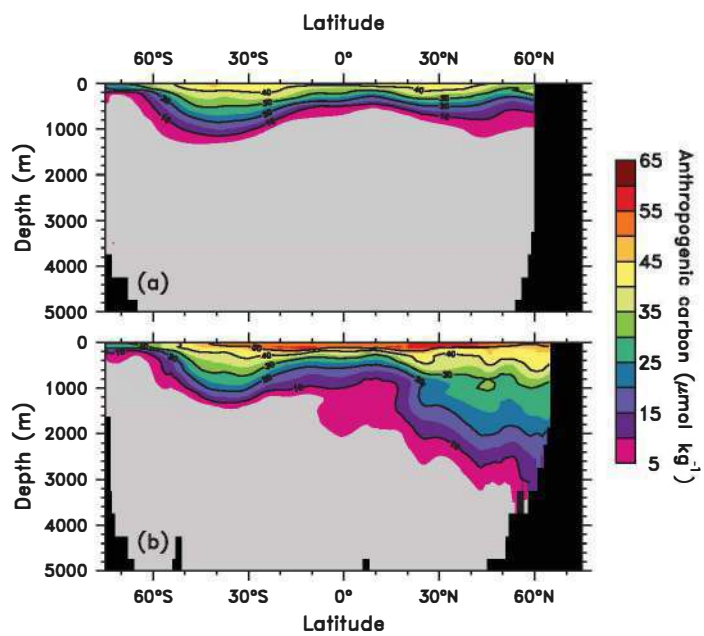

Figure 5.11. *Mean concentration of anthropogenic carbon as of 1994 in µmol kg^{-1} from Sabine et al. (2004b) averaged over (a) the Pacific and Indian Oceans and (b) the Atlantic Ocean. The calculation of anthropogenic carbon is described in the caption of Figure 5.10 and in the text (Section 5.4).*

[1] Acidity is a measure of the concentration of H^+ ions and is reported in pH units, where pH = $-\log_{10}(H^+)$. A pH decrease of 1 unit means a 10-fold increase in the concentration of H^+, or acidity.

ocean, so the ocean remains alkaline (pH > 7) even after these decreases. For comparison, pH was higher by 0.1 unit during glaciations, and there is no evidence of pH values more than 0.6 units below the pre-industrial pH during the past 300 million years (Caldeira and Wickett, 2003). A decrease in ocean pH of 0.1 units corresponds to a 30% increase in the concentration of H^+ in seawater, assuming that alkalinity and temperature remain constant. Changes in surface temperature may have induced an additional decrease in pH of <0.01. The calculated anthropogenic impact on pH is consistent with results from time series stations where a decrease in pH of 0.02 per decade was observed (Figure 5.9). Results from time series stations include not only the increase in anthropogenic carbon, but also other changes due to local physical and biological variability. The consequences of changes in pH on marine organisms are poorly known (see Section 7.3.4 and Box 7.3).

5.4.2.4 Change in Carbonate Species

The uptake of anthropogenic carbon occurs through the injection of CO_2 and causes a shift in the distribution of carbon species (i.e., the balance between CO_2, carbonate and bicarbonate). The availability of carbonate is particularly important because it controls the maximum amount of CO_2 that the ocean is able to absorb. Marine organisms use carbonate to produce shells of calcite and aragonite (both consisting of calcium carbonate; $CaCO_3$). Currently, the surface ocean is super-saturated with respect to both calcite and aragonite, but undersaturated below a depth called the 'saturation horizon'. The undersaturation starts at a depth varying between 200 m in parts of the high-latitude and the Indian Ocean and 3,500 m in the Atlantic. Calcium carbonate dissolves either when it sinks below the calcite or aragonite saturation horizons or under the action of biological activity.

Shoaling of the aragonite saturation horizon has been observed in all ocean basins based on alkalinity, DIC and oxygen measurements (Feely and Chen, 1982; Feely et al., 2002; Sabine et al., 2002; Sarma et al., 2002). The amplitude and direction of the signal was everywhere consistent with the uptake of anthropogenic carbon, with potentially smaller contributions from changes in circulation, temperature and biology. Feely et al. (2004) calculated that the uptake of anthropogenic carbon alone has caused a shoaling of the aragonite saturation horizon between 1750 and 1994 by 30 to 200 m in the eastern Atlantic (50°S–15°N), the North Pacific and the North Indian Ocean, and a shoaling of the calcite saturation horizon by 40 to 100 m in the Pacific (north of 20°N). This calculation is based on the anthropogenic DIC increase estimated by Sabine et al. (2004a), on a global compilation of biogeochemical data and on carbonate chemistry equations. Furthermore, an increase in total alkalinity (primarily controlled by carbonate and bicarbonate) at the depth of the aragonite saturation horizon between 1970 and 1990 has been reported (Sarma et al., 2002). These results are consistent with the calculated increase in $CaCO_3$ dissolution as a result of the shoaling of the aragonite saturation horizon, but with large uncertainty. Carbonate decreases at high latitudes and particularly in the Southern Ocean may have consequences for marine ecosystems because the current saturation horizon is closer to the surface than in other basins (Orr et al., 2005; see Section 7.3.4).

5.4.3 Oxygen

In the thermocline (~100 to 1,000 m), a decrease in the O_2 concentration has been observed between about the early 1970s and the late 1990s or later in several repeated hydrographic sections in the North and South Pacific, North Atlantic, and Southern Indian Oceans (Figure 5.12; see summary table in Emerson et al., 2004, and Section 5.3). Section 5.3 reports on a number of O_2 decreases that fit the overall message of Section 5.4. The reported O_2 decreases range from 0.1 to 6 μmol kg^{-1} yr^{-1}, superposed on decadal variations of ±2 μmol kg^{-1} yr^{-1} (Ono et al., 2001; Andreev and Watanabe, 2002). In all published studies, the observed O_2 decrease appeared to be driven primarily by changes in ocean circulation, and less by changes in the rate of O_2 demand from downward settling of organic matter. A few studies have quantified the contribution of the change in ocean circulation using estimates of changes in apparent CFC ages (Doney et al., 1998; Watanabe et al., 2001; Mecking et al., 2006). In nearly all cases, the decrease in O_2 could entirely be accounted for by the increased apparent CFC age that resulted from reduced rate of renewal of intermediate waters. Changes in biological processes were only significant at the coast of California and may result from assumptions in the method (Mecking et al., 2006).

It is unclear whether the recent changes in O_2 are indicative of trends or of variability. Recent data in the Indian Ocean have shown a reversal of the O_2 decrease between 1987 and 2002 in the South Indian Ocean of similar amplitude to the decrease observed during the previous decades (McDonagh et al., 2005). Variability has been observed on decadal time scales in the North Atlantic large enough to mask any potential trends (Johnson and Gruber, 2007).

In the upper 100 m of the global ocean surface, decadal variations of ±0.5 μmol kg^{-1} in O_2 concentration were observed for the period 1956 to 1998 based on a global analysis of 530,000 oxygen profiles, with no clear trends (Garcia et al., 2005). However, the near-surface changes in O_2 concentration are difficult to interpret. They can be caused by changes in biological activity, by changes in the physical transport of O_2 from intermediate waters or by changes in temperature and salinity. Because there is less confidence in the early measurements and the reported changes cannot be explained by known processes, it cannot be said whether the absence of a long-term trend in surface O_2 is realistic or not.

5.4.4 Nutrients

Changes in nutrient concentrations can provide information on changes in the physical and biological processes that affect the carbon cycle and could potentially be used as indicators for large-scale changes in marine biology. However, only a

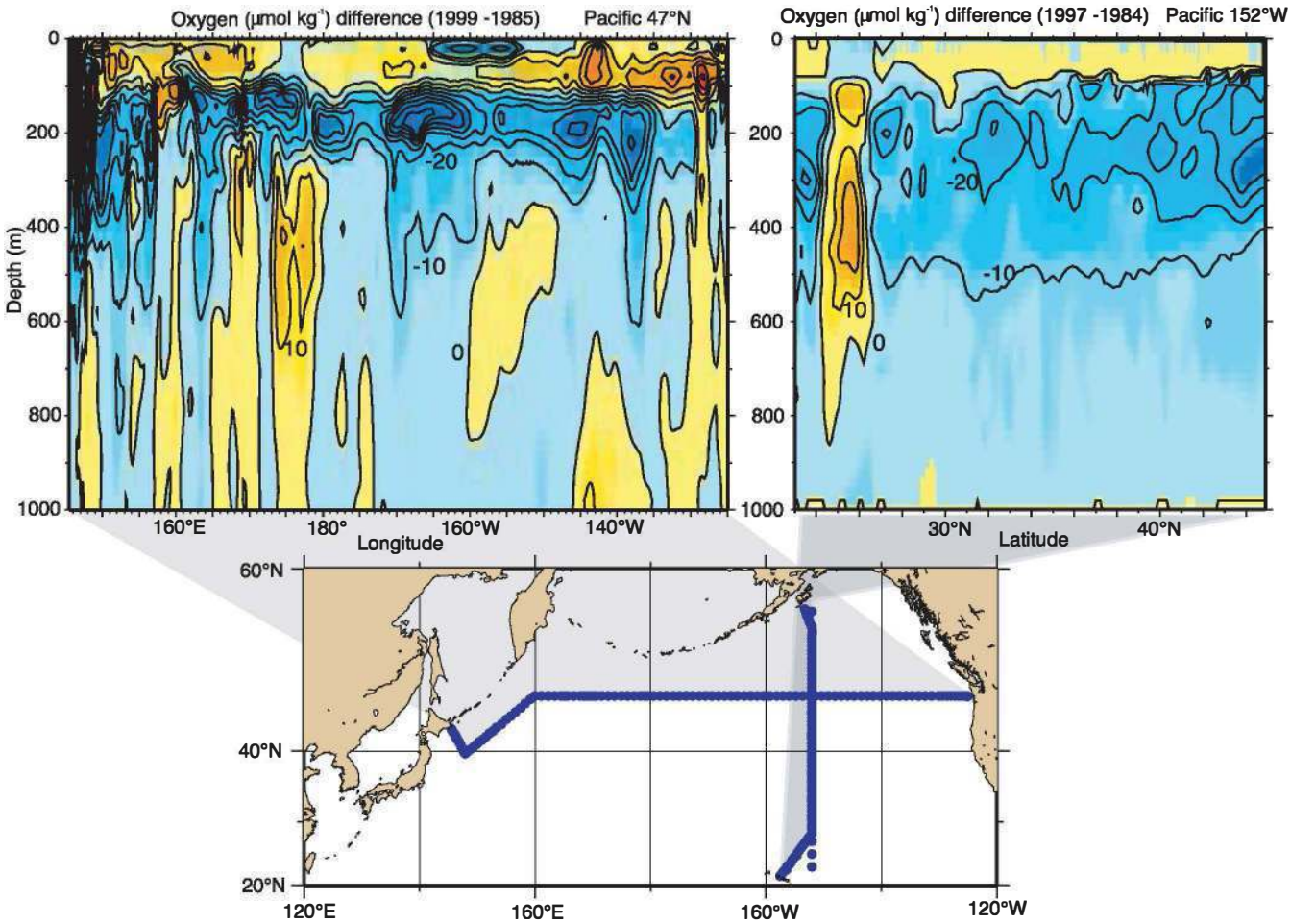

Figure 5.12. *Changes in oxygen concentration (µmol kg⁻¹) along two sections in the North Pacific (see map, bottom panel). Top left panel: Difference (1999 minus 1985) along 47°N. Top right panel: Difference (1997 minus 1984) at 152°W. Blue colours indicate a decrease and yellow colours indicate an increase in oxygen over time. The differences were calculated using density as the vertical coordinate. After Deutsch et al. (2005).*

few studies reported decadal changes in inorganic nutrient concentrations. In the North Pacific, the concentration of nitrate plus nitrite (N) and phosphate decreased at the surface (Freeland et al., 1997; Watanabe et al., 2005) and increased below the surface (Emerson et al., 2001; Ono et al., 2001; Keller et al., 2002) in the past two decades. Nutrient changes were observed in the deep ocean of all basins but no clear pattern emerges from available observations. Pahlow and Riebesell (2000) found changes in the ratio of nutrients in the North Pacific and Atlantic Oceans, and no significant changes in the South Pacific. In the North Pacific, Keller et al. (2002) observed a decrease in N associated with the increase in O_2 between 1970 and 1990 at 1,050 m, opposite to the results of Pahlow and Riebesell's longer study. Using the same data set extended to the world, large regional changes in nutrient ratios were observed (Li and Peng, 2002) but no consistent basin-scale patterns. Uncertainties in deep ocean nutrient observations may be responsible for the lack of coherence in the nutrient changes. Sources of inaccuracy include the limited number of observations and the lack of compatibility between measurements from different laboratories at different times.

In some cases, the observed trends in nutrients can be explained by either a change in thermocline ventilation or a change in biological activity (Pahlow and Riebesell, 2000; Emerson et al., 2001), but in other cases are mostly consistent with a reduction in thermocline ventilation (Freeland et al., 1997; Ono et al., 2001; Watanabe et al., 2005). Thus, all of the reported trends are consistent with a physical explanation of the observed changes, although changes in biological activity cannot be ruled out.

The concentration of surface nutrients can also be influenced by surface mixing, as a reduction in mixing leads to a decreased concentration of surface nutrients. The observed changes in surface temperature and salinity (see Sections 5.2.3 and 5.3) are indicative of changes in the surface mixing (see Section 7.3.4.3). In most of the Pacific Ocean, surface warming and freshening act in the same direction and contribute to reduced mixing (Figures 5.2 and 5.5), consistent with regional observations (Freeland et al., 1997; Watanabe et al., 2005). In the Atlantic and Indian Oceans, temperature and salinity trends generally act in opposite directions and changes in mixing have not been quantified regionally.

5.4.5 Biological Changes Relevant to Ocean Biogeochemistry

Changes in biological activity are an important part of the carbon cycle but are difficult to quantify at the global scale. Marine export production (the fraction of primary production that is not respired at the ocean surface and thus sinks to depth) is the biological process that has the largest influence on element cycles. There are no global observations on changes in export production or respiration. However, estimates of changes in primary production provide partial information. A reduction in global oceanic primary production by about 6% between the early 1980s and the late 1990s was estimated based on the comparison of chlorophyll data from two satellites (Gregg et al., 2003). The errors in this estimate are potentially large because it is based on the comparison of data from two different sensors. Nevertheless, a change in biological fluxes of this order of magnitude is plausible considering that biological production is controlled primarily by nutrient input from intermediate waters, and that a decrease in intermediate water renewal has been observed during that period as indicated by the decrease in O_2. Shifts and trends in plankton biomass have been observed for instance in the North Atlantic (Beaugrand and Reid, 2003), the North Pacific (Karl, 1999; Chavez et al., 2003) and in the Southern Indian Ocean (Hirawake et al., 2005), but the spatial and temporal coverage is limited. The potential impacts of changes in marine ecosystems or dissolved organic matter on climate are discussed in Section 7.3.4, and the impact of climate on marine ecosystems in Chapter 4 of the Working Group II contribution to the IPCC Fourth Assessment Report.

5.4.6 Consistency with Physical Changes

It is clearly established that climate variability affects the oceanic content of natural and anthropogenic DIC and the air-sea flux of CO_2, although the amplitude and physical processes responsible for the changes are less well known. Variability in the marine carbon cycle has been observed in response to physical changes associated with the dominant modes of climate variability such as El Niño events and the PDO (Feely et al., 1999; Takahashi et al., 2006), and the NAO (Bates et al., 2002; Johnson and Gruber, 2007). The regional patterns of anthropogenic CO_2 storage are consistent with those of CFCs and with changes in heat content. The observed trends in CO_2, DIC, pH and carbonate species can be primarily explained by the response of the ocean to the increase in atmospheric CO_2.

Large-scale changes in the O_2 content of the thermocline have been observed between the 1970s and the late 1990s. These changes are everywhere consistent with the local changes in ocean ventilation as identified either by changes in density gradients or by changes in apparent CFC ages. Nevertheless, an influence of changes in marine biology cannot be ruled out. The available data are insufficient to say if the changes in O_2 are caused by natural variability or are trends that are likely to persist in the future, but they do indicate that large-scale changes in ocean physics influence natural biogeochemical cycles, and thus the cycles of O_2 and CO_2 are likely to undergo changes if ocean circulation changes persist in the future.

5.5 Changes in Sea Level

5.5.1 Introductory Remarks

Present-day sea level change is of considerable interest because of its potential impact on human populations living in coastal regions and on islands. This section focuses on global and regional sea level variations, over time spans ranging from the last decade to the past century; a brief discussion of sea level change in previous centuries is given in Section 5.5.2.4. Changes over previous millennia are discussed in Section 6.4.3.

Processes in several nonlinearly coupled components of the Earth system contribute to sea level change, and understanding these processes is therefore a highly interdisciplinary endeavour. On decadal and longer time scales, global mean sea level change results from two major processes, mostly related to recent climate change, that alter the volume of water in the global ocean: i) thermal expansion (Section 5.5.3), and ii) the exchange of water between oceans and other reservoirs (glaciers and ice caps, ice sheets, other land water reservoirs - including through anthropogenic change in land hydrology, and the atmosphere; Section 5.5.5). All these processes cause geographically non-uniform sea level change (Section 5.5.4) as well as changes in the global mean; some oceanographic factors (e.g., changes in ocean circulation or atmospheric pressure) also affect sea level at the regional scale, while contributing negligibly to changes in the global mean. Vertical land movements such as resulting from glacial isostatic adjustment (GIA), tectonics, subsidence and sedimentation influence local sea level measurements but do not alter ocean water volume; nonetheless, they affect global mean sea level through their alteration of the shape and hence the volume of the ocean basins containing the water.

Measurements of present-day sea level change rely on two different techniques: tide gauges and satellite altimetry (Section 5.5.2). Tide gauges provide sea level variations with respect to the land on which they lie. To extract the signal of sea level change due to ocean water volume and other oceanographic change, land motions need to be removed from the tide gauge measurement. Land motions related to GIA can be simulated in global geodynamic models. The estimation of other land motions is not generally possible unless there are adequate nearby geodetic or geological data, which is usually not the case. However, careful selection of tide gauge sites such that records reflecting major tectonic activity are rejected, and averaging over all selected gauges, results in a small uncertainty for global sea level estimates (Appendix 5.A.4). Sea level change based on satellite altimetry is measured with respect to the Earth's centre of mass, and thus is not distorted by land motions, except for a small component due to large-scale deformation of ocean basins from GIA.

Frequently Asked Question 5.1
Is Sea Level Rising?

Yes, there is strong evidence that global sea level gradually rose in the 20th century and is currently rising at an increased rate, after a period of little change between AD 0 and AD 1900. Sea level is projected to rise at an even greater rate in this century. The two major causes of global sea level rise are thermal expansion of the oceans (water expands as it warms) and the loss of land-based ice due to increased melting.

Global sea level rose by about 120 m during the several millennia that followed the end of the last ice age (approximately 21,000 years ago), and stabilised between 3,000 and 2,000 years ago. Sea level indicators suggest that global sea level did not change significantly from then until the late 19th century. The instrumental record of modern sea level change shows evidence for onset of sea level rise during the 19th century. Estimates for the 20th century show that global average sea level rose at a rate of about 1.7 mm yr^{-1}.

Satellite observations available since the early 1990s provide more accurate sea level data with nearly global coverage. This decade-long satellite altimetry data set shows that since 1993, sea level has been rising at a rate of around 3 mm yr^{-1}, significantly higher than the average during the previous half century. Coastal tide gauge measurements confirm this observation, and indicate that similar rates have occurred in some earlier decades.

In agreement with climate models, satellite data and hydrographic observations show that sea level is not rising uniformly around the world. In some regions, rates are up to several times the global mean rise, while in other regions sea level is falling. Substantial spatial variation in rates of sea level change is also inferred from hydrographic observations. Spatial variability of the rates of sea level rise is mostly due to non-uniform changes in temperature and salinity and related to changes in the ocean circulation.

Near-global ocean temperature data sets made available in recent years allow a direct calculation of thermal expansion. It is believed that on average, over the period from 1961 to 2003, thermal expansion contributed about one-quarter of the observed sea level rise, while melting of land ice accounted for less than half. Thus, the full magnitude of the observed sea level rise during that period was not satisfactorily explained by those data sets, as reported in the IPCC Third Assessment Report.

During recent years (1993–2003), for which the observing system is much better, thermal expansion and melting of land ice each account for about half of the observed sea level rise, although there is some uncertainty in the estimates.

The reasonable agreement in recent years between the observed rate of sea level rise and the sum of thermal expansion and loss of land ice suggests an upper limit for the magnitude of change in land-based water storage, which is relatively poorly known. Model results suggest no net trend in the storage of water over land due to climate-driven changes but there are large interannual and decadal fluctuations. However, for the recent period 1993 to 2003, the small discrepancy between observed sea level rise and the sum of known contributions might be due to unquantified human-induced processes (e.g., groundwater extraction, impoundment in reservoirs, wetland drainage and deforestation).

Global sea level is projected to rise during the 21st century at a greater rate than during 1961 to 2003. Under the IPCC Special Report on Emission Scenarios (SRES) A1B scenario by the mid-2090s, for instance, global sea level reaches 0.22 to 0.44 m above 1990 levels, and is rising at about 4 mm yr^{-1}. As in the past, sea level change in the future will not be geographically uniform, with regional sea level change varying within about ±0.15 m of the mean in a typical model projection. Thermal expansion is projected to contribute more than half of the average rise, but land ice will lose mass increasingly rapidly as the century progresses. An important uncertainty relates to whether discharge of ice from the ice sheets will continue to increase as a consequence of accelerated ice flow, as has been observed in recent years. This would add to the amount of sea level rise, but quantitative projections of how much it would add cannot be made with confidence, owing to limited understanding of the relevant processes.

Figure 1 shows the evolution of global mean sea level in the past and as projected for the 21st century for the SRES A1B scenario.

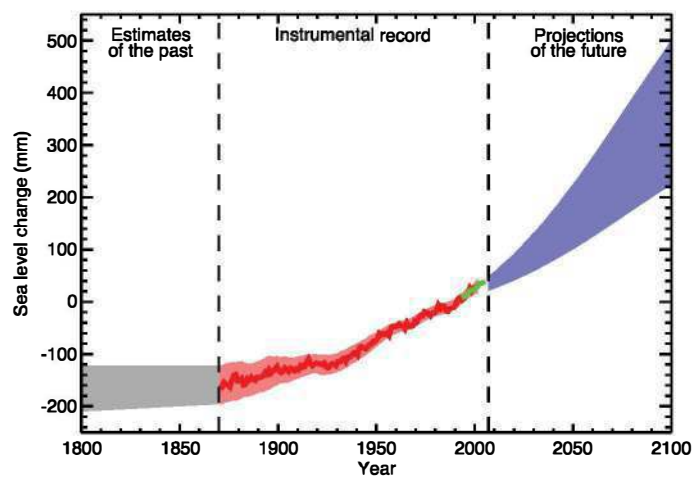

FAQ 5.1, Figure 1. *Time series of global mean sea level (deviation from the 1980-1999 mean) in the past and as projected for the future. For the period before 1870, global measurements of sea level are not available. The grey shading shows the uncertainty in the estimated long-term rate of sea level change (Section 6.4.3). The red line is a reconstruction of global mean sea level from tide gauges (Section 5.5.2.1), and the red shading denotes the range of variations from a smooth curve. The green line shows global mean sea level observed from satellite altimetry. The blue shading represents the range of model projections for the SRES A1B scenario for the 21st century, relative to the 1980 to 1999 mean, and has been calculated independently from the observations. Beyond 2100, the projections are increasingly dependent on the emissions scenario (see Chapter 10 for a discussion of sea level rise projections for other scenarios considered in this report). Over many centuries or millennia, sea level could rise by several metres (Section 10.7.4).*

The TAR chapter on sea level change provided estimates of climate and other anthropogenic contributions to 20th-century sea level rise, based mostly on models (Church et al., 2001). The sum of these contributions ranged from –0.8 to 2.2 mm yr^{-1}, with a mean value of 0.7 mm yr^{-1}, and a large part of this uncertainty was due to the lack of information on anthropogenic land water change. For observed 20th-century sea level rise, based on tide gauge records, Church et al. (2001) adopted as a best estimate a value in the range of 1 to 2 mm yr^{-1}, which was more than twice as large as the TAR's estimate of climate-related contributions. It thus appeared that either the processes causing sea level rise had been underestimated or the rate of sea level rise observed with tide gauges was biased towards higher values.

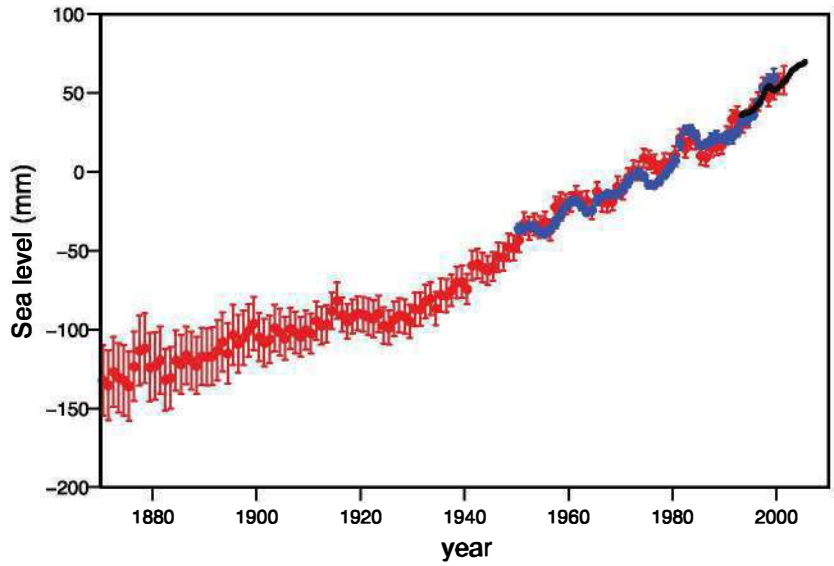

Figure 5.13. *Annual averages of the global mean sea level (mm). The red curve shows reconstructed sea level fields since 1870 (updated from Church and White, 2006); the blue curve shows coastal tide gauge measurements since 1950 (from Holgate and Woodworth, 2004) and the black curve is based on satellite altimetry (Leuliette et al., 2004). The red and blue curves are deviations from their averages for 1961 to 1990, and the black curve is the deviation from the average of the red curve for the period 1993 to 2001. Error bars show 90% confidence intervals.*

Since the TAR, a number of new results have been published. The global coverage of satellite altimetry since the early 1990s (TOPography EXperiment (TOPEX)/Poseidon and Jason) has improved the estimate of global sea level rise and has revealed the complex geographical patterns of sea level change in open oceans. Near-global ocean temperature data for the last 50 years have been recently made available, allowing the first observationally based estimate of the thermal expansion contribution to sea level rise in past decades. For recent years, better estimates of the land ice contribution to sea level are available from various observations of glaciers, ice caps and ice sheets.

In this section, we summarise the current knowledge of present-day sea level rise. The observational results are assessed, followed by our current interpretation of these observations in terms of climate change and other processes, and ending with a discussion of the sea level budget (Section 5.5.6).

5.5.2 Observations of Sea Level Changes

5.5.2.1 20th-Century Sea Level Rise from Tide Gauges

Table 11.9 of the TAR listed several estimates for global and regional 20th-century sea level trends based on the Permanent Service for Mean Sea Level (PSMSL) data set (Woodworth and Player, 2003). The concerns about geographical bias in the PSMSL data set remain, with most long sea level records stemming from the NH, and most from continental coastlines rather than ocean interiors. Based on a small number (~25) of high-quality tide gauge records from stable land regions, the rate of sea level rise has been estimated as 1.8 mm yr^{-1} for the past 70 years (Douglas, 2001; Peltier, 2001), and Miller and Douglas (2004) find a range of 1.5 to 2.0 mm yr^{-1} for the 20th century from 9 stable tide gauge sites. Holgate and Woodworth (2004) estimated a rate of 1.7 ± 0.4 mm yr^{-1} sea level change averaged along the global coastline during the period 1948 to 2002, based on data from 177 stations divided into 13 regions. Church et al. (2004) (discussed further below) determined a global rise of 1.8 ± 0.3 mm yr^{-1} during 1950 to 2000, and Church and White (2006) determined a change of 1.7 ± 0.3 mm yr^{-1} for the 20th century. Changes in global sea level as derived from analyses of tide gauges are displayed in Figure 5.13. Considering the above results, and allowing for the ongoing higher trend in recent years shown by altimetry (see Section 5.5.2.2), we assess the rate for 1961 to 2003 as 1.8 ± 0.5 mm yr^{-1} and for the 20th century as 1.7 ± 0.5 mm yr^{-1}.

While the recently published estimates of sea level rise over the last decades remain within the range of the TAR values (i.e., 1–2 mm yr^{-1}), there is an increasing opinion that the best estimate lies closer to 2 mm yr^{-1} than to 1 mm yr^{-1}. The lower bound reported in the TAR resulted from local and regional studies; local and regional rates may differ from the global mean, as discussed below (see Section 5.5.2.5).

A critical issue concerns how the records are adjusted for vertical movements of the land upon which the tide gauges are located and of the oceans. Trends in tide gauge records are corrected for GIA using models, but not for other land motions. The GIA correction ranges from about 1 mm yr^{-1} (or more) near to former ice sheets to a few tenths of a millimetre per year in the far field (e.g., Peltier, 2001); the error in tide-gauge based global average sea level change resulting from GIA is assessed as 0.15 mm yr^{-1}. The TAR mentioned the developing geodetic technologies (especially the Global Positioning System; GPS) that hold the promise of measuring rates of vertical land movement at tide gauges, no matter if those movements are due to GIA or to other geological processes. Although there has been some model validation, especially for GIA models, systematic problems with such techniques, including short data spans, have yet to be fully resolved.

5.5.2.2 *Sea Level Change during the Last Decade from Satellite Altimetry*

Since 1992, global mean sea level can be computed at 10-day intervals by averaging the altimetric measurements from the TOPEX/Poseidon (T/P) and Jason satellites over the area of coverage (66°S to 66°N) (Nerem and Mitchum, 2001). Each 10-day estimate of global mean sea level has an accuracy of approximately 5 mm. Numerous papers on the altimetry results (see Cazenave and Nerem, 2004, for a review) show a current rate of sea level rise of 3.1 ± 0.7 mm yr^{-1} over 1993 to 2003 (Cazenave and Nerem, 2004; Leuliette et al., 2004; Figure 5.14). A significant fraction of the 3 mm yr^{-1} rate of change has been shown to arise from changes in the Southern Ocean (Cabanes et al., 2001).

The accuracy needed to compute mean sea level change pushes the altimeter measurement system to its performance limits, and thus care must be taken to ensure that the instrument is precisely calibrated (see Appendix 5.A.4.1). The tide gauge calibration method (Mitchum, 2000) provides diagnoses of problems in the altimeter instrument, the orbits, the measurement corrections and ultimately the final sea level data. Errors in determining the altimeter instrument drift using the tide gauge calibration, currently estimated to be about 0.4 mm yr^{-1}, are almost entirely driven by errors in knowledge of vertical land motion at the gauges (Mitchum, 2000).

Altimetry-based sea level measurements include variations in the global ocean basin volume due to GIA. Averaged over the oceanic regions sampled by the altimeter satellites, this effect yields a value close to –0.3 mm yr^{-1} in sea level (Peltier, 2001), with possible uncertainty of 0.15 mm yr^{-1}. This number is subtracted from altimetry-derived global mean sea level in order to obtain the contribution due to ocean (water) volume change.

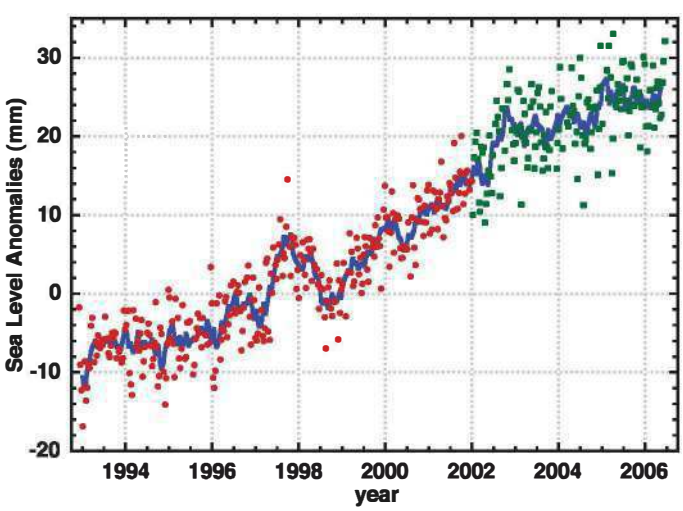

Figure 5.14. *Variations in global mean sea level (difference to the mean 1993 to mid-2001) computed from satellite altimetry from January 1993 to October 2005, averaged over 65°S to 65°N. Dots are 10-day estimates (from the TOPEX/Poseidon satellite in red and from the Jason satellite in green). The blue solid curve corresponds to 60-day smoothing. Updated from Cazenave and Nerem (2004) and Leuliette et al. (2004).*

Altimetry from T/P allows the mapping of the geographical distribution of sea level change (Figure 5.15a). Although regional variability in coastal sea level change had been reported from tide gauge analyses (e.g., Douglas, 1992; Lambeck, 2002), the global coverage of satellite altimetry provides unambiguous evidence of non-uniform sea level change in open oceans, with some regions exhibiting rates of sea level change about five times the global mean. For the past decade, sea level rise shows the highest magnitude in the western Pacific and eastern Indian oceans, regions that exhibit large interannual variability associated with ENSO. Except for the Gulf Stream region, most of the Atlantic Ocean shows sea level rise during the past decade. Despite the global mean rise, Figure 5.15a shows that sea level has been dropping in some regions (eastern Pacific and western Indian Oceans). These spatial patterns likely reflect decadal fluctuations rather than long-term trends. Empirical Orthogonal Functions (EOF) analyses of altimetry-based sea level maps over 1993 to 2003 show a strong influence of the 1997–1998 El Niño, with the geographical patterns of the dominant mode being very similar to those of the sea level trend map (e.g., Nerem et al., 1999).

5.5.2.3 *Reconstructions of Sea Level Change during the Last 50 Years Based on Satellite Altimetry and Tide Gauges*

Attempts have been made to reconstruct historical sea level fields by combining the near-global coverage from satellite altimeter data with the longer but spatially sparse tide gauge records (Chambers et al., 2002; Church et al., 2004). These sea level reconstructions use the short altimeter record to determine the principal EOF of sea level variability, and the tide gauge data to estimate the evolution of the amplitude of the EOFs over time. The method assumes that the geographical patterns of decadal sea level trends can be represented by a superposition of the patterns of variability that are manifest in interannual variability. The sea level for the period 1870 to 2000 (Church and White, 2006) shown in Figure 5.13 is based on this approach. As a caveat, note that variability on different time scales may have different characteristic patterns (see Section 5.5.4.1).

The trends in the EOF amplitudes (and the implied global correlations) allow the reconstruction of a spatially variable rate of sea level rise. Figure 5.16a (updated from Church et al., 2004) shows the geographical distribution of linear sea level trends for 1955 to 2003 based on this reconstruction technique. Comparison with the altimetry-based trend map for the shorter period (1993 to 2003) indicates quite different geographical patterns. These differences mainly arise from thermal expansion changes through time (see Section 5.5.3)

Changes in spatial sea level patterns through time may help reconcile apparently inconsistent estimates of regional variations in tide-gauge based sea level rise. For example, the minimum in rise along the northwest Australian coast is consistent with the results of Lambeck (2002) in having smaller rates of sea level rise and indeed sea level fall off north-western Australia over the last few decades. In addition, for the North Atlantic Ocean,

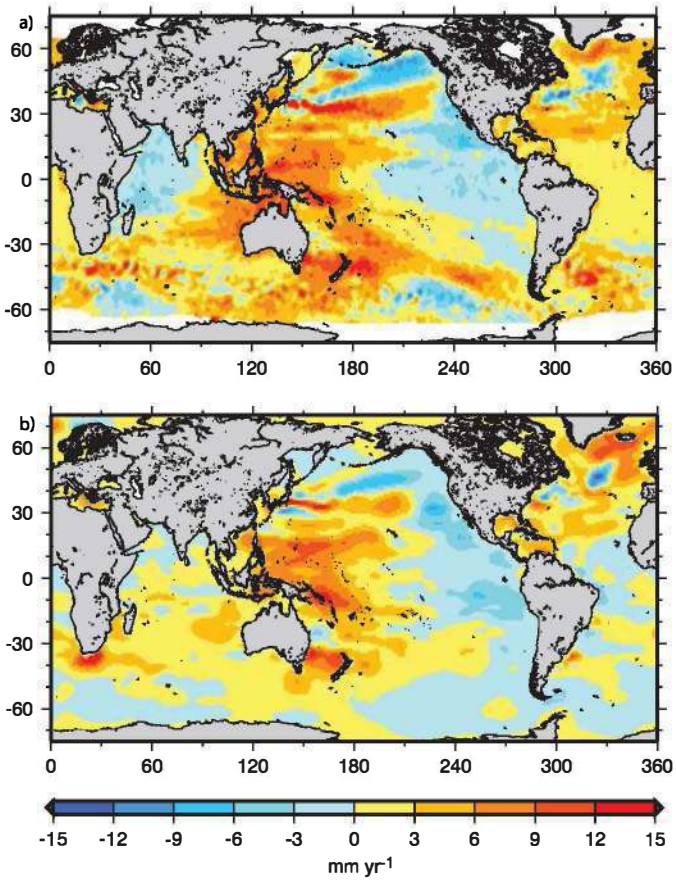

Figure 5.15. *(a) Geographic distribution of short-term linear trends in mean sea level (mm yr^{-1}) for 1993 to 2003 based on TOPEX/Poseidon satellite altimetry (updated from Cazenave and Nerem, 2004) and (b) geographic distribution of linear trends in thermal expansion (mm yr^{-1}) for 1993 to 2003 (based on temperature data down to 700 m from Ishii et al., 2006).*

the rate of rise reaches a maximum (over 2 mm yr^{-1}) in a band running east-northeast from the US east coast. The trends are lower in the eastern than in the western Atlantic (Lambeck et al., 1998; Woodworth et al., 1999; Mitrovica et al., 2001).

5.5.2.4 Interannual and Decadal Variability and Long-Term Changes in Sea Level

Sea level records contain a considerable amount of interannual and decadal variability, the existence of which is coherent throughout extended parts of the ocean. For example, the global sea level curve in Figure 5.13 shows an approximately 10 mm rise and fall of global mean sea level accompanying the 1997–1998 ENSO event. Over the past few decades, the time series of the first EOF of Church et al. (2004) represents ENSO variability, as shown by a significant (negative) correlation with the Southern Oscillation Index. The signature of the 1997–1998 El Niño is also clear in the altimetric maps of sea level anomalies (see Section 5.5.2.2). Model results suggest that large volcanic eruptions produce interannual to decadal fluctuations in the global mean sea level (see Section 9.5.2).

Holgate and Woodworth (2004) concluded that the 1990s had one of the fastest recorded rates of sea level rise averaged along the global coastline (~4 mm yr^{-1}), slightly higher than the altimetry-based open ocean sea level rise (3 mm yr^{-1}). However, their analysis also shows that some previous decades had comparably large rates of coastal sea level rise (e.g., around 1980; Figure 5.17). White et al. (2005) confirmed the larger sea level rise during the 1990s around coastlines compared to the open ocean but found that in some previous periods the coastal rate was smaller than the open ocean rate, and concluded that over the last 50 years the coastal and open ocean rates of change were the same on average. The global reconstruction of Church et al. (2004) and Church and White (2006) also exhibits large decadal variability in the rate of global mean sea level rise, and the 1993 to 2003 rate has been exceeded in some previous decades (Figure 5.17). The variability is smaller in the global reconstruction (standard deviation of overlapping 10-year rates is 1.1 mm yr^{-1}) than in the Holgate and Woodworth (2004) coastal time series (standard deviation 1.7 mm yr^{-1}). The rather

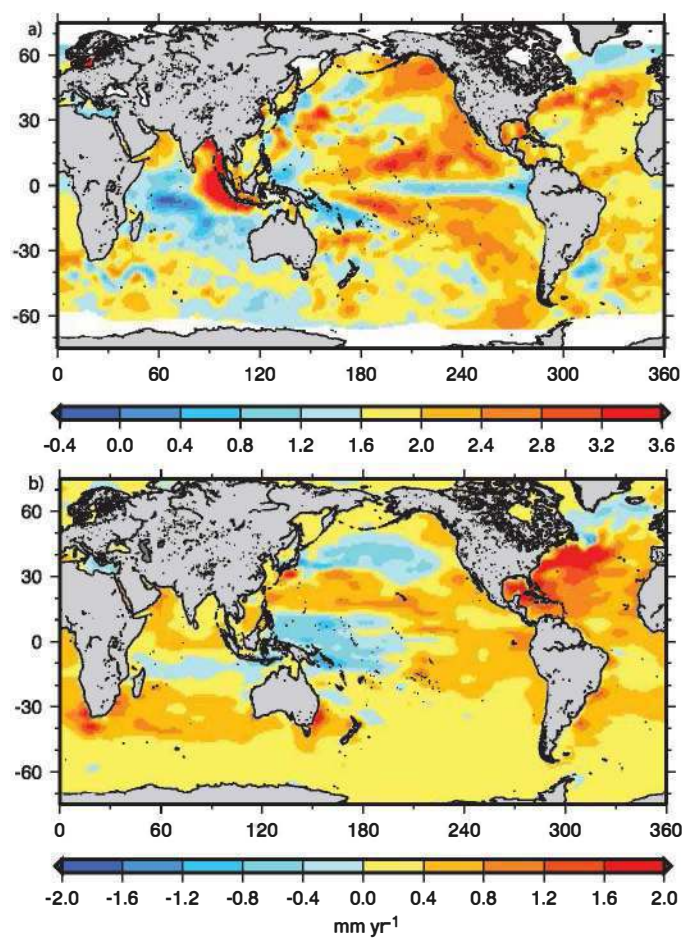

Figure 5.16. *(a) Geographic distribution of long-term linear trends in mean sea level (mm yr^{-1}) for 1955 to 2003 based on the past sea level reconstruction with tide gauges and altimetry data (updated from Church et al., 2004) and (b) geographic distribution of linear trends in thermal expansion (mm yr^{-1}) for 1955 to 2003 (based on temperature data down to 700 m from Ishii et al., 2006). Note that colours in (a) denote 1.6 mm yr^{-1} higher values than those in (b).*

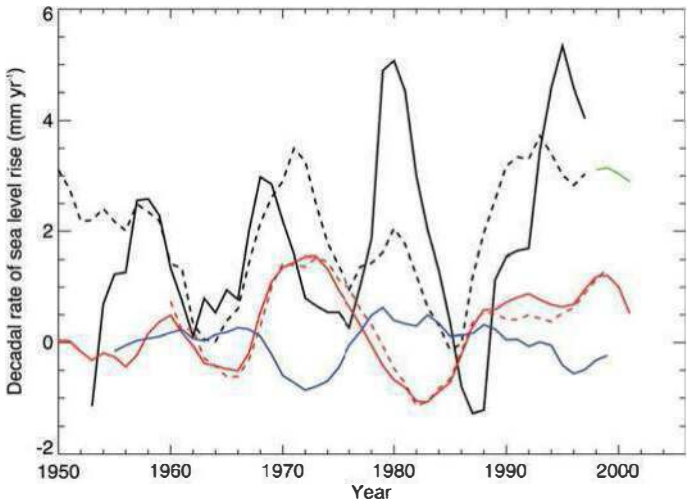

Figure 5.17. *Overlapping 10-year rates of global sea level change from tide gauge data sets (Holgate and Woodworth, 2004, in solid black; Church and White, 2006, in dashed black) and satellite altimetry (updated from Cazenave and Nerem, 2004, in green), and contributions to global sea level change from thermal expansion (Ishii et al., 2006, in solid red; Antonov et al., 2005, in dashed red) and climate-driven land water storage (Ngo-Duc et al., 2005, in blue). Each rate is plotted against the middle of its 10-year period.*

low temporal correlation (r = 0.44) between the two time series suggests that the statistical uncertainty in the linear trends calculated from either data set probably underestimates the systematic uncertainty in the results (Section 5.5.6).

Interannual or longer variability is a major reason why no long-term acceleration of sea level has been identified using 20th-century data alone (Woodworth, 1990; Douglas, 1992). Another possibility is that the sparse tide gauge network may have been inadequate to detect it if present (Gregory et al., 2001). The longest records available from Europe and North America contain accelerations of the order of 0.4 mm yr^{-1} per century between the 19th and 20th century (Ekman, 1988; Woodworth et al., 1999). For the reconstruction shown in Figure 5.13, Church and White (2006) found an acceleration of 1.3 ± 0.5 mm yr^{-1} per century over the period 1870 to 2000. These data support an inference that the onset of acceleration occurred during the 19th century (see Section 9.5.2).

Geological observations indicate that during the last 2,000 years (i.e., before the recent rise recorded by tide gauges), sea level change was small, with an average rate of only 0.0 to 0.2 mm yr^{-1} (see Section 6.4.3). The use of proxy sea level data from archaeological sources is well established in the Mediterranean. Oscillations in sea level from 2,000 to 100 yr before present did not exceed ±0.25 m, based on the Roman-Byzantine-Crusader well data (Sivan et al., 2004). Many Roman and Greek constructions are relatable to the level of the sea. Based on sea level data derived from Roman fish ponds, which are considered to be a particularly reliable source of such information, together with nearby tide gauge records, Lambeck et al. (2004) concluded that the onset of the modern sea level rise occurred between 1850 and 1950. Donnelly et al. (2004) and Gehrels et al. (2004), employing geological data from Connecticut, Maine and Nova Scotia salt-marshes together with nearby tide gauge records, demonstrated that the sea level rise observed during the 20th century was in excess of that averaged over the previous several centuries.

The joint interpretation of the geological observations, the longest instrumental records and the current rate of sea level rise for the 20th century gives a clear indication that the rate of sea level rise has increased between the mid-19th and the mid-20th centuries.

5.5.2.5 Regional Sea Level Change

Two regions are discussed here to give examples of local variability in sea level: the northeast Atlantic and small Pacific Islands.

Interannual variability in northeast Atlantic sea level records exhibits a clear relationship to the air pressure and wind changes associated with the NAO, with the magnitude and sign of the response depending primarily upon latitude (Andersson, 2002; Wakelin et al., 2003; Woolf et al., 2003). The signal of the NAO can also be observed to some extent in ocean temperature records, suggesting a possible, smaller NAO influence on regional mean sea level via steric (density) changes (Tsimplis et al., 2006). In the Russian Arctic Ocean, sea level time series for recent decades also have pronounced decadal variability that correlates with the NAO index. In this region, wind stress and atmospheric pressure loading contribute nearly half of the observed sea level rise of 1.85 mm yr^{-1} (Proshutinsky et al., 2004).

Small Pacific Islands are the subject of much concern in view of their vulnerability to sea level rise. The Pacific Ocean region is the centre of the strongest interannual variability of the climate system, the coupled ocean-atmosphere ENSO mode. There are only a few Pacific Island sea level records extending back to before 1950. Mitchell et al. (2001) calculated rates of relative sea level rise for the stations in the Pacific region. Using their results (from their Table 1) and focusing on only the island stations with more than 50 years of data (only 4 locations), the average rate of sea level rise (relative to the Earth's crust) is 1.6 mm yr^{-1}. For island stations with record lengths greater than 25 years (22 locations), the average rate of relative sea level rise is 0.7 mm yr^{-1}. However, these data sets contain a large range of rates of relative sea level change, presumably as a result of poorly quantified vertical land motions.

An example of the large interannual variability in sea level is Kwajalein (8°44'N, 167°44'E) (Marshall Archipelago). As shown in Figure 5.18, the local tide gauge data, the sea level reconstructions of Church et al. (2004) and Church and White (2006) and the shorter satellite altimeter record all agree and indicate that interannual variations associated with ENSO events are greater than 0.2 m. The Kwajalein data also suggest increased variability in sea level after the mid-1970s, consistent with the trend towards more frequent, persistent and intense ENSO events since the mid-1970s (Folland et al., 2001). For the Kwajalein record, the rate of sea level rise, after correction for GIA land motions and isostatic response to atmospheric pressure changes, is 1.9 ± 0.7 mm yr^{-1}. However,

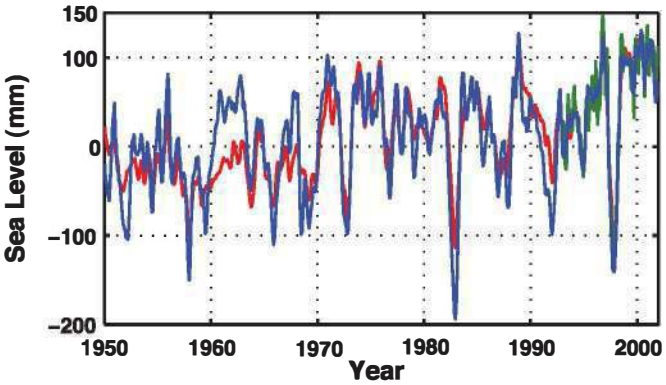

Figure 5.18. *Monthly mean sea level curve for 1950 to 2000 at Kwajalein (8°44'N, 167°44'E). The observed sea level (from tide gauge measurements) is in blue, the reconstructed sea level in red and the satellite altimetry record in green. Annual and semi-annual signals have been removed from each time series and the tide gauge data have been smoothed. The figure was drawn using techniques in Church et al. (2004) and Church and White (2006).*

the uncertainties in rates of sea level change increase rapidly with decreasing record length and can be several mm yr^{-1} for decade-long records (depending on the magnitude of the interannual variability). Sea level change on the atolls of Tuvalu (western Pacific) has been the subject of intense interest as a result of their low-lying nature and increasing incidence of flooding. There are two records available at Funafuti, Tuvalu; the first record commences in 1977 and the second (with rigorous datum control) in 1993. After allowing for subsidence affecting the first record, Church et al. (2006) estimate sea level rise at Tuvalu to be 2.0 ± 1.7 mm yr^{-1}, in agreement with the reconstructed rate of sea level rise.

5.5.2.6 Changes in Extreme Sea Level

Societal impacts of sea level change primarily occur via the extreme levels rather than as a direct consequence of mean sea level changes. Apart from non-climatic events such as tsunamis, extreme sea levels occur mainly in the form of storm surges generated by tropical or extra tropical cyclones. Secular changes and decadal variability in storminess are discussed in Chapter 3. Studies of variations in extreme sea levels during the 20th century based on tide gauge data are fewer than studies of changes in mean sea level for several reasons. A study on changes in extremes, which are caused by changes in mean sea level as well as changes in surges, is more complex than the study of mean sea level changes. Moreover, the hourly sampling interval normally used in tide gauge records is not always sufficient to accurately capture the true extreme. Among the different parameters often used to describe extremes, annual maximum surge is a good indicator of climatic trends. For study of long records extending back to the 19th century or before, annual maximum surge-at-high-water (defined as the maximum of the difference between observed high water and the predicted tide at high water) is a better-suited parameter because during that period high waters and not the full tidal curve were recorded.

Studies of the longest records of extremes are inevitably restricted to a small number of locations. From observed sea level extremes at Liverpool since 1768, Woodworth and Blackman (2002) concluded that the annual maximum surge-at-high-water was larger in the late 18th, late 19th and late 20th centuries than for most of the 20th century, qualitatively consistent with the long-term variability in storminess from meteorological data. From the tide gauge record at Brest from 1860 to 1994, Bouligand and Pirazzoli (1999) found an increasing trend in annual maxima and 99th percentile of surges; however, a decreasing trend was found during the period 1953 to 1994. From non-tidal residuals ('surges') at San Francisco since 1858, Bromirski et al. (2003) concluded that extreme winter residuals have exhibited a significant increasing trend since about 1950, a trend that is attributed to an increase in storminess during this period. Zhang et al. (2000) concluded from records at 10 stations along the east coast of the USA since 1900 that the rise in extreme sea level closely followed the rise in mean sea level. A similar conclusion can be drawn from a recent study of Firing and Merrifield (2004), who found long-term increases in the number and height of daily extremes at Honolulu (interestingly, the highest-ever value being due an anticyclonic oceanic eddy system in 2003), but no evidence for an increase relative to the underlying upward mean sea level trend.

An analysis of 99th percentiles of hourly sea level at 141 stations over the globe for recent decades (Woodworth and Blackman, 2004) showed that there is evidence for an increase in extreme high sea level worldwide since 1975. In many cases, the secular changes in extremes were found to be similar to those in mean sea level. Likewise, interannual variability in extremes was found to be correlated with regional mean sea level, as well as to indices of regional climate patterns.

5.5.3 Ocean Density Changes

Sea level will rise if the ocean warms and fall if it cools, since the density of the water column will change. If the thermal expansivity were constant, global sea level change would parallel the global ocean heat content discussed in Section 5.2. However, since warm water expands more than cold water (with the same input of heat), and water at higher pressure expands more than at lower pressure, the global sea level change depends on the three-dimensional distribution of ocean temperature change.

Analysis of the last half century of temperature observations indicates that the ocean has warmed in all basins (see Section 5.2). The average rate of thermosteric sea level rise caused by heating of the global ocean is estimated to be 0.40 ± 0.09 mm yr^{-1} over 1955 to 1995 (Antonov et al., 2005), based on five-year mean temperature data down to 3,000 m. For the 0 to 700 m layer and the 1955 to 2003 period, the averaged thermosteric trend, based on annual mean temperature data from Levitus et al. (2005a), is 0.33 ± 0.07 mm yr^{-1} (Antonov et al., 2005). For the same period and depth range, the mean thermosteric rate based on monthly ocean temperature data from Ishii et al. (2006) is 0.36 ± 0.12 mm yr^{-1}. Figure 5.19

shows the thermosteric sea level curve over 1955 to 2003 for both the Levitus and Ishii data sets. The rate of thermosteric sea level rise is clearly not constant in time and shows considerable fluctuations (Figure 5.17). A rise of more than 20 mm occurred from the late 1960s to the late 1970s (giving peak 10-year rates in the early 1970s) with a smaller drop afterwards. Another large rise began in the 1990s, but after 2003, the steric sea level is decreasing in both estimates (peak rates in the late 1990s). Overlapping 10-year rates from these two estimates have a very high temporal correlation (r = 0.97) and the standard deviation of the rates is 0.7 mm yr^{-1}.

The Levitus and Ishii data sets both give 0.32 ± 0.09 mm yr^{-1} for the upper 700 m during 1961 to 2003, but the Levitus data set of temperature down to 3,000 m ends in 1998. From the results of Antonov et al. (2005) for thermal expansion, the difference between the trends in the upper 3,000 m and the upper 700 m for 1961 to 1998 is about 0.1 mm yr^{-1}. Assuming that the ocean below 700 m continues to contribute beyond 1998 at a similar rate, with an uncertainty similar to that of the upper-ocean contribution, we assess the thermal expansion of the ocean down to 3,000 m during 1961 to 2003 as 0.42 ± 0.12 mm yr^{-1}.

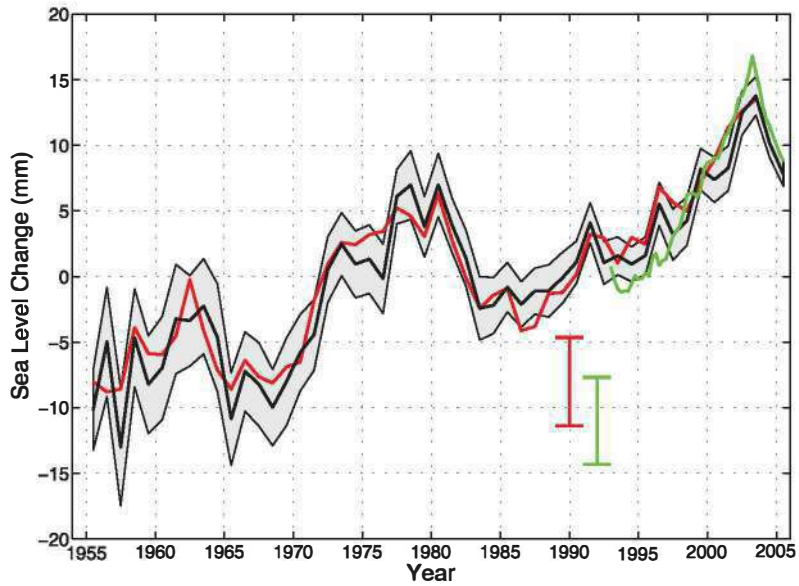

Figure 5.19. *Global sea level change due to thermal expansion for 1955 to 2003, based on Levitus et al. (2005a; black line) and Ishii et al. (2006; red line) for the 0 to 700 m layer, and based on Willis et al. (2004; green line) for the upper 750 m. The shaded area and the vertical red and green error bars represent the 90% confidence interval. The black and red curves denote the deviation from their 1961 to 1990 average, the shorter green curve the deviation from the average of the black curve for the period 1993 to 2003.*

For the recent period 1993 to 2003, a value of 1.2 ± 0.5 mm yr^{-1} for thermal expansion in the upper 700 m is estimated both by Antonov et al. (2005) and Ishii et al. (2006). Willis et al. (2004) estimate thermal expansion to be 1.6 ± 0.5 mm yr^{-1}, based on combined *in situ* temperature profiles down to 750 m and satellite measurements of altimetric height. Including the satellite data reduces the error caused by the inadequate sampling of the profile data. Error bars were estimated to be about 2 mm for individual years in the time series, with most of the remaining error due to inadequate profile availability. A close result (1.8 ± 0.4 mm yr^{-1} steric sea level rise for 1993 to 2003) was recently obtained by Lombard et al. (2006), based on a combined analysis of *in situ* hydrographic data and satellite sea surface height and SST data (Guinehut et al., 2004). It is presently unclear why the latter two estimates are significantly larger than the thermosteric rates based on temperature data alone. It is possible that the *in situ* data underestimate thermal expansion because of poor coverage in Southern Oceans, and it is interesting to note that a model based on assimilation of hydrographic data yields a somewhat higher estimate of 2.3 mm yr^{-1} (Carton et al., 2005). Published estimates of the steric sea level rates for 1955 to 2003 and 1993 to 2003 are shown in Table 5.2.

We assess the thermal expansion of the upper 700 m during 1993 to 2003 as 1.5 ± 0.5 mm yr^{-1}, and that of the upper 3,000 m as 1.6 ± 0.5 mm yr^{-1}, allowing for the ocean below 700 m as for the earlier period (see also Section 5.5.6, Table 5.3).

Table 5.2. *Recent estimates for steric sea level trends from different studies.*

Reference	Steric sea level change with errors (mm yr^{-1})	Period	Depth range (m)	Data Source
Antonov et al. (2005)	0.40 ± 0.09	1955–1998	0–3,000	Levitus et al. (2005b)
Antonov et al. (2005)	0.33 ± 0.07	1955–2003	0–700	Levitus et al. (2005b)
Ishii et al. (2006)	0.36 ± 0.06	1955–2003	0–700	Ishii et al. (2006)
Antonov et al. (2005)	1.2 ± 0.5	1993–2003	0–700	Levitus et al. (2005b)
Ishii et al. (2006)	1.2 ± 0.5	1993–2003	0–700	Ishii et al. (2006)
Willis et al. (2004)	1.6 ± 0.5	1993–2003	0–750	Willis et al. (2004)
Lombard et al. (2006)	1.8 ± 0.4	1993-2003	0-700	Guinehut et al. (2004)

Antonov et al. (2002) attributed about 10% of the global average steric sea level rise during recent decades to halosteric expansion (i.e., the volume increase caused by freshening of the water colunm). A similar result was obtained by Ishii et al. (2006) who estimated a halosteric contribution to 1955 to 2003 sea level rise of 0.04 ± 0.02 mm yr^{-1}. While it is of interest to quantify this effect, only about 1% of the halosteric expansion contributes to the global sea level rise budget. This is because the halosteric expansion is nearly compensated by a decrease in volume of the added freshwater when its salinity is raised (by mixing) to the mean ocean value; the compensation would be exact for a linear state equation (Gille, 2004; Lowe and Gregory, 2006). Hence, for global sums of sea level change, halosteric expansion cannot be counted separately from the volume of added land freshwater (which Antonov et al., 2002, also calculate; see Section 5.5.5.1). However, for regional changes in sea level, thermosteric and halosteric contributions can be comparably important (see, e.g., Section 5.5.4.1).

5.5.4 Interpretation of Regional Variations in the Rate of Sea Level Change

Sea level observations show that whatever the time span considered, rates of sea level change display considerable regional variability (see Sections 5.5.2.2 and 5.5.2.3). A number of processes can cause regional sea level variations.

5.5.4.1 Steric Sea Level Changes

Like the sea level trends observed by satellite altimetry (see Section 5.5.2.3), the global distribution of thermosteric sea level trends is not spatially uniform. This is illustrated by Figure 5.15b and Figure 5.16b, which show the geographical distribution of thermosteric sea level trends over two different periods, 1993 to 2003 and 1955 to 2003 respectively (updated from Lombard et al., 2005). Some regions experienced sea level rise while others experienced a fall, often with rates that are several times the global mean. However, the patterns of thermosteric sea level rise over the approximately 50-year period are different from those seen in the 1990s. This occurs because the spatial patterns, like the global average, are also subject to decadal variability. In other words, variability on different time scales may have different characteristic patterns.

An EOF analysis of gridded thermosteric sea level time series since 1955 (updated from Lombard et al., 2005) displays a spatial pattern that is similar to the spatial distribution of thermosteric sea level trends over the same time span (compare Figure 5.20 with Figure 5.16b). In addition, the first principal component is negatively correlated with the Southern Oscillation Index. Thus, it appears that ENSO-related ocean variability accounts for the largest fraction of variance in spatial patterns of thermosteric sea level. Similarly, decadal thermosteric sea level in the North Pacific and North Atlantic appears strongly influenced by the PDO and NAO respectively.

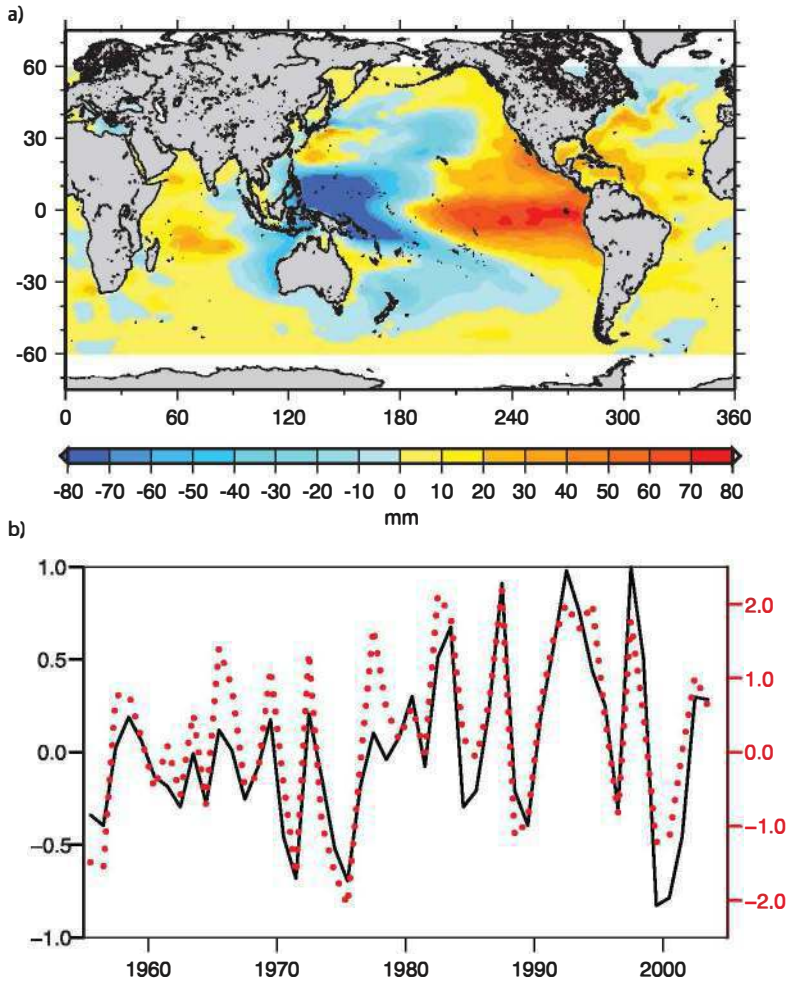

Figure 5.20. *(a) First mode of the EOF decomposition of the gridded thermosteric sea level time series of yearly temperature data down to 700 m from Ishii et al. (2006). (b) The normalised principal component (black solid curve) is highly correlated with the negative Southern Oscillation Index (dotted red curve).*

For the recent years (1993–2003), the geographic distribution of observed sea level trends (Figure 5.15a) shows correlation with the spatial patterns of thermosteric sea level change (Figure 5.15b). This suggests that at least part of the non-uniform pattern of sea level rise observed in the altimeter data over the past decade can be attributed to changes in the ocean's thermal structure, which is itself driven by surface heating effects and ocean circulation. Note that the steric changes due to salinity changes have not been included in these figures due to insufficient salinity data in parts of the World Ocean.

Ocean salinity changes, while unimportant for sea level at the global scale, can have an effect on regional sea level (e.g., Antonov et al., 2002; Ishii et al., 2006; Section 5.5.3). For example, in the subpolar gyre of the North Atlantic, especially in the Labrador Sea, the halosteric contribution nearly

counteracts the thermosteric contribution. This observational result is supported by results from data assimilation into models (e.g., Stammer et al., 2003). Since density changes can result not only from surface buoyancy fluxes but also from the wind, a simple attribution of density changes to buoyancy forcing is not possible.

While much of the non-uniform pattern of sea level change can be attributed to thermosteric volume changes, the difference between observed and thermosteric spatial trends show a high residual signal in a number of regions, especially in the southern oceans. Part of these residuals is likely due to the lack of ocean temperature coverage in remote oceans as well as in deep layers (below 700 m), and to regional salinity change.

5.5.4.2 Ocean Circulation Changes

The highly non-uniform geographical distribution of steric sea level trends is closely connected, through geostrophic balance, with changes in ocean surface circulation. Density and circulation changes result from changes in atmospheric forcing that is primarily by surface wind stress and buoyancy flux (i.e., heat and freshwater fluxes). The wind alone can therefore cause local (but not global) changes in steric sea level. Ocean general circulation models based on the assimilation of ocean data satisfactorily reproduce the spatial structure of sea level trends for the past decade, and show in particular that the tropical Pacific pattern results from decadal fluctuations in the depth of the tropical thermocline and change in equatorial trade winds (Carton et al., 2005; Köhl et al., 2006). The similarity of the patterns of steric and actual sea level change indicates that density changes are the dominant influence. Discrepancies may indicate a significant contribution from changes in the wind-driven barotropic circulation, especially at high latitudes.

5.5.4.3 Surface Atmospheric Pressure Changes

Surface atmospheric pressure also causes regional sea level variations. Over time scales longer than a few days, the ocean adjusts nearly isostatically to changes in atmospheric pressure (inverted barometer effect), that is, for each 1 hPa sea level pressure increase the ocean is depressed by approximately 10 mm, shifting the underlying mass sideways to other regions. For the temporal average, regional changes in sea level caused by atmospheric pressure loading reach about 0.2 m (e.g., between the subtropical Atlantic and the subpolar Atlantic). Such effects are generally corrected for in tide gauge and altimetry-based sea level analyses. The inverted barometer effect has a negligible effect on global mean sea level, because water is nearly incompressible, but is significant when averaged over the area of T/P and Jason-1 altimetry, which does not cover the whole World Ocean (Ponte, 2006). For that reason, the altimetry-based mean sea level curve is corrected for the inverted barometer effect.

5.5.4.4 Solid Earth and Geoid Changes

Geodynamical processes related to the solid Earth's elastic and viscoelastic response to spatially variable ice melt loading (due to the last deglaciation and present-day land ice melt) also cause non-uniform sea level change (e.g., Mitrovica et al., 2001; Peltier, 2001, 2004; Plag, 2006). The solid Earth and oceans continue to respond to the ice and complementary water loads associated with the late Pleistocene and early Holocene glacial cycles through GIA. This process not only drives large crustal uplift near the location of former ice complexes, but also produces a worldwide signature in sea level that results from gravitational, deformational and rotational effects: as the viscous mantle material flows to restore isostasy during and after the last deglaciation, uplift occurs under the former centres of the ice sheets while the surrounding peripheral bulges experience a subsidence. The return of the melt water to the oceans produces an ongoing geoid change resulting in subsidence of the ocean basins and an upward warping of the continents, while the flow of water into the subsiding peripheral bulges contributes a broad scale sea level fall in the far field of the ice complexes. The combined gravitational and deformational effects also perturb the rotation vector of the planet, and this perturbation feeds back into variations in the position of the crust and the geoid (an equipotential surface of the Earth's gravity field that coincides with the mean surface of the oceans). Corrections for GIA effects are made to both tide gauge and altimeter estimates of global sea level change (see Sections 5.5.2.1 and 5.5.2.2).

Self-gravitation and deformation of the Earth's surface in response to the ongoing change in loading by glaciers and ice sheets is another cause of regional sea level variations. Model predictions show quite different patterns of non-uniform sea level change depending on the source of the ice melt (Mitrovica et al., 2001; Plag, 2006), and associated regional sea level variations reach up to a few 0.1 mm yr^{-1}.

5.5.5 Ocean Mass Change

Global mean sea level will rise if water is added to the ocean from other reservoirs in the climate system. Water storage in the atmosphere is equivalent to only about 35 mm of global mean sea level, and the observed atmospheric storage trend of about 0.04 mm yr^{-1} in recent decades (Section 3.4.2.1) is unimportant compared with changes in ice and water stored on land, described in this subsection. Variations in land water storage result from variations in climatic conditions, direct human intervention in the water cycle and human modification of the land surface.

5.5.5.1 Ocean Mass Change Estimated from Salinity Change

Global salinity changes can be caused by changes in the global sea ice volume (which do not influence sea level) and by ocean mass changes (which do). Thus in principle, global salinity

changes can be used to estimate the global average sea level change due to fresh water input (Antonov et al., 2002; Munk, 2003; Wadhams and Munk, 2004). However, the accuracy of these estimates depends on the accuracy of the estimates for both sea ice volume (Hilmer and Lemke, 2000; Wadhams and Munk, 2004; see also Section 4.4) and global salinity change (Section 5.2.3). We assess that the error in estimates of ocean mass changes derived from salinity changes and sea ice melt is too large to provide useful constraints on the sea level change budget (Section 5.5.6).

5.5.5.2 Land Ice

During the 20th century, glaciers and ice caps have experienced considerable mass losses, with strong retreats in response to global warming after 1970. For 1961 to 2003, their contribution to sea level is assessed as 0.50 ± 0.18 mm yr^{-1} and for 1993 to 2003 as 0.77 ± 0.22 mm yr^{-1} (see Section 4.5.2).

As discussed in Section 4.6.2.2 and Table 4.6, the Greenland Ice Sheet has also been losing mass in recent years, contributing 0.05 ± 0.12 mm yr^{-1} to sea level rise during 1961 to 2003 and 0.21 ± 0.07 mm yr^{-1} during 1993 to 2003. Assessments of contributions to sea level rise from the Antarctic Ice Sheet are less certain, especially before the advent of satellite measurements, and are 0.14 ± 0.41 mm yr^{-1} for 1961 to 2003 and 0.21 ± 0.35 mm yr^{-1} for 1993 to 2003. Geodetic data on Earth rotation and polar wander allow a late-20th century sea level contribution of up to about 1 mm yr^{-1} from land ice (Mitrovica et al., 2006). However, recent estimates of ice sheet mass change exclude the large contribution inferred for Greenland by Mitrovica et al. (2001) from the geographical pattern of sea level change, confirming the lower rates reported above.

5.5.5.3 Climate-Driven Change in Land Water Storage

Continental water storage includes water (both liquid and solid) stored in subsurface saturated (groundwater) and unsaturated (soil water) zones, in the snowpack, and in surface water bodies (lakes, artificial reservoirs, rivers, floodplains and wetlands). Changes in concentrated stores, most notably very large lakes, are relatively well known from direct observation. In contrast, global estimates of changes in distributed surface stores (soil water, groundwater, snowpack and small areas of surface water) rely on computations with detailed hydrological models coupled to global ocean-atmosphere circulation models or forced by observations. Such models estimate the variation in land water storage by solving the water balance equation. The Land Dynamics (LaD) model developed by Milly and Shmakin (2002) provides global 1° by 1° monthly gridded time series of root zone soil water, groundwater and snowpack for the last two decades. With these data, the contributions of time-varying land water storage to sea level rise in response to climate change have been estimated, resulting in a small positive sea level trend of about 0.12 mm yr^{-1} for the last two decades, with larger interannual and decadal fluctuations (Milly et al., 2003). From a land surface model forced by a global climatic data set based on standard reanalysis products and on observations, land water changes during the past five decades were found to have low-frequency (decadal) variability of about 2 mm in amplitude but no significant trend (Ngo-Duc et al., 2005). These decadal variations are related to groundwater and are caused by precipitation variations. They are strongly negatively correlated with the de-trended thermosteric sea level (Figure 5.17). This suggests that the land water contribution to sea level and thermal expansion partly compensate each other on decadal time scales. However, this conclusion depends on the accuracy of the precipitation in reanalysis products.

5.5.5.4 Anthropogenic Change in Land Water Storage

The amount of anthropogenic change in land water storage systems cannot be estimated with much confidence, as already discussed by Church et al. (2001). A number of factors can contribute to sea level rise. First, natural groundwater systems typically are in a condition of dynamic equilibrium where, over long time periods, recharge and discharge are in balance. When the rate of groundwater pumping greatly exceeds the rate of recharge, as is often the case in arid or even semi-arid regions, water is removed permanently from storage. The water that is lost from groundwater storage eventually reaches the ocean through the atmosphere or surface flow, resulting in sea level rise. Second, wetlands contain standing water, soil moisture and water in plants equivalent to water roughly 1 m deep. Hence, wetland destruction contributes to sea level rise. Over time scales shorter than a few years, diversion of surface waters for irrigation in the internally draining basins of arid regions results in increased evaporation. The water lost from the basin hydrologic system eventually reaches the ocean. Third, forests store water in living tissue both above and below ground. When a forest is removed, transpiration is eliminated so that runoff is favoured in the hydrologic budget.

On the other hand, impoundment of water behind dams removes water from the ocean and lowers sea level. Dams have led to a sea level drop over the past few decades of –0.5 to –0.7 mm yr^{-1} (Chao, 1994; Sahagian et al., 1994). Infiltration from dams and irrigation may raise the water table, storing more water. Gornitz (2001) estimated –0.33 to –0.27 mm yr^{-1} sea level change equivalent held by dams (not counting additional potential storage due to subsurface infiltration).

It is very difficult to provide accurate estimates of the net anthropogenic contribution, given the lack of worldwide information on each factor, although the effect caused by dams is possibly better known than other effects. According to Sahagian (2000), the sum of the above effects could be of the order of 0.05 mm yr^{-1} sea level rise over the past 50 years, with an uncertainty several times as large.

In summary, our assessment of the land hydrology contribution to sea level change has not led to a reduction in the uncertainty compared to the TAR, which estimated the rather wide ranges of –1.1 to +0.4 mm yr^{-1} for 1910 to 1990

and –1.9 to +1.0 mm yr^{-1} for 1990. However, indirect evidence from considering other contributions to the sea level budget (see Section 5.5.6) suggests that the land contribution either is small (<0.5 mm yr^{-1}) or is compensated for by unaccounted or underestimated contributions.

5.5.6 Total Budget of the Global Mean Sea Level Change

The various contributions to the budget of sea level change are summarised in Table 5.3 and Figure 5.21 for 1961 to 2003 and 1993 to 2003. Some terms known to be small have been omitted, including changes in atmospheric water vapour and climate-driven change in land water storage (Section 5.5.5), permafrost and sedimentation (see, e.g., Church et al., 2001), which very likely total less than 0.2 mm yr^{-1}. The poorly known anthropogenic contribution from terrestrial water storage (see Section 5.5.5.4) is also omitted.

For 1961 to 2003, thermal expansion accounts for only 23 ± 9% of the observed rate of sea level rise. Miller and Douglas (2004) reached a similar conclusion by computing steric sea level change over the past 50 years in three oceanic regions (northeast Pacific, northeast Atlantic and western Atlantic); they found it to be too small by about a factor of three to account for the observed sea level rise based on nine tide gauges in these regions. They concluded that sea level rise in the second half of the 20th century was mostly due to water mass added to the oceans. However, Table 5.3 shows that the sum of thermal expansion and contributions from land ice is smaller by 0.7 ± 0.7 mm yr^{-1} than the observed global average sea level rise. This is likely to be a significant difference. The assessment of Church et al. (2001) could allow this difference to be explained by positive anthropogenic terms (especially groundwater mining) but these are expected to have been outweighed by negative terms (especially impoundment). We conclude that the budget has not yet been closed satisfactorily.

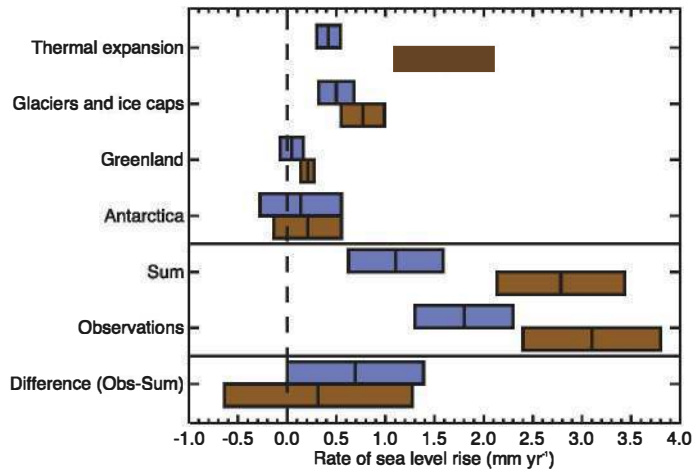

Figure 5.21. *Estimates of the various contributions to the budget of the global mean sea level change (upper four entries), the sum of these contributions and the observed rate of rise (middle two), and the observed rate minus the sum of contributions (lower), all for 1961 to 2003 (blue) and 1993 to 2003 (brown). The bars represent the 90% error range. For the sum, the error has been calculated as the square root of the sum of squared errors of the contributions. Likewise the errors of the sum and the observed rate have been combined to obtain the error for the difference.*

Given the large temporal variability in the rate of sea level rise evaluated from tide gauges (Section 5.5.2.4 and Figure 5.17), the budget is rather problematic on decadal time scales. The thermosteric contribution has smaller variability (though still substantial; Section 5.5.3) and there is only moderate temporal correlation between the thermosteric rate and the tide gauge rate. The difference between them has to be explained by ocean mass change. Because the thermosteric and climate-driven land water contributions are negatively correlated (Section 5.5.5.3.),

Table 5.3. *Estimates of the various contributions to the budget of global mean sea level change for 1961 to 2003 and 1993 to 2003 compared with the observed rate of rise. Ice sheet mass loss of 100 Gt yr^{-1} is equivalent to 0.28 mm yr^{-1} of sea level rise. A GIA correction has been applied to observations from tide gauges and altimetry. For the sum, the error has been calculated as the square root of the sum of squared errors of the contributions. The thermosteric sea level changes are for the 0 to 3,000 m layer of the ocean.*

	Sea Level Rise (mm yr^{-1})		
Source	**1961–2003**	**1993–2003**	**Reference**
Thermal Expansion	0.42 ± 0.12	1.6 ± 0.5	Section 5.5.3
Glaciers and Ice Caps	0.50 ± 0.18	0.77 ± 0.22	Section 4.5
Greenland Ice Sheet	0.05 ± 0.12	0.21 ± 0.07	Section 4.6.2
Antarctic Ice Sheet	0.14 ± 0.41	0.21 ± 0.35	Section 4.6.2
Sum	1.1 ± 0.5	2.8 ± 0.7	
Observed	1.8 ± 0.5		Section 5.5.2.1
		3.1 ± 0.7	Section 5.5.2.2
Difference (Observed –Sum)	0.7 ± 0.7	0.3 ± 1.0	

the apparent difference implies contributions during some 10-year periods from land ice, the only remaining term, exceeding 2 mm yr^{-1} (Figure 5.17). Since it is unlikely that the land ice contributions of 1993 to 2003 were exceeded in earlier decades (Figure 4.14 and Section 4.6.2.2), we conclude that the maximum 10-year rates of global sea level rise are likely overestimated from tide gauges, indicating that the estimated variability is excessive.

For 1993 to 2003, thermal expansion is much larger and land ice contributes 1.2 ± 0.4 mm yr^{-1}. These increases may partly reflect decadal variability rather than an acceleration (Section 5.5.3; attribution of changes in rates and comparison with model results are discussed in Section 9.5.2). The sum is still less than the observed trend but the discrepancy of 0.3 ± 1.0 mm yr^{-1} is consistent with zero. It is interesting to note that the difference between the observed total and thermal expansion (assumed to be due to ocean mass change) is about the same in the two periods. The more satisfactory assessment for recent years, during which individual terms are better known and satellite altimetry is available, indicates progress since the TAR.

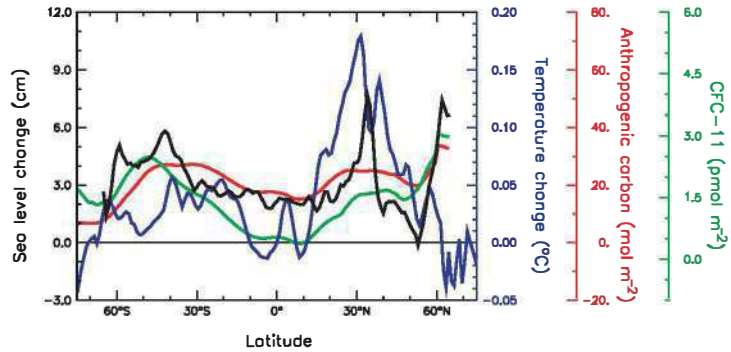

Figure 5.22. *Averages of temperature change (blue, from Levitus et al., 2005a), anthropogenic carbon (red, from Sabine et al., 2004b) and CFC-11 (green, from Willey et al., 2004) along lines of constant latitude over the top 700-m layer of the upper ocean. Also shown is sea level change averaged along lines of constant latitude (black, from Cazenave and Nerem, 2004). The temperature changes are for the 1955 to 2003 period, the anthropogenic carbon is since pre-industrial times (i.e., 1750), CFC-11 concentrations are for the period 1930 to 1994 and sea level for the period 1993 to 2003.*

5.6 Synthesis

The patterns of observed changes in global heat content and salinity, sea level, steric sea level, water mass evolution and biogeochemical cycles described in the previous four sections are broadly consistent with known characteristics of the large-scale ocean circulation (e.g., ENSO, NAO and SAM).

There is compelling evidence that the heat content of the World Ocean has increased since 1955 (Section 5.2). In the North Atlantic, the warming is penetrating deeper than in the Pacific, Indian and Southern Oceans (Figure 5.3), consistent with the strong convection, subduction and deep overturning circulation cell that occurs in the North Atlantic Ocean. The overturning cell in the North Atlantic region (carrying heat and water downwards through the water column) also suggests that there should be a higher anthropogenic carbon content as observed (Figure 5.11). Subduction of SAMW (and to a lesser extent AAIW) also carries anthropogenic carbon into the ocean, which is observed to be higher in the formation areas of these subantarctic water masses (Figure 5.10). The transfer of heat into the ocean also leads to sea level rise through thermal expansion, and the geographical pattern of sea level change since 1955 is largely consistent with thermal expansion and with the change in heat content (Figure 5.2).

Although salinity measurements are relatively sparse compared with temperature measurements, the salinity data also show significant changes. In global analyses, the waters at high latitudes (poleward of 50°N and 70°S) are fresher in the upper 500 m (Figure 5.5 World). In the upper 500 m, the subtropical latitudes in both hemispheres are characterised by an increase in salinity. The regional analyses of salinity also show a similar distributional change with a freshening of key high-latitude water masses such as LSW, AAIW and NPIW, and increased salinity in some of the subtropical gyres such as that at 24°N. The North Atlantic (and other key ocean water masses) also shows significant decadal variations, such as the recent increase in surface salinity in the North Atlantic subpolar gyre. At high latitudes (particularly in the NH), there is an observed increase in melting of perennial sea ice, precipitation, and glacial melt water (see Chapter 4), all of which act to freshen high-latitude surface waters. At mid-latitudes it is likely that evaporation minus precipitation has increased (i.e., the transport of freshwater from the ocean to the atmosphere has increased). The pattern of salinity change suggests an intensification in the Earth's hydrological cycle over the last 50 years. These trends are consistent with changes in precipitation and inferred greater water transport in the atmosphere from low latitudes to high latitudes and from the Atlantic to the Pacific.

Figure 5.22 shows zonal means of changes in temperature, anthropogenic carbon, sea level rise and a passive tracer (CFC). It is remarkable that these independent variables (albeit with widely varying reference periods) show a common pattern of change in the ocean. Specifically, the close similarity of higher levels of warming, sea level rise, anthropogenic carbon and CFC-11 at mid-latitudes and near the equator strongly suggests that these changes are the result of changes in ocean ventilation and circulation. Warming of the upper ocean should lead to a decrease in ocean ventilation and subduction rates, for which there is some evidence from observed decreases in O_2 concentrations.

In the equatorial Pacific, the pattern of steric sea level rise also shows that strong west to east gradients in the Pacific have weakened (i.e., it is now cooler in the western Pacific and warmer in the eastern Pacific). This decrease in the equatorial temperature gradient is consistent with a tendency towards more prolonged and stronger El Niños over this same period (see Section 3.6.2).

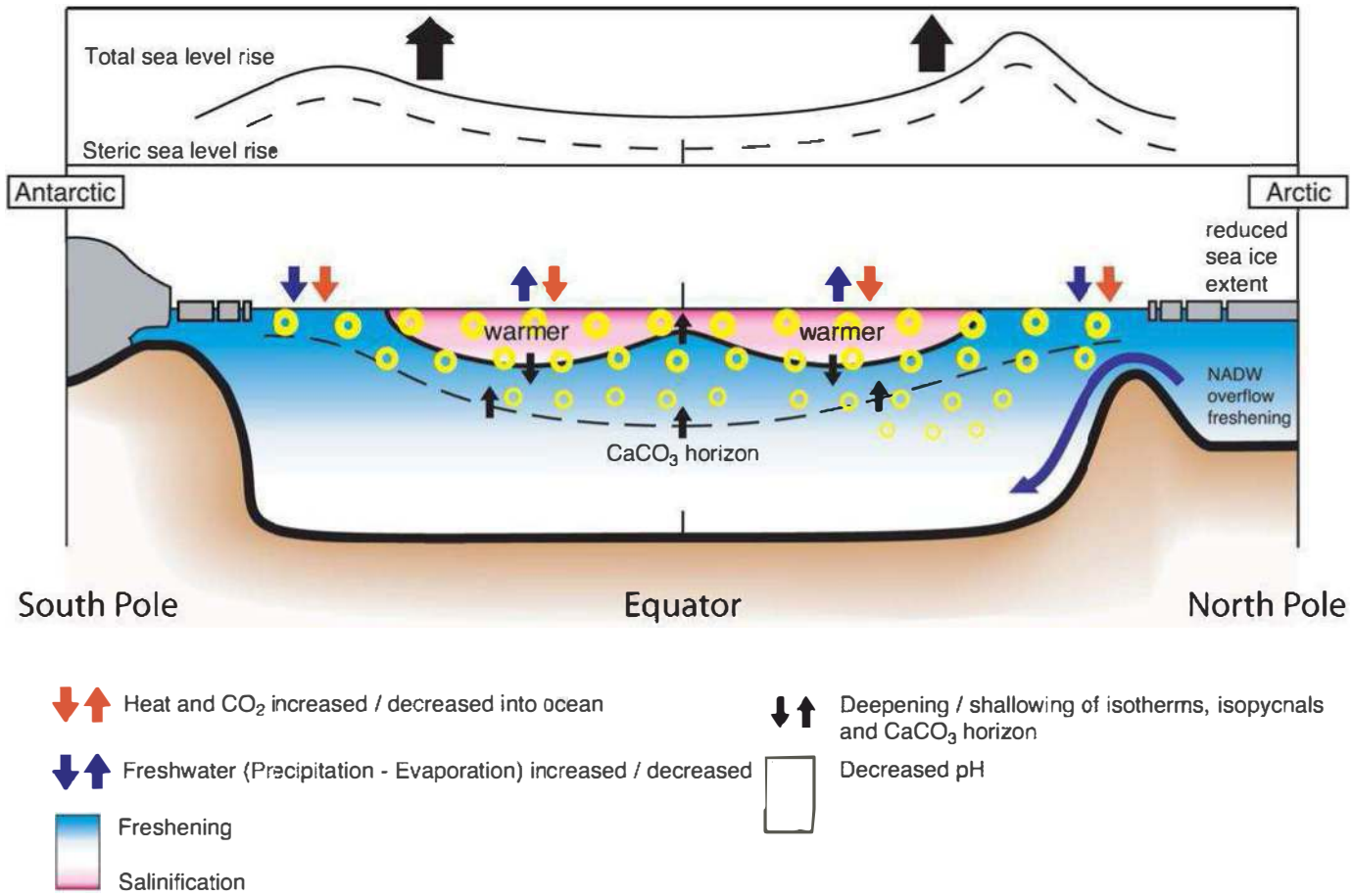

Figure 5.23. *Schematic of the observed changes in the ocean state, including ocean temperature, ocean salinity, sea level, sea ice and biogeochemical cycles. The legend identifies the direction of the changes in these variables.*

The subduction of carbon into the ocean has resulted in calcite and aragonite saturation horizons generally becoming shallower and pH decreasing primarily in the surface and near-surface ocean causing the ocean to become more acidic.

Since the TAR, the capability to measure most of the processes that contribute to sea level has been developed. In the 1990s, the observed sea level rise that was not explained through steric sea level rise could largely be explained by the transfer of mass from glaciers, ice sheets and river runoff (see Section 5.5). Figure 5.23 is a schematic that summarises the observed changes.

All of these observations taken together give high confidence that the ocean state has changed, that the spatial distribution of the changes is consistent with the large-scale ocean circulation and that these changes are in response to changed ocean surface conditions.

While there are many robust findings regarding the changed ocean state, key uncertainties still remain. Limitations in ocean sampling (particularly in the SH) mean that decadal variations in global heat content, regional salinity patterns, and rates of global sea level rise can only be evaluated with moderate confidence. Furthermore, there is low confidence in the evidence for trends in the MOC and the global ocean freshwater budget. Finally, the global average sea level rise for the last 50 years is likely to be larger than can be explained by thermal expansion and loss of land ice due to increased melting, and thus for this period it is not possible to satisfactorily quantify the known processes causing sea level rise.

References

AchutaRao, K.M. et al., 2006: Variability of ocean heat uptake: Reconciling observations and models, *J. Geophys. Res.,* **111**, C05019, doi:10.1029/2005JC003136.

Andersson, H.C., 2002: Influence of long-term regional and large-scale atmospheric circulation on the Baltic sea level. *Tellus*, **A54**, 76–88.

Andreev, A., and S. Watanabe, 2002: Temporal changes in dissolved oxygen of the intermediate water in the subarctic North Pacific. *Geophys. Res. Lett.*, **29**(14), 1680, doi:10.1029/2002GL015021.

Andrie, C., et al., 2003: Variability of AABW properties in the equatorial channel at 35 degrees W. *Geophys. Res. Lett.*, **30**(5), 8007, doi:10.1029/2002GL015766.

Antonov, J.I., S. Levitus, and T.P. Boyer, 2002: Steric sea level variations during 1957-1994: Importance of salinity. *J. Geophys. Res.*, **107**(C12), 8013, doi:10.1029/2001JC000964.

Antonov, J.I., S. Levitus, and T.P. Boyer, 2005: Steric variability of the world ocean, 1955-2003. *Geophys. Res. Lett.*, **32**(12), L12602, doi:10.1029/2005GL023112.

Aoki, S., M. Yoritaka, and A. Masuyama, 2003: Multidecadal warming of subsurface temperature in the Indian sector of the Southern Ocean. *J. Geophys. Res.*, **108**(C4), 8081, doi:10.1029/JC000307.

Aoki, S., N.L. Bindoff, and J.A. Church, 2005a: Interdecadal water mass changes in the Southern Ocean between 30E and 160E. *Geophys. Res. Lett.*, **32**, L07607, doi:10.1029/2004GL022220.

Aoki, S., S.R. Rintoul, S. Ushio, and S. Watanabe, 2005b: Freshening of the Adélie Land Bottom water near 140•E. *Geophys. Res. Lett.*, **32**, L23601, doi:10.1029/2005GL024246.

Baringer, M.O., and J.C. Larsen, 2001: Sixteen years of Florida Current transport at 27• N. *Geophys. Res. Lett.*, **28**(16), 3179–3182.

Bates, N.R., A.C. Pequignet, R.J. Johnson, and N. Gruber, 2002: A short-term sink for atmospheric CO_2 in subtropical mode water of the North Atlantic Ocean. *Nature*, **420**(6915), 489–493.

Beaugrand, G., and P.C. Reid, 2003: Long-term changes in phytoplankton, zooplankton and salmon related to climate. *Global Change Biol.*, **9**(6), 801–817.

Belkin, I.M., 2004: Propagation of the "Great Salinity Anomaly" of the 1990s around the northern North. *Geophys. Res. Lett.*, **31**, L08306, doi:10.1029/2003GL019334.

Beltrami, H., J.E. Smerdon, H.N. Pollack, and S. Huang, 2002: Continental heat gain in the global climate system. *Geophys. Res. Lett.*, **29**, doi:10.1029/2001GL014310.

Bersch, M., 2002: North Atlantic Oscillation-induced changes of the upper layer circulation in the northern North Atlantic Ocean. *J. Geophys. Res.*, **107**(C10), 3156, doi:10.1029/JC000901.

Bi, D.H., W.F. Budd, A.C. Hirst, and X.R. Wu, 2001: Collapse and reorganisation of the Southern Ocean overturning under global warming in a coupled model. *Geophys. Res. Lett.*, **28**(20), 3927–3930.

Biasutti, M., D.S. Battisti, and E.S. Sarachik, 2003: The annual cycle over the tropical Atlantic, South America, and Africa. *J. Clim.*, **16**(15), 2491–2508.

Bindoff, N.L., and T.J. McDougall, 2000: Decadal changes along an Indian Ocean section at 32 degrees S and their interpretation. *J. Phys. Oceanogr.*, **30**(6), 1207–1222.

Björk, G., et al., 2002: Return of the cold halocline layer to the Amundsen Basin of the Arctic Ocean: Implications for the sea ice mass balance. *Geophys. Res. Lett.*, **29**(11), 1513, doi:10.1029/2001GL014157.

Bouligand, R., and P.A. Pirazzoli, 1999: Les surcotes et les décotes marines à Brest, étude statistique et évolution. *Oceanol. Acta*, **22**(2), 153–166.

Boyer, T.P., J.I. Antonov, S. Levitus, and R. Locarnini, 2005: Linear trends of salinity for the world ocean, 1955-1998. *Geophys. Res. Lett.*, **32**, L01604, doi:1029/2004GL021791.

Boyer, T.P., et al., 2002: World ocean database 2001, Volume 2: Temporal distribution of bathythermograph profiles. In: *NOAA Atlas NESDIS 43* [Levitus, S. (ed.)]. Vol. 2. U.S. Government Printing Office, Washington, DC, 119 pp, CD-ROMs.

Brankart, J.M., and N. Pinardi, 2001: Abrupt cooling of the Mediterranean Levantine Intermediate Water at the beginning of the 1980s: Observational evidence and model simulation. *J. Phys. Oceanogr.*, **31**(8), 2307–2320.

Bromirski, P.D., R.E. Flick, and D.R. Cayan, 2003: Storminess variability along the California coast: 1858-2000. *J. Clim.*, **16**, 982–993.

Bryden, H.L., E.L. McDonagh, and B.A. King, 2003: Changes in ocean water mass properties: Oscillations or trends? *Science*, **300**, 2086–2088.

Bryden, H.L., H.R. Longworth, and S.A. Cunningham, 2005: Slowing of the Atlantic meridional overturning circulation at 25•N. *Nature*, **438**, 655–657, doi:10.1038/nature04385.

Bryden, H.L., et al., 1996: Decadal changes in water mass characteristics at 24 degrees N in the subtropical North Atlantic Ocean. *J. Clim.*, **9**(12), 3162–3186.

Cabanes, C., A. Cazenave, and C. Le Provost, 2001: Sea level change from Topex-Poseidon altimetry for 1993-1999 and possible warming of the southern oceans. *Geophys. Res. Lett.*, **28**(1), 9–12.

Cai, W., 2006: Antarctic ozone depletion causes an intensification of the Southern Ocean super-gyre circulation. *Geophys. Res. Lett.*, **33**, doi:1029/2005GL024911.

Caldeira, K., and M.E. Wickett, 2003: Anthropogenic carbon and ocean pH. *Nature*, **425**(6956), 365.

Carmack, E.C., et al., 1995: Evidence for warming of Atlantic Water in the southern Canadian Basin of the Arctic-Ocean - Results from the Larsen-93 Expedition. *Geophys. Res. Lett.*, **22**(9), 1061–1064.

Carton, J., B. Giese, and S. Grodsky, 2005: Sea level rise and the warming of the oceans in the Simple Ocean Data Assimilation (SODA) ocean reanalysis. *J. Geophys. Res.*, **110**, C09006, doi:1029/2004JC002817.

Cazenave, A., and R.S. Nerem, 2004: Present-day sea level change: observations and causes. *Rev. Geophys.*, **42**(3), RG3001, doi:10.1029/2003RG000139.

Chambers, D., J.C. Ries, C.K. Shum, and B.D. Tapley, 1998: On the use of tide gauges to determine altimeter drift. *J. Geophys. Res.*, **103**(C6), 12885–12890.

Chambers, D.P., et al., 2002: Low-frequency variations in global mean sea level: 1950-2000. *J. Geophys. Res.*, **107**(C4), doi:10.1029/2001JC001089.

Chao, B., 1994: Man-made lakes and global sea level. *Nature*, **370**, 258.

Chavez, F.P., J. Ryan, S.E. Lluch-Cota, and M. Niquen, 2003: From anchovies to sardines and back: Multidecadal change in the Pacific Ocean. *Science*, **299**(5604), 217–221.

Chelton, B., et al., 2001: Satellite altimetry. In: *Satellite Altimetry and Earth Sciences: A Handbook of Techniques and Applications* [Fu, L.-L., and A. Cazenave (eds.)]. Academic Press, San Diego, pp. 1–131.

Church, J.A., and N.J. White, 2006: A 20th century acceleration in global sea-level rise. *Geophys. Res. Lett.*, **33**, L01602, doi:10.1029/2005GL024826.

Church, J.A., N.J. White, and J.R. Hunter, 2006: Sea-level rise at tropical Pacific and Indian Ocean islands. *Global Planet. Change*, **53**, 155–168.

Church, J.A., et al., 2001: Changes in sea level. In: *Climate Change 2001: The Scientific Basis. Contribution of Working Group I to the Third Assessment Report of the Intergovernmental Panel on Climate Change* [Houghton, J.T., et al. (eds.)]. Cambridge University Press, Cambridge, United Kingdom and New York, NY, USA, pp. 639–693.

Church, J.A., et al., 2004: Estimates of the regional distribution of sea-level rise over the 1950 to 2000 period. *J. Clim.*, **17**(13), 2609–2625.

Clark, P.U., N.G. Pisias, T.F. Stocker, and A.J. Weaver, 2002: The role of the thermohaline circulation in abrupt climate change. *Nature*, **415**, 863–869.

Comiso, J.C., 2002: A rapidly declining perennial sea ice cover in the Arctic. *Geophys. Res. Lett.*, **29**, 1956–1959.

Comiso, J.C., 2003: Warming trends in the Arctic from clear sky satellite observations. *J. Clim.*, **16**(21), 3498–3510.

Conkright, M.E., et al., 2002: World ocean database 2001, Volume 1: Introduction. In: *NOAA Atlas NESDIS 42* [Levitus, S. (ed.). Vol. 1. U.S. Government Printing Office, Washington, DC, 159 pp, CD-ROMs.

Cunningham, S.A., S.G. Alderson, B.A. King, and M.A. Brandon, 2003: Transport and variability of the Antarctic Circumpolar Current in Drake Passage. *J. Geophys. Res.*, **108**(C5), 8084, doi:10.1029/2001JC001147.

Curry, R., and C. Mauritzen, 2005: Dilution of the northern North Atlantic Ocean in recent decades. *Science*, **308**(5729), 1772–1774.

Curry, R., B. Dickson, and I. Yashayaev, 2003: A change in the freshwater balance of the Atlantic Ocean over the past four decades. *Nature*, **426**(6968), 826–829.

Deutsch, C., S. Emerson, and L. Thompson, 2005: Fingerprints of climate change in North Pacific oxygen. *Geophys. Res. Lett.*, **32**, L16604, doi:10.1029/2005GL023190.

Dickson, B., et al., 2002: Rapid freshening of the deep North Atlantic Ocean over the past four decades. *Nature*, **416**(6883), 832–837.

Dickson, R., et al., 1996: Long-term coordinated changes in the convective activity of the North Atlantic. *Prog. Oceanogr.*, **38**, 241–295.

Dickson, R.R., R. Curry, and I. Yashayaev, 2003: Recent changes in the North Atlantic. *Philos. Trans. R. Soc. London Ser. A*, **361**(1810), 1917–1933.

Dickson, R.R., J. Meincke, S.A. Malmberg, and A.J. Lee, 1988: The Great Salinity Anomaly in the Northern North Atlantic 1968-1982. *Prog. Oceanogr.*, **20**(2), 103–151.

Doney, S.C., J.L. Bullister, and R. Wanninkhof, 1998: Climatic variability in upper ocean ventilation rates diagnosed using chlorofluorocarbons. *Geophys. Res. Lett.*, **25**(9), 1399–1402.

Donnelly, J.P., P. Cleary, P. Newby, and R. Ettinger, 2004: Coupling instrumental and geological records of sea-level change: Evidence from southern New England of an increase in the rate of sea-level rise in the late 19th century. *Geophys. Res. Lett.*, **31**(5), L05203, doi:10.1029/2003GL018933.

Dore, J.E., R. Lukas, D.W. Sadler, and D.M. Karl, 2003: Climate-driven changes to the atmospheric CO_2 sink in the subtropical North Pacific Ocean. *Nature*, **424**(6950), 754–757.

Douglas, B.C., 1992: Global sea level acceleration. *J. Geophys. Res.*, **97**(C8), 12699–12706.

Douglas, B.C., 2001: Sea level change in the era of the recording tide gauges. In: *Sea Level Rise: History and Consequences* [Douglas, B.C., Kearney, M.S., and S.P. Leatherman (eds.)]. Academic Press, New York, pp. 37–64.

Ekman, M., 1988: The world's longest continued series of sea level observations. *Pure Appl. Geophys.*, **127**, 73–77.

Emerson, S., S. Mecking, and J. Abell, 2001: The biological pump in the subtropical North Pacific Ocean: Nutrient sources, Redfield ratios, and recent changes. *Global Biogeochem. Cycles*, **15**(3), 535–554.

Emerson, S., Y.W. Watanabe, T. Ono, and S. Mecking, 2004: Temporal trends in apparent oxygen utilization in the upper pycnocline of the North Pacific: 1980-2000. *J. Oceanogr.*, **60**(1), 139–147.

Fahrbach, E., et al., 2004: Decadal-scale variations of water mass properties in the deep Weddell Sea. *Ocean Dyn.*, **54**(1), 77–91.

Feely, R.A., and C.T.A. Chen, 1982: The effect of excess CO_2 on the calculated calcite and aragonite saturation horizons in the northeast Pacific. *Geophys. Res. Lett.*, **9**(11), 1294–1297.

Feely, R.A., R. Wanninkhof, T. Takahashi, and P. Tans, 1999: Influence of El Niño on the equatorial Pacific contribution to atmospheric CO_2 accumulation. *Nature*, **398**(6728), 597–601.

Feely, R.A., et al., 2002: In situ calcium carbonate dissolution in the Pacific Ocean. *Global Biogeochem. Cycles*, **16**(4), 1144, doi:10.1029/2002GB001866.

Feely, R.A., et al., 2004: Impact of anthropogenic CO_2 on the $CaCO_3$ system in the oceans. *Science*, **305**(5682), 362–366.

Feng, M., and G. Meyers, 2003: Interannual variability in the tropical Indian Ocean: A two-year time-scale of Indian Ocean Dipole. *Deep-Sea Res. II*, **50**, 2263–2284.

Firing, Y.L., and M.A. Merrifield, 2004: Extreme sea level events at Hawaii: the influence of mesoscale eddies. *Geophys. Res. Lett.*, **31**(24), L24306, doi:10.1029/2004GL021539.

Folland, C.K., et al., 2001: Observed climate variability and change. In: *Climate Change 2001: The Scientific Basis. Contribution of Working Group I to the Third Assessment Report of the Intergovernmental Panel on Climate Change* [Houghton, J.T., et al. (eds.)]. Cambridge University Press, Cambridge, United Kingdom and New York, NY, pp. 99–181.

Freeland, H., et al., 1997: Evidence of change in the winter mixed layer in the Northeast Pacific Ocean. *Deep-Sea Res. I*, **44**(12), 2117–2129.

Fu, L.L., and A. Cazenave, 2001: *Satellite Altimetry and Earth Sciences: A Handbook of Techniques and Applications.* International Geophysics Series Vol. 69, Academic Press, San Diego, 457 pp.

Fukasawa, M., et al., 2004: Bottom water warming in the North Pacific Ocean. *Nature*, **427**(6977), 825–827.

Gamo, T., et al., 1986: Spatial and temporal variations of water characteristics in the Japan Sea bottom layer. *J. Mar. Res.*, **44**(4), 781–793.

Ganachaud, A., and C. Wunsch, 2003: Large-scale ocean heat and freshwater transports during the World Ocean Circulation Experiment. *J. Clim.*, **16**(4), 696–705.

Garcia, H.E., et al., 2005: On the variability of dissolved oxygen and apparent oxygen utilization content for the upper world ocean: 1955 to 1998. *Geophys. Res. Lett.*, **32**, L09604, doi:10.1029/GL022286.

Gasparini, G.P., et al., 2005: The effect of the Eastern Mediterranean Transient on the hydrographic characteristics in the Strait of Sicily and in the Tyrrhenian Sea. *Deep-Sea Res. I*, **52**(6), 915–935.

Gehrels, W.R., et al., 2004: Late Holocene sea-level changes and isostatic crustal movements in Atlantic Canada. *Quat. Int.*, **120**, 79–89.

Gertman, I., N. Pinardi, Y. Popov, and A. Hecht, 2006: Aegean sea water masses during the early stages of the eastern Mediterranean climatic transient (1988-1990). *J. Phys. Oceanogr.*, **36**(9), 1841–1859.

Gille, S.T., 2002: Warming of the Southern Ocean since the 1950s. *Science*, **295**(5558), 1275–1277.

Gille, S.T., 2004: How nonlinearities in the equation of state of seawater can confound estimates of steric sea level change. *J. Geophys. Res.*, **109**(3), C03005, doi:10.1029/2003JC002012.

Gonzalez-Dávila, M., et al., 2003: Seasonal and interannual variability of sea-surface carbon dioxide species at the European Station for Time Series in the Ocean at the Canary Islands (ESTOC) between 1996 and 2000. *Global Biogeochem. Cycles*, **17**(3), 1076, doi:10.1029/2002GB001993.

González-Pola, C., A. Lavin, and M. Vargas-Yanez, 2005: Intense warming and salinity modification of intermediate water masses in the southeastern corner of the Bay of Biscay for the period 1992-2003. *J. Geophys. Res.*, **110**, C05020, doi:10.1029/2004JC002367.

Gornitz, V., 2001: Impoundment, groundwater mining, and other hydrologic transformations: Impacts on global sea level rise. In: *Sea Level Rise: History and Consequences* [Douglas, B.C., M.S. Kearney, and S.P. Leatherman (eds.)]. Academic Press, San Diego, pp. 97–119.

Gregg, W.W., et al., 2003: Ocean primary production and climate: Global decadal changes. *Geophys. Res. Lett.*, **30**(15), 1809, doi:10.1029/2003GL016889.

Gregory, J.M., et al., 2001: Comparison of results from several AOGCMs for global and regional sea-level changes 1900-2100. *Clim. Dyn.*, **18**, 225–240.

Gregory, J.M., et al., 2004: Simulated and observed decadal variability in ocean heat content. *Geophys. Res. Lett.*, **31**, L15312, doi:10.1029/2004/GL020258.

Gregory, J.M., et al., 2005: A model intercomparison of changes in the Atlantic thermohaline circulation in response to increasing atmospheric CO_2 concentration. *Geophys. Res. Lett.*, **32**, L12703, doi:10.1029/2005GL023209.

Grist, J.P., and S.A. Josey, 2003: Inverse analysis adjustment of the SOC air-sea flux climatology using ocean heat transport constraints. *J. Clim.*, **16**(20), 3274–3295.

Gruber, N., J.L. Sarmiento, and T.F. Stocker, 1996: An improved method for detecting anthropogenic CO_2 in the oceans. *Global Biogeochem. Cycles*, **10**(4), 809–837.

Gruber, N., C.D. Keeling, and N.R. Bates, 2002: Interannual variability in the North Atlantic Ocean carbon sink. *Science*, **298**(5602), 2374–2378.

Guinehut, S., P.-Y. Le Traon, G. Larnicol, and S. Phillips, 2004: Combining ARGO and remote-sensing data to estimate the ocean three-dimensional temperature fields. *J. Mar. Syst.*, **46**, 85–98.

Gulev, S.K., T. Jung, and E. Ruprecht, 2006: Estimation of the sampling errors in global surface flux fields based on VOS data. *J. Clim.*, **20**(2), 279-301.

Häkkinen, S., 2002: Surface salinity variability in the northern North Atlantic during recent decades. *J. Geophys. Res.*, **107**(C12), doi:10.1029/2001JC000812.

Häkkinen, S., and P.B. Rhines, 2004: Decline of subpolar North Atlantic circulation during the 1990s. *Science*, **304**, 555–559.

Hanawa, K., 1995: Southward penetration of the Oyashio water system and the wintertime condition of midlatitude westerlies over the North Pacific. *Bull. Hokkaido Natl. Fish. Res. Inst.*, **59**, 103–119.

Hanawa, K., and J. Kamada, 2001: Variability of core layer temperature (CLT) of the North Pacific subtropical mode water. *Geophys. Res. Lett.*, **28**(11), 2229–2232.

Hanawa, K., and L.D. Talley, 2001: Mode waters. In: *Ocean Circulation and Climate* [Siedler, G., J.A. Church, and J. Gould (eds.)]. Academic Press, San Diego, pp. 373–386.

Harrison, D.E., and M. Carson, 2006: Is the World Ocean warming? Upper ocean temperature trends, 1950-2000. *J. Phys. Oceanogr.*, **37** (2), 174–187.

Hátún, H., et al., 2005: Influence of the Atlantic Subpolar Gyre on the thermohaline circulation. *Science*, **309**, 1841–1844.

Hazeleger, W., and S.S. Drijfhout, 1998: Mode water variability in a model of the subtropical gyre: Response to anomalous forcings. *J. Phys. Oceanogr.*, **28**, 266–288.

Hazeleger, W., P. de Vries, and Y. Friocourt, 2003: Sources of the Equatorial Undercurrent in the Atlantic in a high-resolution ocean model. *J. Phys. Oceanogr.*, **33**, 677–693.

Hill, K.L., A.J. Weaver, H.J. Freeland, and A. Bychkov, 2003: Evidence of change in the Sea of Okhotsk: Implications for the North Pacific. *Atmos.-Ocean*, **41**(1), 49–63.

Hilmer, M., and P. Lemke, 2000: On the decrease of Arctic sea ice volume. *Geophys. Res. Lett.*, **27**(22), 3751–3754.

Hirawake, T., T. Odate, and M. Fukuchi, 2005: Long-term variation of surface phytoplankton chlorophyll a in the Southern Ocean during 1965-2002. *Geophys. Res. Lett.*, **32**(5), L05606, doi:10.1029/2004GL021394.

Hogg, N.G., 2001: Quantification of the deep circulation. In: *Ocean Circulation and Climate* [Siedler, G., J.A. Church, and J. Gould (eds.)]. Academic Press, San Diego, pp. 259–270.

Hogg, N.G., and W. Zenk, 1997: Long-period changes in the bottom water flowing through Vema Channel. *J. Geophys. Res.*, **102**, 15639–15646.

Holgate, S.J., and P.L. Woodworth, 2004: Evidence for enhanced coastal sea level rise during the 1990s. *Geophys. Res. Lett.*, **31**, L07305, doi:10.1029/2004GL019626.

Houghton, R.W., and M. Visbeck, 2002: Quasi-decadal salinity fluctuations in the Labrador Sea. *J. Phys. Oceanogr.*, **32**, 687–701.

ICES, 2005: *The Annual ICES Ocean Climate Status Summary 2004/2005.* ICES Cooperative Research Report No.275, International Council for the Exploration of the Sea, Copenhagen, Denmark, 37 pp.

IOC, 2002: *Manual on Sea-Level Measurement and Interpretation. Volume 3 - Reappraisals and Recommendations as of the Year 2000.* Manuals and Guides No. 14, Intergovernmental Oceanographic Commission, Paris, 47 pp.

IPCC, 2001: *Climate Change 2001: The Scientific Basis. Contribution of Working Group I to the Third Assessment Report of the Intergovernmental Panel on Climate Change* [Houghton, J.T., et al. (eds.)]. Cambridge University Press, Cambridge, United Kingdom and New York, NY, USA, 881 pp.

Ishii, M., M. Kimoto, K. Sakamoto, and S.I. Iwasaki, 2006: Steric sea level changes estimated from historical ocean subsurface temperature and salinity analyses. *J. Oceanogr.*, **62**(2), 155–170.

Jacobs, S.S., C.F. Giulivi, and P.A. Mele, 2002: Freshening of the Ross Sea during the late 20th century. *Science*, **297**(5580), 386–389.

Johnson, G.C., and A.H. Orsi, 1997: Southwest Pacific Ocean water-mass changes between 1968/69 and 1990/91. *J. Clim.*, **10**(2), 306–316.

Johnson, G.C., and N. Gruber, 2007: Decadal water mass variations along 20°W in the northeastern Atlantic Ocean. *Prog. Oceanogr.*, in press.

Johnson, G.C., D.L. Rudnick, and B.A. Taft, 1994: Bottom water variability in the Samoa Passage. *J. Mar. Res.*, **52**, 177–196.

Josey, S.A., 2003: Changes in the heat and freshwater forcing of the eastern Mediterranean and their influence on deep water formation. *J. Geophys. Res.*, **108**(C7), 3237, doi:10.1029/2003JC001778.

Josey, S.A., and R. Marsh, 2005: Surface freshwater flux variability and recent freshening of the North Atlantic in the eastern Subpolar Gyre. *J. Geophys. Res.*, **110**, C05008, doi:10.1029/2004JC002521.

Joyce, T.M., and P.E. Robbins, 1996: The long-term hydrographic record at Bermuda. *J. Clim.*, **9**, 3121–3131.

Joyce, T.M., and J. Dunworth-Baker, 2003: Long-term hydrographic variability in the Northwest Pacific Ocean. *Geophys. Res. Lett.*, **30**(2), 1043, doi:10.1029/2002GL015225.

Joyce, T.M., R.S. Pickart, and R.C. Millard, 1999: Long-term hydrographic changes at 52 and 66 degrees W in the North Atlantic Subtropical Gyre & Caribbean. *Deep-Sea Res. II*, **46**(1–2), 245–278.

Joyce, T.M., C. Deser, and M.A. Spall, 2000: The relation between decadal variability of subtropical mode water and the North Atlantic Oscillation. *J. Clim.*, **13**(14), 2550–2569.

Karl, D.M., 1999: A sea of change: Biogeochemical variability in the North Pacific Subtropical Gyre. *Ecosystems*, **2**(3), 181–214.

Keeling, R.F., 2005: Comment on "The ocean sink for anthropogenic CO_2". *Science*, **308**(5729), 1743c.

Keigwin, L.D., W.B. Curry, S.J. Lehman, and S. Johnsen, 1994: The role of the deep ocean in North Atlantic climate change between 70 and 130 kyr ago. *Nature*, **371**, 323–326.

Keller, K., R.D. Slater, M. Bender, and R.M. Key, 2002: Possible biological or physical explanations for decadal scale trends in North Pacific nutrient concentrations and oxygen utilization. *Deep-Sea Res. II*, **49**(1–3), 345–362.

Kieke, D., et al., 2006: Changes in the CFC inventories and formation rates of Upper Labrador Sea water. *J. Phys. Oceanogr.*, **36**, 64–86.

Kim, K., et al., 2004: Water masses and decadal variability in the East Sea (Sea of Japan). *Prog. Oceanogr.*, **61**(2–4), 157–174.

Kim, K.R., et al., 2002: A sudden bottom-water formation during the severe winter 2000-2001: The case of the East/Japan Sea. *Geophys. Res. Lett.*, **29**(8), doi:10.1029/2001GL014498.

Klein, B., et al., 2000: Is the Adriatic returning to dominate the production of Eastern Mediterranean Deep Water? *Geophys. Res. Lett.*, **27**(20), 3377–3380.

Knight, J.R., et al., 2005: A signature of persistent natural thermohaline circulation cycles in observed climate. *Geophys. Res. Lett.*, **32**, L20708, doi:1029/2005GL024233.

Köhl, A., D. Stammer, and B. Cornuelle, 2006: Interannual to decadal changes in the ECCO global synthesis. *J. Phys. Oceanogr.*, **37**(2), 313-337.

Krahmann, G., and F. Schott, 1998: Long-term increases in Western Mediterranean salinities and temperatures: anthropogenic and climatic sources. *Geophys. Res. Lett.*, **25**(22), 4209–4212.

Kwon, Y.O., and S.C. Riser, 2004: North Atlantic Subtropical Mode Water: A history of ocean-atmosphere interaction 1961-2000. *Geophys. Res. Lett.*, **31**(19), L19307, doi:10.1029/2004GL021116.

Kwon, Y.O., K. Kim, Y.G. Kim, and K.R. Kim, 2004: Diagnosing long-term trends of the water mass properties in the East Sea (Sea of Japan). *Geophys. Res. Lett.*, **31**(20), L20306, doi:10.1029/2004GL020881.

Lambeck, K., 2002: Sea-level change from mid-Holocene to recent time: An Australian example with global implications. In: *Ice Sheets, Sea Level and the Dynamic Earth* [Mitrovica, J.X., and B. L.A. Vermeersen (eds.)]. Geodynamics Series Vol. 29, American Geophysical Union, Washington, DC, doi:10.1029/029GD03. 33–50.

Lambeck, K., C. Smither, and M. Ekman, 1998: Tests of glacial rebound models for Fennoscandinavia based on instrumental sea- and lake-level records. *Geophys. J. Int.*, **135**, 375–387.

Lambeck, K., et al., 2004: Sea level in Roman time in the Central Mediterranean and implications for recent change. *Earth Planet. Sci. Lett.*, **224**, 563–575.

Latif, M., et al., 2006: Is the thermohaline circulation changing? *J. Clim.*, **19**, 4631–4637.

Lazar, A., et al., 2002: Seasonality of the ventilation of the tropical Atlantic thermocline in an ocean general circulation mode. *J. Geophys. Res.*, **107**(C8), doi:10.1029/2000JC000667.

Lazier, J.R.N., 1995: The salinity decrease in the Labrador Sea over the past thirty years. In: *Natural Climate Variability on Decade-to-Century Time Scales* [Martinson, D.G., et al. (eds.)]. National Academy Press, Washington, DC, pp. 295–304.

Lazier, J.R.N., et al., 2002: Convection and restratification in the Labrador Sea, 1990-2000. *Deep-Sea Res. I*, **49**(10), 1819–1835.

Le Quéré, C., et al., 2003: Two decades of ocean CO_2 sink and variability. *Tellus*, **B55**(2), 649–656.

Lee, T., 2004: Decadal weakening of the shallow overturning circulation of the South Indian Ocean. *Geophys. Res. Lett.*, **31**, L18305, doi:10.1029/2004GL020884.

Lefèvre, N., et al., 2004: A decrease in the sink for atmospheric CO_2 in the North Atlantic. *Geophys. Res. Lett.*, **31**(7), L07306, doi:10.1029/2003GL018957.

Leuliette, E.W., R.S. Nerem, and G.T. Mitchum, 2004: Calibration of TOPEX/Poseidon and Jason altimeter data to construct a continuous record of mean sea level change. *Mar. Geodesy*, **27**(1–2), 79–94.

Levitus, S., 1989: Interpentadal variability of salinity in the upper 150m of the North-Atlantic Ocean, 1970-1974 versus 1955-1959. *J. Geophys. Res.*, **94**(C7), 9679–9685.

Levitus, S., J.I. Antonov, and T.P. Boyer, 2005a: Warming of the World Ocean, 1955-2003. *Geophys. Res. Lett.*, **32**, L02604, doi:10.1029/2004GL021592.

Levitus, S., J. Antonov, T.P. Boyer, and C. Stephens, 2000: Warming of the World Ocean. *Science*, **287**, 2225–2229.

Levitus, S., et al., 2005b: *Building Ocean Profile-Plankton Databases for Climate and Ecosystem System Research.* NOAA Technical Report NESDIS 117, U.S. Government Printing Office, Washington, DC, 29 pp.

Levitus, S., et al., 2005c: EOF analysis of upper ocean heat content, 1956-2003. *Geophys. Res. Lett.*, **32**, L18607, doi:10.1029/2005GL023606.

Li, M., P.G. Myers, and H. Freeland, 2005: An examination of historical mixed layer depths along Line-P in the Gulf of Alaska. *Geophys. Res. Lett.*, **32**, L05613, doi:10.1029/2004GL021911.

Li, Y.-H., and T.-H. Peng, 2002: Latitudinal change of remineralization ratios in the oceans and its implication for nutrient cycles. *Global Biogeochem. Cycles*, **16**(4), 1130, doi:10.1029/2001GB001828.

Locarnini, R.A., et al., 2002: World ocean database 2001. In: *NOAA Atlas NESDIS 45. Vol. 4: Temporal Distribution of Temperature, Salinity and Oxygen Profiles* [Levitus, S. (ed.)]. U.S. Government Printing Office, Washington, DC, 332 pp, CD-ROMs.

Lombard, A., et al., 2005: Thermosteric sea level rise for the past 50 years; comparison with tide gauges and inference on water mass contribution. *Global Planet. Change*, **48**, 303–312.

Lombard, A., et al., 2006: Perspectives on present-day sea level change: a tribute to Christian le Provost. *Ocean Dyn.*, **56**(5-6), doi:10.1007/s10236-005-0046-x.

Lowe, J.A., and J.M. Gregory, 2006: Understanding projections of sea level rise in a Hadley Centre coupled climate model. *J. Geophys. Res.*, **111**, C11014, doi:10.1029/2005JC003421.

Luterbacher, J., et al., 2004: European seasonal and annual temperature variability, trends, and extremes since 1500. *Science*, **303**(5663), 1499–1503.

Lyman, J.M., J.K. Willis, and G.C. Johnson, 2006: Recent cooling of the upper ocean. *Geophys. Res. Lett.*, **33**, L18604, doi:10.1029/2006GL027033.

Macrander, A., et al., 2005: Interannual changes in the overflow from the Nordic Seas into the Atlantic Ocean through Denmark Strait. *Geophys. Res. Lett.*, **32**, L06606, doi:10.1029/2004GL021463.

Manca, B.B., V. Kovacevic, M. Gacic, and D. Viezzoli, 2002: Dense water formation in the Southern Adriatic Sea and spreading into the Ionian Sea in the period 1997-1999. *J. Mar. Syst.*, **33**, 133–154.

Mariotti, A., et al., 2002: The hydrological cycle in the Mediterranean region and implications for the water budget of the Mediterranean Sea. *J. Clim.*, **15**(13), 1674.

Marsh, R., 2000: Recent variability of the North Atlantic thermohaline circulation inferred from surface heat and freshwater fluxes. *J. Clim.*, **13**(18), 3239–3260.

Matsumoto, K., and N. Gruber, 2005: How accurate is the estimation of anthropogenic carbon in the ocean? An evaluation of the delta C* method. *Global Biogeochem. Cycles*, **19**, GB3014, doi:10.1029/2004GB002397.

McDonagh, E.L., et al., 2005: Decadal changes in the south Indian Ocean thermocline. *J. Clim.*, **18**, 1575–1590.

McLaughlin, F.A., E.C. Carmack, R.W. Macdonald, and J.K.B. Bishop, 1996: Physical and geochemical properties across the Atlantic Pacific water mass front in the southern Canadian Basin. *J. Geophys. Res.*, **101**(C1), 1183–1197.

McNeil, B.I., et al., 2003: Anthropogenic CO_2 uptake by the ocean based on the global chlorofluorocarbon data set. *Science*, **299**(5604), 235–239.

McPhaden, M.J., and D.X. Zhang, 2002: Slowdown of the meridional overturning circulation in the upper Pacific Ocean. *Nature*, **415**(6872), 603–608.

McPhaden, M.J., and D.X. Zhang, 2004: Pacific Ocean circulation rebounds. *Geophys. Res. Lett.*, **31**(18), L18301, doi:10.1029/2004GL020727.

Mecking, S., M.J. Warner, and J.L. Bullister, 2006: Temporal changes in pCFC-12 ages and AOU along two hydrographic sections in the eastern subtropical North Pacific. *Deep-Sea Res.*, **53**(1), 169–187.

Meredith, M.P., and J.C. King, 2005: Rapid climate change in the ocean west of the Antarctic Peninsula during the second half of the 20th century. *Geophys. Res. Lett.*, **32**, L19604, doi:1029/2005GL024042.

Meyers, G., 1996: Variation of the Indonesian throughflow and the El Nino-Southern Oscillation. *J. Geophys. Res.*, **101**, 12255–12263.

Miller, L., and B.C. Douglas, 2004: Mass and volume contributions to 20th century global sea level rise. *Nature*, **428**, 406–409.

Millot, C., J.-L. Fuda, J. Candela, and Y. Tber, 2006: Large warming and salinification of the Mediterranean outflow due to changes in its composition. *Deep-Sea Res. I*, **53**, 656–666.

Milly, P.C.D., and A.B. Shmakin, 2002: Global modeling of land water and energy balances: 1. The land dynamics (LaD) model. *J. Hydrometeorol.*, **3**, 283–299.

Milly, P.C.D., A. Cazenave, and M.C. Gennero, 2003: Contribution of climate-driven change in continental water storage to recent sea-level rise. *Proc. Natl. Acad. Sci. U.S.A.*, **100**(213), 13158–13161.

Minami, H., Y. Kano, and K. Ogawa, 1998: Long-term variations of potential temperature and dissolved oxygen of the Japan Sea Water. *J. Oceanogr.*, **55**, 197–205.

Mitchell, T.P., and J.M. Wallace, 1992: The annual cycle in equatorial convection and sea-surface temperature. *J. Clim.*, **5**(10), 1140–1156.

Mitchell, W., J. Chittleborough, B. Ronai, and G.W. Lennon, 2001: Sea level rise in Australia and the Pacific. In: *Pacific Islands Conference on Climate Change, Climate Variability and Sea Level Rise, National Tidal Facility Australia, Rarotonga, Cook Islands, 3-7 April 2000*. Flinders Press, Adelaide, Australia, pp. 47–57.

Mitchum, G.T., 1994: Comparison of Topex sea surface heights and tide gauge sea levels. *J. Geophys. Res.*, **99**(C12), 24541–24554.

Mitchum, G.T., 2000: An improved calibration of satellite altimetric heights using tide gauge sea levels with adjustment for land motion. *Mar. Geodesy*, **23**, 145–166.

Mitrovica, J.X., M. Tamisiea, J.L. Davis, and G.A. Milne, 2001: Recent mass balance of polar ice sheets inferred from patterns of global sea-level change. *Nature*, **409**, 1026–1029.

Mitrovica, J.X., et al., 2006: Reanalysis of ancient eclipses, astronomic and geodetic data: a possible route to resolving the enigma of global sea level rise. *Earth Planet. Sci. Lett.*, **243**, 390–399.

Molinari, R.L., 2004: Annual and decadal variability in the western subtropical North Atlantic: signal characteristics and sampling methodologies. *Prog. Oceanogr.*, **62**(1), 33–66.

Morison, J., M. Steele, and R. Andersen, 1998: Hydrography of the upper Arctic Ocean measured from the nuclear submarine USS Pargo. *Deep-Sea Res. I*, **45**(1), 15–38.

Munk, W., 2003: Ocean freshening, sea level rising. *Science*, **300**, 2041–2043.

Murray, R.J., N.L. Bindoff, and C.J.C. Reason, 2007: Modelling decadal changes on the Indian Ocean Section I5 at 32°S. *J. Clim.*, in press.

Nerem, R.S., and G.T. Mitchum, 2001: Observations of sea level change from satellite altimetry. In: *Sea Level Rise: History and Consequences* [Douglas, B.C., M.S. Kearney, and S.P. Leatherman (eds.)]. Academic Press, San Diego, pp. 121–163.

Nerem, R.S., et al., 1999: Variations in global mean sea level associated with the 1997-1998 ENSO event: Implications for measuring long term sea level change. *Geophys. Res. Lett.*, **26**, 3005–3008.

Ngo-Duc, T., et al., 2005: Effects of land water storage on the global mean sea level over the last half century. *Geophys. Res. Lett.*, **32**, L09704, doi:10.1029/2005GL022719.

Ono, T., et al., 2001: Temporal increases of phosphate and apparent oxygen utilization in the subsurface waters of western subarctic Pacific from 1968 to 1998. *Geophys. Res. Lett.*, **28**(17), 3285–3288.

Orr, J.C., et al., 2005: 21st century decline in ocean carbonate and high latitude aragonitic organisms. *Nature*, **437**, 681–686.

Orsi, A.H., W.M. Smethie, and J.L. Bullister, 2002: On the total input of Antarctic waters to the deep ocean: A preliminary estimate from chlorofluorocarbon measurements. *J. Geophys. Res.*, **107**(C8), 3122, doi:10.1029/2001JC000976.

Østerhus, S., W.R. Turrell, S. Jónsson, and B. Hansen, 2005: Measured volume, heat, and salt fluxes from the Atlantic to the Arctic Mediterranean. *Geophys. Res. Lett.*, **32**, L07603, doi:10.1029/2004GL022188.

Pahlow, M., and U. Riebesell, 2000: Temporal trends in deep ocean Redfield ratios. *Science*, **287**(5454), 831–833.

Palmer, M.H., H.L. Bryden, J.L. Hirschi, and J. Marotzke, 2004: Observed changes in the South Indian Ocean gyre circulation, 1987-2002. *Geophys. Res. Lett.*, **31**(15), L15303, doi:15310.11029/12004GL020506.

Parrish, R.H., F.B. Schwing, and R. Mendelssohn, 2000: Midlatitude wind stress: the energy source for climatic regimes in the North Pacific Ocean. *Fish. Oceanogr.*, **9**, 224–238.

Peltier, W.R., 2001: Global glacial isostatic adjustment and modern instrumental records of relative sea level history. In: *Sea Level Rise: History and Consequences* [Douglas, B.C., M.S. Kearney, and S.P. Leatherman (eds.)]. Academic Press, San Diego, pp. 65–95.

Peltier, W.R., 2004: Global glacial isostasy and the surface of the ice-age earth: the ICE-5G (VM2) model and GRACE. *Annu. Rev. Earth Planet. Sci.*, **32**, 111–149.

Penduff, T., B. Barnier, W.K. Dewar, and J.J. O'Brien, 2004: Dynamical response of the oceanic eddy field to the North Atlantic Oscillation: A model-data comparison. *J. Phys. Oceanogr.*, **34**, 2615–2629.

Peng, T.-H., R. Wanninkhof, and R.A. Feely, 2003: Increase of anthropogenic CO_2 in the Pacific Ocean over the last two decades. *Deep-Sea Res. II*, **50**, 3065–3082.

Peng, T.-H., et al., 1998: Quantification of decadal anthropogenic CO_2 uptake in the ocean based on dissolved inorganic carbon measurements. *Nature*, **396**(6711), 560–563.

Plag, H.-P., 2006: Recent relative sea level trends: an attempt to quantify the forcing factors. *Philos. Trans. R. Soc. London A*, **364**(1841), 821–844.

Polyakov, I.V., et al., 2004: Variability of the intermediate Atlantic water of the Arctic Ocean over the last 100 years. *J. Clim.*, **17**(23), 4485–4497.

Polyakov, I.V., et al., 2005: One more step toward a warmer Arctic. *Geophys. Res. Lett.*, **32**, L17605, doi:10.1029/2005GL023740.

Ponte, R.M., 2006: Low frequency sea level variability and the inverted barometer effect. *J. Atmos. Ocean. Technol.*, **23**(4), 619–629.

Potter, R.A., and M.S. Lozier, 2004: On the warming and salinification of the Mediterranean outflow waters in the North Atlantic. *Geophys. Res. Lett.*, **31**(1), L01202, doi:10.1029/2003GL018161.

Prentice, I.C., et al., 2001: The carbon cycle and atmospheric carbon dioxide. In: *Climate Change 2001: The Scientific Basis. Contribution of Working Group I to the Third Assessment Report of the Intergovernmental Panel on Climate Change* [Houghton, J.T., et al. (eds.)]. Cambridge University Press, Cambridge, United Kingdom and New York, NY, USA, pp. 183–237.

Proshutinsky, A.Y., and M.A. Johnson, 1997: Two circulation regimes of the wind-driven Arctic Ocean. *J. Geophys. Res.*, **102**(C6), 12493–12514.

Proshutinsky, A., et al., 2004: Secular sea level change in the Russian sector of the Arctic Ocean. *J. Geophys. Res.*, **109**(C3), C03042, doi:10.1029/2003JC002007.

Qian, H., Y. Yin, and Y. Ni, 2003: Tropical Indian Ocean subsurface dipole mode and diagnostic analysis of dipole event in 1997-1998. *J. Appl. Meteorol. Sci.*, **14**, 129–139 (in Chinese).

Quadfasel, D., A. Sy, D. Wells, and A. Tunik, 1991: Warming in the Arctic. *Nature*, **350**(6317), 385.

Raven, J., et al., 2005: *Ocean Acidification due to Increasing Atmospheric Carbon Dioxide.* The Royal Society, London, 59 pp.

Reverdin, G., D. Cayan, and Y. Kushnir, 1997: Decadal variability of hydrography in the upper northern North Atlantic in 1948-1990. *J. Geophys. Res.*, **102**(C4), 8505–8531.

Rigor, I.G., J.M. Wallace, and R.L. Colony, 2002: Response of sea ice to the Arctic Oscillation. *J. Clim.*, **15**, 2648–2663.

Rixen, M., et al., 2005: The Western Mediterranean Deep Water: A new proxy for global climate change. *Geophys. Res. Lett.*, **32**, L12608, doi:10.1029/2005GL022702.

Robertson, R., M. Visbeck, A.L. Gordon, and E. Fahrbach, 2002: Long-term temperature trends in the deep waters of the Weddell Sea. *Deep-Sea Res. II*, **49**(21), 4791–4806.

Roemmich, et al., 2007: Decadal spin-up of the South Pacific Subtropical Gyre. *J. Phys. Oceanogr.*, 37, 162-173.

Roether, W., et al., 1996: Recent changes in eastern Mediterranean deep waters. *Science*, **271**(5247), 333–335.

Rohling, E.J., and H.L. Bryden, 1992: Man-induced salinity and temperature increases in western Mediterranean deep-water. *J. Geophys. Res.*, **97**(C7), 11191–11198.

Rupolo, V., S. Marullo, and D. Iudicone, 2003: Eastern Mediterranean transient studied with Lagrangian diagnostics applied to a Mediterranean OGCM forced by satellite SST and ECMWF wind stress for the years 1988-1993. *J. Geophys. Res.*, **108**(C9), 8121.

Sabine, C.L., R.M. Key, R.A. Feely, and D. Greeley, 2002: Inorganic carbon in the Indian Ocean: Distribution and dissolution processes. *Global Biogeochem. Cycles*, **16**(4), 1067, doi:10.1029/2002GB001869.

Sabine, C.L., R.A. Feely, Y.W. Watanabe, and M. Lamb, 2004a: Temporal evolution of the North Pacific CO_2 uptake rate. *J. Oceanogr.*, **60**(1), 5–15.

Sabine, C.L., et al., 1999: Anthropogenic CO_2 inventory of the Indian Ocean. *Global Biogeochem. Cycles*, **13**, 179–198.

Sabine, C.L., et al., 2004b: The oceanic sink for anthropogenic CO_2. *Science*, **305**(5682), 367–371.

Sahagian, D.L., 2000: Global physical effects of anthropogenic hydrological alterations: sea level and water redistribution. *Global Planet. Change*, **25**, 39–48.

Sahagian, D.L., F.W. Schwartz, and D.K. Jacobs, 1994: Direct anthropogenic contributions to sea level rise in the twentieth century. *Nature*, **367**, 54–56.

Sarma, V.V.S.S., T. Ono, and T. Saino, 2002: Increase of total alkalinity due to shoaling of aragonite saturation horizon in the Pacific and Indian Oceans: Influence of anthropogenic carbon inputs. *Geophys. Res. Lett.*, **29**(20), 1971, doi:10.1029/2002GL015135.

Sarmiento, J.L., C. Le Quéré, and S.W. Pacala, 1995: Limiting future atmospheric carbon dioxide. *Global Biogeochem. Cycles*, **9**(1), 121–137.

Schauer, U., E. Fahrbach, and S. Østerhus, 2004: Arctic warming through the Fram Strait - Oceanic heat transport from three years of measurements. *J. Geophys. Res.*, **109**, C06026, doi:10.1029/2003JC001823.

Schneider, N., and B.D. Cornuelle, 2005: The forcing of the Pacific Decadal Oscillation. *J. Clim.*, **18**(21), 4355–4373.

Schoenefeldt, R., and F. Schott, 2006: Decadal variability of the Indian Ocean cross-equatorial exchange in SODA. *Geophys. Res. Lett.*, **33**, L08602, doi:10.1029/2006GL025891.

Schott, F.A., et al., 2004: Circulation and deep-water export at the western exit of the subpolar North Atlantic. *J. Phys. Oceanogr.*, **34**, 817–843.

Seager, R., et al., 2001: Wind-driven shifts in the latitude of the Kuroshio-Oyashio Extension and generation of SST anomalies on decadal timescales. *J. Clim.*, **14**(22), 4249–4265.

Sekine, Y., 1988: Anomalous southward intrusion of the Oyashio east of Japan.1. Influence of the seasonal and interannual variations in the wind stress over the North Pacific. *J. Geophys. Res.*, **93**(C3), 2247–2255.

Sekine, Y., 1999: On variations in the subarctic circulation in the North Pacific. *Prog. Oceanogr.*, **43**(2–4), 193–203.

Senjyu, T., et al., 2002: Renewal of the bottom water after the winter 2000-2001 may spin-up the thermohaline circulation in the Japan Sea. *Geophys. Res. Lett.*, **29**(7), 1149, doi:10.1029/2001GL014093.

Sivan, D., et al., 2004: Ancient coastal wells of Caesarea Maritima, Israel, an indicator for sea level changes during the last 2000 years. *Earth Planet. Sci. Lett.*, **222**, 315–330.

Smith, T.M., and R.W. Reynolds, 2003: Extended reconstructions of global sea surface temperatures based on COADS Data (1854-1997). *J. Clim.*, **16**, 1495–1510.

Sprintall, J., et al., 2004: INSTANT: A new international array to measure the Indonesian Throughflow. *EOS*, **85**(39), 369.

Stammer, D., et al., 2003: Volume, heat and freshwater transports of the global ocean circulation 1993-2000. *J. Geophys. Res.*, **108**(C1), doi:10.1029/2001JC001115.

Stark, S., R.A. Wood, and H.T. Banks, 2006: Re-evaluating the causes of observed changes in Indian Ocean water masses. *J. Clim.*, **19**(16), 4075–4086.

Steele, M., and T. Boyd, 1998: Retreat of the cold halocline layer in the Arctic Ocean. *J. Geophys. Res.*, **103**(C5), 10419–10435.

Stephens, C., S. Levitus, J. Antonov, and T. Boyer, 2001: On the Pacific Ocean regime shift. *Geophys. Res. Lett.*, **28**, 3721–3724.

Stephens, C., et al., 2002: World ocean database 2001, Volume 3: Temporal distribution of conductivity-temperature-depth profiles. In: *NOAA Atlas NESDIS 44* [Levitus, S. (ed.)]. U.S. Government Printing Office, Washington, DC, pp. 47, CD-ROMs.

Sterl, A., and W. Hazeleger, 2003: Coupled variability and air-sea interaction in the South Atlantic Ocean. *J. Clim.*, **21**, 559–571.

Stramma, L., J. Fischer, P. Brandt, and F. Schott, 2003: Circulation, variability and near-equatorial meridional flow in the central tropical Atlantic. In: *Interhemispheric Water Exchange in the Atlantic Ocean* [Goni, G., and P. Malanotte-Rizzoli (eds.)]. Elsevier, Amsterdam, pp. 1–22.

Stramma, L., et al., 2004: Deep water changes at the western boundary of the subpolar North Atlantic during 1996 to 2001. *Deep-Sea Res.*, **51A**, 1033–1056.

Sy, A., et al., 1997: Surprisingly rapid spreading of newly formed intermediate waters across the North Atlantic Ocean. *Nature*, **386**(6626), 675–679.

Takahashi, T., S.C. Sutherland, R.A. Feely, and R. Wanninkhof, 2006: Decadal change of the surface water pCO_2 in the North Pacific: A synthesis of 35 years of observations. *J. Geophys. Res.*, **111**, C07S05, doi:10.1029/2005JC003074.

Takahashi, T., et al., 2002: Global sea-air CO_2 flux based on climatological surface ocean pCO_2, and seasonal biological and temperature effects. *Deep-Sea Res. II*, **49**(9–10), 1601–1622.

Talley, L.D., 1996: North Atlantic circulation and variability, reviewed for the CNLS conference. *Physica D*, **98**(2–4), 625–646.

Talley, L.D., and M.S. McCartney, 1982: Distribution and circulation of Labrador Sea-water. *J. Phys. Oceanogr.*, **12**(11), 1189–1205.

Talley, L.D., J.L. Reid, and P.E. Robbins, 2003a: Data-based meridional overturning streamfunctions for the global ocean. *J. Clim.*, **16**, 3213–3226.

Talley, L.D., et al., 2003b: Deep convection and brine rejection in the Japan Sea. *Geophys. Res. Lett.*, **30**(4), 1159, doi:10.1029/2002GL0165451.

Trenberth, K.E., and J.M. Caron, 2001: Estimates of meridional atmosphere and ocean heat transports. *J. Clim.*, **14**(16), 3433–3443.

Trenberth, K.E., J.M. Caron, and D.P. Stepaniak, 2001: The atmospheric energy budget and implications for surface fluxes and ocean heat transports. *Clim. Dyn.*, **17**, 259–276.

Tsimplis, M.N., and M. Rixen, 2002: Sea level in the Mediterranean Sea: The contribution of temperature and salinity changes. *Geophys. Res. Lett.*, **29**(23), 2136, doi:10.1029/2002GL015870.

Tsimplis, M.N., A.G.P. Shaw, R.A. Flather, and D.K. Woolf, 2006: The influence of the North Atlantic Oscillation on the sea level around the northern European coasts reconsidered: the thermosteric effects. *Phil. Trans. R. Soc.London A*, **364**(1841), 845–856, doi:10.1098/rsta.2006.1740.

Vargas-Yáñez, M., et al., 2004: Temperature and salinity increase in the eastern North Atlantic along the 24.5°N in the last ten years. *Geophys. Res. Lett.*, **31**, L06210, doi:10.1029/2003GL019308.

Vaughan, D., et al., 2003: Recent rapid regional climate warming on the Antarctic Peninsula. *Clim. Change*, **60**, 243–274.

Vellinga, M., and R.A. Wood, 2002: Global climatic impacts of a collapse of the Atlantic thermohaline circulation. *Clim. Change*, **54**, 251–267.

Venegas, S.A., L.A. Mysak, and D.N. Straub, 1998: An interdecadal climate cycle in the South Atlantic and its links to other ocean basins. *J. Geophys. Res.*, **103**(C11), 24723–24736.

Vignudelli, S., G.P. Gasparini, M. Astraldi, and M.E. Schiano, 1999: A possible influence of the North Atlantic Oscillation on the circulation of the Western Mediterranean Sea. *Geophys. Res. Lett.*, **26**(5), 623–626.

Vranes, K., A.L. Gordon, and A. Ffield, 2002: The heat transport of the Indonesian Throughflow and implications for the Indian Ocean heat budget. *Deep-Sea Res. I*, **49**, 1391–1410.

Wadhams, P., and W. Munk, 2004: Ocean freshening, sea level rising, sea ice melting. *Geophys. Res. Lett.*, **31**(11), L11311, doi:10.1029/2004GL020039.

Wakelin, S.L., P.L. Woodworth, R.A. Flather, and J.A. Williams, 2003: Sea-level dependence on the NAO over the NW European continental shelf. *Geophys. Res. Lett.*, **30**(7), 1403, doi:10.1029/2003GL017041.

Watanabe, Y.W., H. Ishida, T. Nakano, and N. Nagai, 2005: Spatiotemporal decreases of nutrients and chlorophyll-a in the surface mixed layer of the western North Pacific from 1971 to 2000. *J. Oceanogr.*, **61**, 1011–1016.

Watanabe, Y.W., et al., 2001: Probability of a reduction in the formation rate of the subsurface water in the North Pacific during the 1980s and 1990s. *Geophys. Res. Lett.*, **28**(17), 3289–3292.

White, N.J., J.A. Church, and J.M. Gregory, 2005: Coastal and global averaged sea-level rise for 1950 to 2000. *Geophys. Res. Lett.*, **32**(1), L01601, doi:10.1029/2004GL021391.

Whitworth, T., 2002: Two modes of bottom water in the Australian-Antarctic Basin. *Geophys. Res. Lett.*, **29**(5), 1973, doi:10.1029/2001GL014282.

Wijffels, S., and G.A. Meyers, 2004: An intersection of oceanic wave guides: Variability in the Indonesian Throughflow region. *J. Phys. Oceanogr.*, **34**, 1232–1253.

Willey, D.A., et al., 2004: Global oceanic chlorofluorocarbon inventory. *Geophys. Res. Lett.*, **31**, L01303, doi:10.1029/2003GL018816.

Willis, J.K., D. Roemmich, and B. Cornuelle, 2004: Interannual variability in upper-ocean heat content, temperature and thermosteric expansion on global scales. *J. Geophys. Res.*, **109**, C12036, doi:10.1029/2003JC002260.

Wong, A.P.S., N.L. Bindoff, and J.A. Church, 1999: Large-scale freshening of intermediate waters in the Pacific and Indian oceans. *Nature*, **400**(6743), 440–443.

Wong, A.P.S., N.L. Bindoff, and J.A. Church, 2001: Freshwater and heat changes in the North and South Pacific Oceans between the 1960s and 1985-94. *J. Clim.*, **14**(7), 1613–1633.

Woodworth, P.L., 1990: A search for accelerations in records of European mean sea level. *Int. J. Climatol.*, **10**, 129–143.

Woodworth, P.L., and D.L. Blackman, 2002: Changes in extreme high waters at Liverpool since 1768. *Int. J. Climatol.*, **22**, 697–714.

Woodworth, P.L., and R. Player, 2003: The Permanent Service for Mean Sea Level: An update to the 21st century. *J. Coastal Res.*, **19**, 287–295.

Woodworth, P.L., and D.L. Blackman, 2004: Evidence for systematic changes in extreme high waters since the mid-1970s. *J. Clim.*, **17**, 1190–1197.

Woodworth, P.L., M.N. Tsimplis, R.A. Flather, and I. Shennan, 1999: A review of the trends observed in British Isles mean sea level data measured by tide gauges. *Geophys. J. Int.*, **136**, 651–670.

Woolf, D., A. Shaw, and M.N. Tsimplis, 2003: The influence of the North Atlantic Oscillation on sea level variability in the North Atlantic Region. *Global Atmos. Ocean System*, **9**(4), 145–167.

Xie, S.P., H. Annamalai, F.A. Schott, and J.P. McCreary, 2002: Structure and mechanisms of South Indian Ocean climate variability. *J. Clim.*, **15**(8), 864–878.

Yamagata, T., et al., 2004: Coupled ocean-atmosphere variability in the tropical Indian Ocean. In: *Earth Climate: The Ocean-Atmosphere Interaction* [Wang, C., S.-P. Xie, and J.A. Carton (eds.)]. American Geophysical Union, Washington, DC, pp. 189–212.

Yashayaev, I., J.R.N. Lazier, and R.A. Clarke, 2003: Temperature and salinity in the central Labrador Sea. *ICES Marine Symposia Series*, **219**, 32–39.

Yasuda, I., T. Tozuka, M. Noto, and S. Kouketsu, 2000: Heat balance and regime shifts of the mixed layer in the Kuroshio Extension. *Prog. Oceanogr.*, **47**(2–4), 257–278.

Yasuda, I., et al., 2001: Hydrographic structure and transport of the Oyashio south of Hokkaido and the formation of North Pacific Intermediate Water. *J. Geophys. Res.*, **106**(C4), 6931–6942.

Zhang, K., B.C. Douglas, and S.P. Leatherman, 2000: Twentieth-century storm activity along the U.S. east coast. *J. Clim.*, **13**, 1748–1761.

Appendix 5.A: Techniques, Error Estimation and Measurement Systems

5.A.1 Ocean Temperature and Salinity

Sections 5.2 and 5.3 report on the changes in the oceans using two different approaches to the oceanic part of the climate system. Section 5.2 documents the changes found in the most comprehensive ocean data sets that exist for temperature and salinity. These data sets are collected from a wide range of organisations and are a composite of heterogeneous measurement systems, including mechanical and expendable bathythermographs, research ship measurements, voluntary observing ships, moored and drifting buoys and Argo floats for recent years. The advantage of these composite data sets is the greater spatial and temporal coverage that they offer for climate studies. The main disadvantage of these composite data sets, relative to the research data sets used in Section 5.3, is that they can have more problems related to the quality and heterogeneity of the measurements systems. This heterogeneity can lead to subtle biases and artificial noise and consequently difficulties in estimating trends at small regional scales (Harrison and Carson, 2006). On the other hand, Section 5.3 described the changes found in detailed analyses of very specific research voyages that consist mainly of very tightly calibrated and monitored temperature and salinity measurements (and other variables). The internal consistency of these research data sets is much higher than the composite data sets, and as a consequence they have significant advantages in their ease of interpretation and analysis. However, research quality oceanographic data sets are only collected occasionally and are focussed more frequently on regional rather than global issues. This means that in the poorly sampled oceans, such as the Indian, South Pacific and Southern Oceans, observational records only cover a relatively short period of time (e.g., the 1960s to present) with some decades poorly covered and highly heterogeneous in space (see Figure 5.A.1).

An example of the distribution of ocean temperature observations in both space and time is shown in Figure 5.A.1. This figure shows the *in situ* temperature data distribution for two five-year periods used to create estimates of global heat content change (e.g., Figure 5.1), one with a low (a) and one with a high (b) density of observations. It is clear that parts of the ocean, in particular in the SH, are not well sampled even in periods of high observation density. Hence, sampling errors resulting from the lack of data are potentially important but cannot easily be quantified.

Several different objective analysis techniques have been used to produce the gridded fields of temperature anomalies used to compute ocean heat content and steric sea level rise presented in this chapter. The technique used by Levitus et al. (2005b), Garcia et al. (2005) and Antonov et al. (2005) in their estimates of temperature (heat content), oxygen and the thermosteric component of sea level change is based on the construction of gridded (1° latitude by 1° longitude grid) fields at standard depth measurement levels. The objective analysis procedure used for interpolation (filling in data-void areas and smoothing the entire field) is described by Boyer et al. (2002). At each standard depth level, all data are averaged within each 1° square, and the deviation from climatology yields the observed anomaly. From all observations within the surrounding region of diameter 888 km, the analysed value is computed. Features with a wavelength of less than 500 to 600 km are substantially reduced in amplitude; in regions without sufficient data, it is essentially the climatological information that is used. Ishii et al. (2006) employed similar techniques, with a smaller de-correlation length scale of 300 km and a least-squares technique for estimating corrections to the climatological field. Willis et al. (2004) used a two-scale covariance function, but also used altimetric data in areas where ocean observations were lacking.

There are some differences in the data used in these studies. In addition to ocean temperature profile data, Ishii et al. (2006) also used the product of climatological mixed layer depth and individual SST measurements in their estimates of ocean heat content. Southern Hemisphere World Ocean Circulation Experiment profiling float temperature profiles for the 1990s were used by Willis et al. (2004) that were not used by Levitus et al. (2005a) and Ishii et al. (2006). The similarity of the three independently estimated heat content time series shown in Figure 5.1 to within confidence intervals indicates that the differences between analysis techniques and data sources do not substantially influence the estimates of the three global ocean heat content time series.

All analyses are subject to statistical errors and sampling errors. Statistical errors are estimated in a straightforward way. For example, for the Levitus et al. (2005a) fields, the uncertainty at any grid point is estimated from the variability of observations that contributed to the analysed value. In this way, 90% errors for all analysed variables are computed as a function of depth and horizontal position, and correspondingly for integrated variables such as heat content. Both Ishii et al. (2006) and Willis et al. (2004) used the interannual variability of heat content as the basis for error analyses.

5.A.2 Heat Transports

Estimates of meridional heat transport (MHT) derived from the surface heat balance involve the integration of the zonally averaged balances in the longitudinal direction. This integration also implies the integration of uncertainties in the zonally averaged estimates. For instance, an uncertainty in zonally averaged estimates of ± 10 W m^{-2} results in an uncertainty of 0.5×10^{15} W in MHT in the Atlantic and nearly twice that value in the Pacific. Thus, all climatological estimates of MHT based on the surface heat balance have considerable uncertainties, and estimates of MHT variability are unlikely to be significant when derived from the surface heat balance.

In addition to the uncertainties in diagnostic computations of transports from vertical sections, estimates of MHT based on oceanic cross sections are largely influenced by sparse sampling of these sections during continuous time periods. As a result, there is no way to discriminate between the long-term signals and interannual variability using the estimates of MHT for individual years.

5.A.3 Estimates of Oxygen Changes

Estimates of changes in O_2 in the surface 100 m of the ocean between 1955 and 1998 were made for each pentad using a total of 530,000 O_2 profiles (Garcia et al., 2005). The measurement method was not reported for all the cruises. Only the Winkler titration was reported, with only manual titrations prior to 1990. The Carpenter method to improve accuracy was reported for some cruises after 1970. An automated titration gives a significant improvement for measurement reproducibility but is not the essential solution for accuracy. Problems of O_2 leakage were reported from the older samples using Nansen bottles (generally before 1970). The Niskin bottles more widely used after 1970 are thought to be more reliable. There are no agreed standards for O_2 measurements because of reagent impurity and the difficulty in preparing a stable solution, which limits accuracy of these measurements to typically less than 10 μmol kg^{-1} for modern methods.

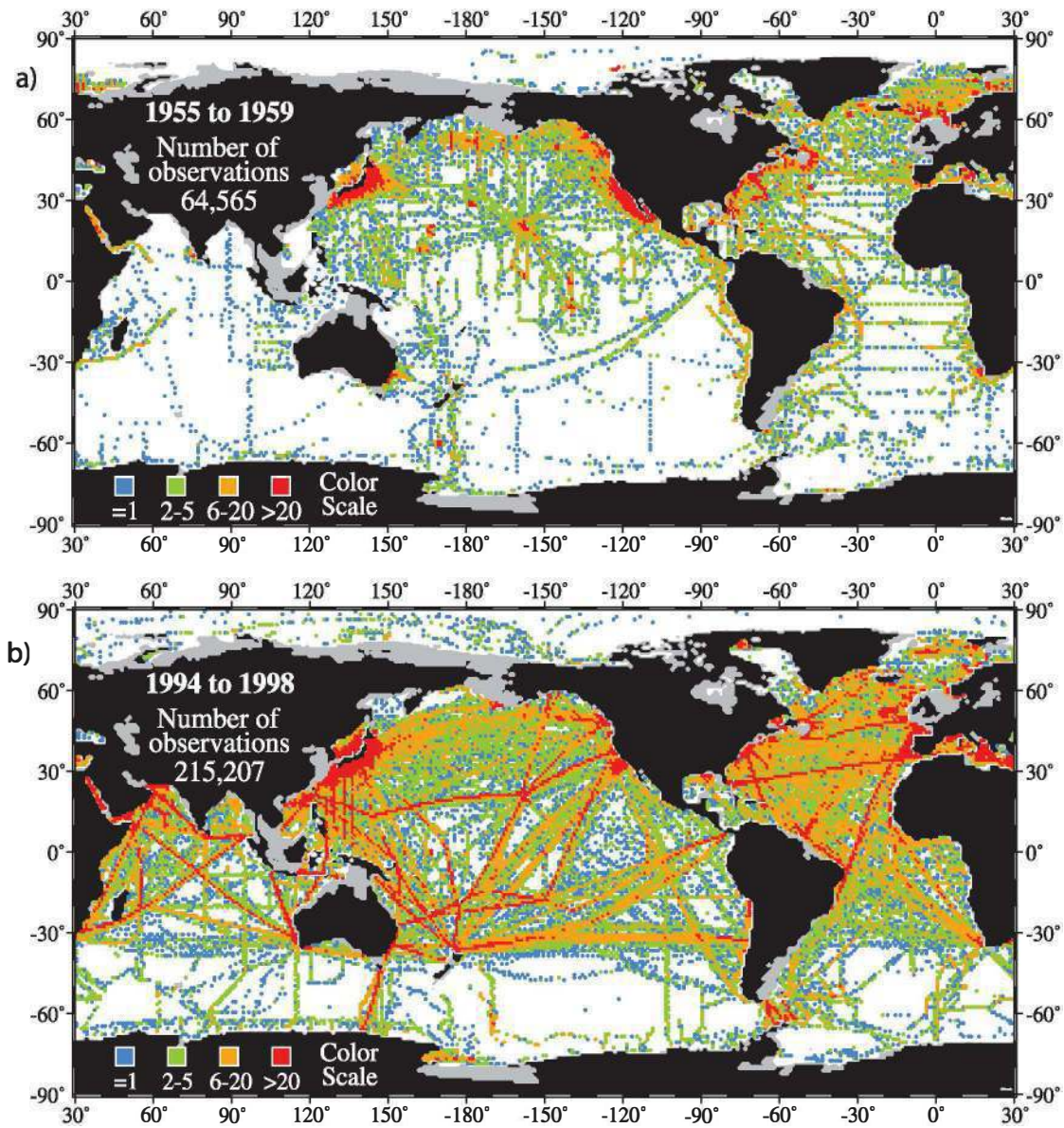

Figure 5.A.1 *The number of ocean temperature observations in each 1° grid box at 250 m depth for two periods: (a) 1955 to 1959, with a low density of observations, and (b) 1994 to 1998, with a high density of observations. A blue dot indicates a 1° grid box containing 1 observation, a green dot 2 to 5 observations, an orange dot 6 to 20 observations, and a red dot more than 20 observations.*

5.A.4 Estimation of Sea Level Change

5.A.4.1 Satellite Altimetry: Measurement Principle and Associated Errors

The concept of satellite altimetry measurement is rather straightforward. The onboard radar altimeter transmits a short pulse of microwave radiation with known power towards the nadir. Part of the incident radiation reflects back to the altimeter. Measurement of the round-trip travel time provides the height of the satellite above the instantaneous sea surface. The quantity of interest in oceanography is the height of the instantaneous sea surface above a fixed reference surface, which is computed as the difference between the altitude of the satellite above the reference ellipsoid and the altimeter range. The satellite position is computed through precise orbit determination, combining accurate modelling of the satellite motion and tracking measurements between the satellite and observing stations on Earth or other observing satellites. A number of corrections must be applied to obtain the correct sea surface height. These include instrumental corrections, ionospheric correction, dry and wet tropospheric corrections, electromagnetic bias correction, ocean and solid Earth tidal corrections, ocean loading correction, pole tide correction and an inverted barometer correction that has to be applied since the altimeter does not cover the global ocean completely. The total measurement accuracy for the TOPEX/Poseidon altimetry-based sea surface height is about 80 mm (95% error) for a single measurement based on one-second along-track averages (Chelton et al., 2001).

The above error estimates concern instantaneous sea surface height measurements. For estimating the mean sea level variations, the procedure consists of simply averaging over the ocean the point-to-point measurements collected by the satellite during a complete orbital cycle (10 days for TOPEX/Poseidon and Jason-1), accounting for the spatial distribution of the data using an equal area weighting. In effect, during this time interval, the satellite realises an almost complete coverage of the oceanic domain. The 95% error associated with a 10-day mean sea level estimate is approximately 8 mm.

When computing global mean sea level variations through time, proper account of instrumental bias and drifts (including the terrestrial reference frame) is of considerable importance. These effects (e.g., the radiometer drift onboard TOPEX/Poseidon used to correct for the wet tropospheric delay) are of the same order of magnitude as the sea level signal. Studies by Chambers et al. (1998) and Mitchum (1994; 2000) have demonstrated that comparing the altimeter sea level measurements to tide gauge sea level measurements produces the most robust way of correcting for instrumental bias and drifts. This approach uses a network of high-quality tide gauges, well distributed over the ocean domain. Current results indicate that the residual error in the mean sea level variation using the tide gauge calibration is about 0.8 mm yr^{-1} (a value resulting mainly from the uncertainties in vertical land motion at the tide gauges). The current altimeter-inferred sea level measurements do not include modelling of the geocenter or mitigating the effect resulting from the potential drift of the terrestrial reference frame.

Detailed information about satellite altimetry, uncertainty and applications can be found in Fu and Cazenave (2001).

5.A.4.2 Sea Level from Tide Gauge Observations

Tide gauges are based on a number of different technologies (float, pressure, acoustic, radar), each of which has its advantages in particular applications. The Global Sea Level Observing System (GLOSS) specifies that a gauge must be capable of measuring sea level to centimetre accuracy (or better) in all weather conditions (i.e., in all wave conditions). The most important consideration is the need to maintain the gauge datum relative to the level of the Tide Gauge Bench Mark (TGBM), which provides the land reference level for the sea level measurements. The specifications for GLOSS require that local levelling must be repeated at least annually between the reference mark of the gauge, TGBM and a set of approximately five ancillary marks in the area, in order to maintain the geodetic integrity of the measurements. In practice, this objective is easier to meet if the area around the gauge is hard rock, rather than reclaimed land, for example. The question of whether the TGBM is moving vertically within a global reference frame (for whatever reason) is being addressed by advanced geodetic methods (GPS, Determination d'Orbite et Radiopositionnement Intégrés par Satellite (DORIS), Absolute Gravity). With typical rates of sea and land level change of order of 1 mm yr^{-1}, it is necessary to maintain the accuracy of the overall gauge system at the centimetre level over many decades. This demanding requirement has been met in many countries for many years (see IOC, 2002 for more information). The tide gauge observation system for three periods is shown in Figure 5.A.2, together with the evolution over time of the number of stations in both hemispheres. The distribution of tide gauge stations was particularly sparse in space at the beginning of the 20th century, but rapidly improved in the 1950s through to the current network of GLOSS standard instruments. This distribution of instruments through time means that confidence in the estimates of sea level rise has been improving and this certainty is reflected in the shrinking confidence intervals (Figure 5.13).
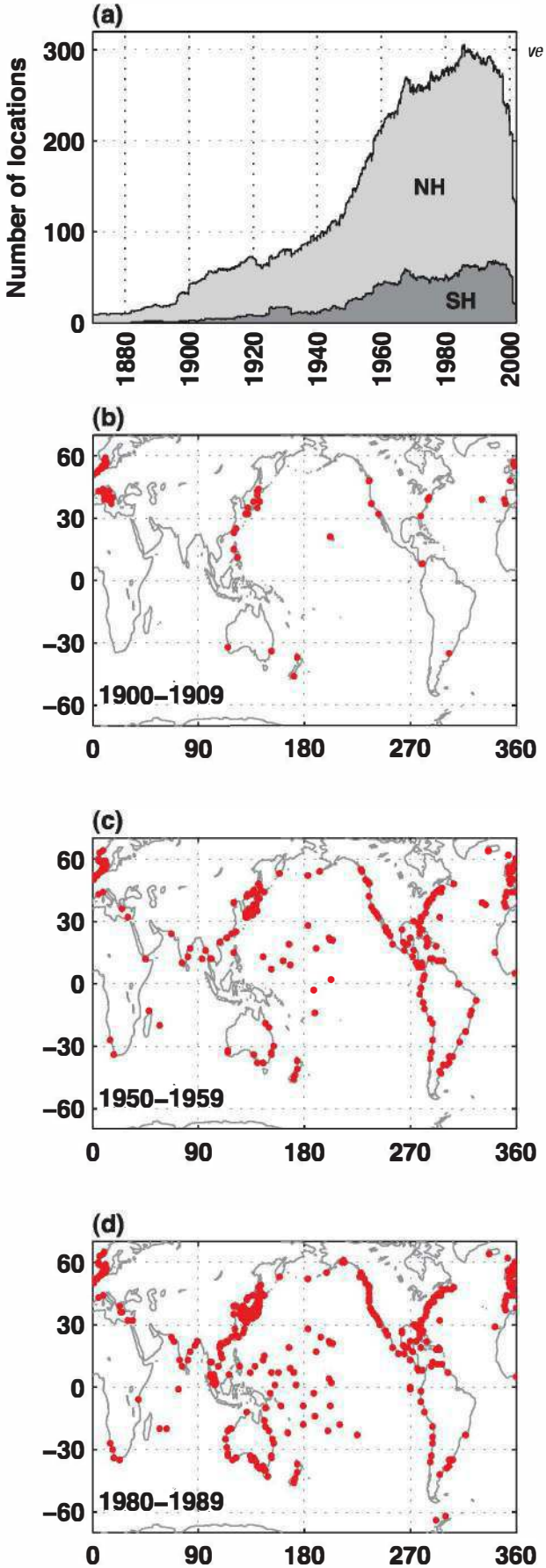
Figure 5.A.2. *(a) Number of tide gauge stations in the Northern Hemisphere (NH) and Southern Hemisphere (SH) used to deri the global sea level curve (red and blue curves in Figure 5.13) as a function of time. Lower panels show the spatial distribution of tide gauge stations (denoted by red dots) for the periods (b) 1900 to 1909, (c) 1950 to 1959 and (d) 1980 to 1989.*